



**STRUCTURAL SYSTEMS
RESEARCH PROJECT**

Report No.
SSRP-04/17

**EFFECTS OF CONSTRUCTION
METHODS ON THE AXIAL
CAPACITY OF DRILLED SHAFTS**

by

**DAIVA A. SEAVEY
SCOTT A. ASHFORD**

Final Report Submitted to Caltrans under Contract No. 59A0337

December 2004

Department of Structural Engineering
University of California, San Diego
La Jolla, California 92093-0085

University of California, San Diego
Department of Structural Engineering
Structural Systems Research Project

Report No. SSRP-04/17

**Effects of Construction Methods on the Axial Capacity of
Drilled Shafts**

by

Daiva A. Seavey

Graduate Research Assistant

Scott A. Ashford

Professor of Geotechnical Engineering

Final Report Submitted to Caltrans under Contract No. 59A0337

Department of Structural Engineering
University of California, San Diego
La Jolla, California 92093-0085

December 2004

Technical Report Documentation Page

1. Report No. SSRP-04/17	2. Government Accession No.	3. Recipient's Catalog No.	
4. Title and Subtitle Effects of Construction Methods on the Axial Capacity of Cast-In-Drilled-Hole Piles		5. Report Date December 2004	
7. Author(s) Daiva A. Seavy, Scott A. Ashford		6. Performing Organization Code	
9. Performing Organization Name and Address Department of Structural Engineering School of Engineering University of California, San Diego La Jolla, California 92093-0085		8. Performing Organization Report No.	
12. Sponsoring Agency Name and Address California Department of Transportation Engineering Service Center 1801 30 th St., West Building MS-9 Sacramento, California 95807		10. Work Unit No. (TRAIS)	
15. Supplementary Notes Prepared in cooperation with the State of California Department of Transportation.		11. Contracts or Grant No. 59A0337	
16. Abstract		13. Type of Report and Period Covered Final Report	
17. Key Words CIDH Pile, Axial Capacity, Grouting		14. Sponsoring Agency Code	
19. Security Classification (of this report) Unclassified		18. Distribution Statement Unlimited	
20. Security Classification (of this page) Unclassified		21. No. of Pages ~134	22. Price

DISCLAIMER

Any opinions, findings, conclusions and recommendations expressed in this final test report are those of the authors and do not necessarily reflect views of the California Department of Transportation.

ACKNOWLEDGEMENT

The research project described in this final report was funded by the California Department of Transportation (Caltrans) under contract No. 59A0337.

ABSTRACT

A Cast-In-Drilled-Hole (CIDH) pile is a type of deep foundation that provides support to structures situated on weak surface soils by transferring loads to deeper and/or stronger soils. CIDH piles are also referred to as drilled shafts, caissons, drilled piers, and bored piles, to name a few. The purpose of this research is to provide a broad overview of the effects of construction methods on the axial capacity of CIDH piles. Axial capacity is the resistance along the sides of the pile and at the tip with the surrounding soils. Case studies by others are discussed to determine where further research efforts on CIDH piles would benefit current design practice.

In comparing current research to current design practice, several conclusions can be drawn. The first of which concerns post-grouting, where grout is added to the sides and/or tip of the pile after construction is complete. Post-grouting increases the axial capacity by improving the friction along the sides of the pile and bearing at the tip, yet this practice is rarely used. The second conclusion concerns the design equations for side resistance, which may need modification for non-typical construction, such as post-grouting and large diameter piles. Regarding large diameter CIDH piles, it should be noted that a very limited amount of information is available, and therefore further research would be beneficial. Another area where research is recommended is the use of self-compacting concrete, which may prove ideal for CIDH pile construction.

TABLE OF CONTENTS

DISCLAIMER	ii
ACKNOWLEDGEMENT	iii
ABSTRACT.....	iv
TABLE OF CONTENTS	v
LIST OF FIGURES.....	viii
LIST OF TABLES.....	x
LIST OF SYMBOLS	xi
1 INTRODUCTION.....	1
2 BACKGROUND	3
2.1 History.....	3
2.2 Uses of CIDH piles	4
2.3 Construction Methods.....	5
2.3.1 Dry Method.....	5
2.3.2 Casing Method.....	6
2.3.3 Slurry Method	7
2.4 Materials	8
2.4.1 Drilling Equipment	8
2.4.2 Slurry Mixes.....	10
2.4.3 Concrete Mixes	12
2.5 Design	13
2.6 Construction Specifications	14
3 CIDH PILE BEHAVIOR AND DESIGN	17
3.1 Side Resistance	17
3.1.1 Alpha-Method (α -Method) for Cohesive Soils	18
3.1.2 Beta-Method (β -Method) for Cohesionless Soils	20

3.2	Bearing (Tip) Resistance.....	22
3.2.1	Tip Resistance in Cohesive Soils.....	22
3.2.2	Tip Resistance in Cohesionless Soils.....	24
3.3	Structural Design (Axial and Lateral Resistance).....	27
3.3.1	Allowable Stress Design (ASD) Method.....	29
3.3.2	Load and Resistance Factor Design (LRFD).....	29
3.4	Testing Methods.....	30
3.4.1	Gamma-Gamma Logging (GGL)	30
3.4.2	Impulse Response Methods	31
3.4.3	Cross-hole Sonic Logging (CSL).....	32
4	CASE HISTORIES AND RESEARCH.....	35
4.1	Construction Method Effects on Capacity	36
4.1.1	Case Study by Camp, Brown, and Mayne (2002)	39
4.1.1.1	Testing Procedure	41
4.1.1.2	Discussion of Results.....	43
4.1.2	Case Study by Reese, Owens, and Hoy (1985)	45
4.1.3	Case Study by Finno, Chao, Gassman, and Zhou (2002).....	48
4.1.4	Case Study by Petek, Felice, and Holtz (2002)	50
4.1.5	Case Study by Sarhan, Tabsh, and O’Neill (2002).....	52
4.2	Post-Grouting.....	54
4.2.1	Case Study by Reese <i>et al.</i> (1985), (Cont’d from 4.1.3).....	57
4.2.2	Case Study by Littlechild, Plumbridge, Hill, and Lee (2000)	59
4.2.3	Case Study by Dapp and Mullins (2002).....	62
4.2.4	Case Study by Brusey (2000)	65
4.2.4.1	Testing Procedure	67
4.2.4.2	Discussion of Results.....	68
4.3	Test Methods.....	70
4.3.1	Case Study by Finno <i>et al.</i> (2002), Cont’d	72
4.3.2	Case Study by Robinson, Rausche, Garland, and Ealy (2002).....	72
4.3.3	Case Study by Branagan, Vanderpool, Murvosh, Klein (2002)	73
4.3.4	Case Study by Caltrans (2003)	73

4.4	Self-Compacting Concrete.....	75
5	DISCUSSION ON DESIGN vs. RESEARCH	77
5.1	Comparisons of Construction Methods and Predictions.....	77
5.1.1	Tip Resistance.....	77
5.1.2	Side Resistance	79
5.1.3	Total Axial Capacity.....	83
5.2	Bottom Cleanliness.....	84
5.3	Anomaly Effects and Non-Destructive Testing.....	87
5.4	Self-Compacting Concrete.....	90
6	RECOMMENDATIONS.....	93
	APPENDIX A.....	95
	APPENDIX B.....	105
	APPENDIX C.....	107
	REFERENCES	120

LIST OF FIGURES

Figure 1 Elementary drilling set-up (ADSC 2002).....	3
Figure 2 Pile casing (Goodman <i>et al.</i> 2002)	6
Figure 3 Rock auger (Goodman <i>et al.</i> 2002)	8
Figure 4 Drilling auger (Stewart <i>et al.</i> 2001).....	9
Figure 5 Core barrel (Goodman <i>et al.</i> 2002).....	9
Figure 6 Variation of a with c_u/p_a based on tested results by Kulhawy and Jackson (1989).....	18
Figure 7 Gamma-gamma log testing (Caltrans 2002).....	31
Figure 8 Load-displacement curves for the minimum shallow-depth value and maximum deep-depth value (Camp <i>et al.</i> 2000).....	42
Figure 9 Load displacement curves for non-grouted (DS) and post-grouted (DSG) piles (Brusey 2000).....	68
Figure 10 Comparison of case histories for tip resistance between tested- and design- values (Camp <i>et al.</i> 2002, Dapp <i>et al.</i> 2002, Reese <i>et al.</i> 1985).....	78
Figure 11 Comparison of case histories between design- and tested-values for side resistance (Camp <i>et al.</i> 2002, Finno <i>et al.</i> 2002, Reese <i>et al.</i> 1985, Littlechild <i>et al.</i> 2000)	79
Figure 12 Tested side resistance values in portions of the pile without casing for Camp <i>et al.</i> (2002).....	80
Figure 13 Tested tip resistances for Camp <i>et al.</i> (2002).....	81
Figure 14 Side resistances reported for the cased areas of CIDH piles compared to design predictions (Camp <i>et al.</i> 2002, Reese <i>et al.</i> 1986).....	82
Figure 15 Comparison of case histories between design- and tested-values for the total resistance (Dapp <i>et al.</i> 2002, Brusey 2000, Finno <i>et al.</i> 2002, and Reese <i>et al.</i> 1985)	83
Figure 16 Average reported sediment depth vs. ultimate end-bearing from the case study by Camp <i>et al.</i> (2002)	85
Figure 17 Comparison of the ultimate settlement to the average sediment depths as reported by Camp <i>et al.</i> (2002).....	86

Figure 18	Comparison of the ultimate settlement to the end-bearing resistance as reported by Camp <i>et al.</i> (2002).....	86
Figure 19	Axial capacity effects from defects in pile located in soft clay (Petek <i>et al.</i> 2002).....	88
Figure 20	Axial capacity effects from defects in pile located in very stiff clay (Petek <i>et al.</i> 2002).....	88
Figure 21	Total axial load versus design limits (Reese <i>et al.</i> 1985).....	107
Figure 22	Total axial load versus design limits (Dapp <i>et al.</i> 2002).....	108
Figure 23	Total axial load versus design limits (Brusey <i>et al.</i> 2000).....	109
Figure 24	Total axial load versus design limits (Finno <i>et al.</i> 2002).....	110
Figure 25	Tested tip resistance versus design limits (Camp <i>et al.</i> 2002).....	111
Figure 26	Tested tip resistance versus design limits (Reese <i>et al.</i> 1985).....	112
Figure 27	Tested tip resistance versus design limits (Reese <i>et al.</i> 1985).....	113
Figure 28	Tested tip resistance versus design limits (Dapp <i>et al.</i> 2002).....	114
Figure 29	Tested side resistance versus design limits (Camp <i>et al.</i> 2002).....	115
Figure 30	Tested side resistance with casing versus design limits (Camp <i>et al.</i> 2002).....	116
Figure 31	Tested side resistance versus design limits (Dapp <i>et al.</i> 2002).....	117
Figure 32	Tested side resistance versus design limits (Littlechild <i>et al.</i> 2000).....	118
Figure 33	Tested side resistance versus design limits (Reese <i>et al.</i> 1985).....	119

LIST OF TABLES

Table 1	Case study checklist for differing methods of construction	36
Table 2	Case study summaries on construction effects on capacity	37
Table 3	Numerical test results (Camp <i>et al.</i> 2002)	40
Table 4	Design values <i>vs.</i> tested results (Camp <i>et al.</i>).....	43
Table 5	Numerical test results (Reese <i>et al.</i> 1985)	45
Table 6	Design values <i>vs.</i> tested results (Reese <i>et al.</i>).....	47
Table 7	Design values <i>vs.</i> tested results by Finno <i>et al.</i> (2002).....	50
Table 8	Numerical modeling results from PLAXIS (Petek <i>et al.</i> 2002).....	51
Table 9	Numerical modeling results on lateral capacity (Sarhan <i>et al.</i> 2002).....	52
Table 10	Case study checklist for post-grouting CIDH piles	56
Table 11	Case study summaries on post-grouting	56
Table 12	Numerical Results for Post-Grouting (Reese <i>et al.</i> 1985)	57
Table 13	Design values <i>vs.</i> tested results (Reese <i>et al.</i>)	58
Table 14	Numerical test results (Littlechild <i>et al.</i> 2000)	60
Table 15	Design values <i>vs.</i> tested results (Littlechild <i>et al.</i>)	61
Table 16	Numerical test results (Dapp & Mullins 2002).....	63
Table 17	Design values <i>vs.</i> tested results (Dapp <i>et al.</i>)	64
Table 18	Numerical test results for post-grouting (Brusey 2000)	66
Table 19	Design estimates <i>vs.</i> tested results (Brusey 2000)	69
Table 20	Case study checklist for testing procedures.....	71
Table 21	Summaries of case studies on testing methods.....	71
Table 22	Self-Compacting Concrete Case Histories	75

LIST OF SYMBOLS

A	Bearing capacity factor (Caltrans)
A_s	Surface area of the pile
A_b	Base area of the pile
B	Bearing capacity factor (Caltrans)
D	Diameter of the pile
L	Length of the pile
N	Uncorrected blow count number
N_c	Bearing capacity factor for cohesive soils
N_q	Bearing capacity factor for cohesionless soils
P_a	Atmospheric pressure (101 kPa)
q_p	Unit tip resistance
q_{pr}	Reduced unit tip resistance
q_s	Unit side resistance
Q_s	Total side resistance
Q_p	Total point resistance
Q	Total axial/bearing capacity
s_u	Undrained shear/cohesion strength
α	Side resistance reduction factor
β	Side resistance reduction factor for cohesionless soils
γ	Unit weight (lb/ft ³ or kN/m ³)
γ'	Effective unit weight (lb/ft ³ or kN/m ³)
λ	Side resistance factor for the Lambda-method
σ_v'	Vertical effective stress
σ_{vb}'	Vertical effective stress at base elevation

1 INTRODUCTION

Since the 1960's, Cast-In-Drilled-Hole (CIDH) piles have been a popular deep foundation choice. A CIDH pile is most commonly constructed by drilling or excavating a 0.9- to 4.6-meter (3-15 foot) diameter hole in the ground that can be anywhere from 4.6- to 76-meters (15-250 feet) deep, lowering a reinforcing cage into the hole and then filling the excavation with concrete. Many different names exist for this foundation, such as cast-in-place (CIP) piles, drilled shafts, caissons, and bored piles. CIDH piles are not to be confused with what the California Department of Transportation (Caltrans) calls a cast-in-steel-shell (CISS) pile, or cased pile. A CISS pile is a steel pipe that extends the full pile length and is filled with reinforced concrete; however, these piles are beyond the scope of this report.

CIDH piles provide support through upper layers of weak soil down to stronger soil layers. This concept is similar to driven piles; however, due to the fact that CIDH piles are drilled rather than driven, the load transfer behavior with the soil is different than with piles. Unique soil conditions at each individual site can cause difficulties in drilling, such as caving soils or water infiltration. Thus, innovative construction practices are essential, and therefore many different methods exist in constructing CIDH piles. Each method introduces variables that may not have been anticipated in the design process, some of which influence the capacity of the pile. Recognizing this, studies have been conducted in recent years to investigate the behavior of CIDH piles resulting from different construction methods. The results obtained from many of these studies have yet to be reflected in the general practice. In order for the design industry to progress, these advances need to be recognized on a national level.

This report provides a broad overview of construction method effects on axial capacity in order to determine where further research efforts on CIDH piles should focus. The first objective of this report is to discuss the history, the current construction and design practices, and the results from recent CIDH pile case studies by others concerning both typical methods of construction and newly developed techniques. A description of

these case studies is presented with a summary of axial capacity test results, if provided. However, it should be noted that the amount of information provided on each case study is limited in this report to details that are most pertinent to this research. Therefore, the reader is encouraged to refer to the original reference for additional information. Ultimately, this report discusses how current design practice relates to what has been shown in these case studies. For example, post-grouting the sides and tips of CIDH piles decreases displacements and increases the axial capacity by 50-200%. Thus, rather than neglecting all bearing capacity from soft bottoms or side resistance due to casing, which is a typical design procedure for Caltrans, post-grouting ensures adequate friction and tip capacity. Other differences between field results and design will also be discussed, such as the accuracy of design equations in predicting capacity. And finally, further research in areas such as self-compacting concrete and testing on large diameter CIDH piles is assessed.

2 BACKGROUND

CIDH piles have been on the rise since the early 1900s; however, there is still much to learn about them. In recent years, a significant amount of research with favorable results has posed the possibility to make changes in the current design and construction of CIDH piles. This chapter presents a background on CIDH piles, as well as an introduction to the current construction and design procedures.

2.1 History

The first recorded use of drilled deep foundations was in the 1920s, where CIDH piles were originally termed *Chicago Caissons* or *Gow Caissons* (ADSC 2002). Weaker top soils in areas such as Chicago, Cleveland, London, and San Antonio called for an alternative foundation to traditional methods. Texan engineer, Mr. Willard Simpson, Sr., recognized this and in 1925 wrote the first specification on a deep foundation site with expanding and contracting surface soils (Greer 1986). Drills were elementary at this time

and excavations were generally carried out by hand or by animals, such as relying on the power of mules to operate converted water well drills by pulling a capstan bar around a circular track. Hand excavations were carried out with Gow Caissons. These piles were constructed by driving a casing into the ground that was large enough in diameter for a person to fit inside and excavate the soil out of the middle. A smaller casing was then driven down beneath the previous casing. This process continued until the bearing stratum was reached (American Pile Driving Equipment, Inc. 2002). By the mid-1930s, contractors were beginning to use steam shovels



Figure 1 Elementary drilling set-up (ADSC 2002)

converted to power drill tables for use on deep foundation digging (ADSC 2002 and O'Neill & Reese 1999). Small auger machines began to appear shortly after WWII

(Greer 1986). As drilling rigs improved and became more efficient, CIDH piles increased in popularity. However, little was known about the performance and load transfer of these relatively new foundations, thus, designs were overly conservative. From 1965 to the 1970s, studies were conducted on skin friction and end-bearing resistance at the University of Texas Center for Highway Research with the support of other state Departments of Transportation, breaking forth to the first set of standard specifications for CIDH piles (ADSC 2002). To date, there is still much to be clarified concerning the impact of construction methods on CIDH pile performance.

2.2 Uses of CIDH piles

CIDH piles are increasingly common today, especially in bridge structures. They are used in situations where deep foundations are recommended, such as areas with weak foundation soils and/or high lateral load requirements. Although pile foundations are more common, CIDH piles are used when piling is not economically feasible. Pile foundations are steel piles that are driven into the ground and are embedded near the ground surface into what is known as a *pile cap*, a reinforced concrete footing or slab. However, there are limits to pile foundations that can make them less economically feasible than using a CIDH pile. For instance, overstressing of the concrete within the pile cap can occur under high lateral loads and in situations where scour depths (amount of erosion expected at the top of the piles) are large (Mullins *et al.* 2000). CIDH piles do not generally depend on a pile cap for integrity with the structure. Therefore, when extreme event limit states govern the design, CIDH piles may be optimal.

Soils in which CIDH piles can be constructed include soft and hard rock, soil with boulders, residual soils with little weathering, karstic foundations (soil with many cavities), caving soils beneath the water table, soft soils, and marine sites (O'Neill and Reese 1999).

CIDH piles are most commonly constructed vertically. Battered CIDH piles, or CIDH piles constructed at an angle, are rare but can provide greater lateral resistance.

However, battered CIDH piles are generally not feasible due to the sloped hole causing difficult concrete placement and the likelihood of caving. Construction dilemmas such as this are common for CIDH piles. The following Section 2.3 will elaborate on the different types of construction methods used.

2.3 Construction Methods

A solid foundation is vital to any structure, and therefore much is dependent on the success of construction. For CIDH piles, good constructability is dependent on appropriate site investigations, an experienced design engineer involved with the construction, and quality control by the inspector. The type of construction method is generally chosen by the contractor based on several factors, such as the site conditions, intended method of load transfer, and economics. If the water table is low and the soil is fairly cohesive, the contractor may opt for the dry method, otherwise, casing or slurry is used. This section focuses on the methods of CIDH pile construction and the potential influence on capacity.

2.3.1 Dry Method

The dry method is employed in soils that will not cave in during and after drilling. Soils of this nature include stiff clays, soft and hard rock, and some sands with cohesive material (O'Neill and Reese 1999). The dry method is acceptable if the ratio of overburden stress to the undrained shear strength of the soil is less than or equal to six (Lukas and Baker 1978). If the ratio exceeds this value, the hole is likely to collapse and slurry or casing should be considered instead.

Construction using the dry method has the least affect on pile capacity. As will be discussed in the following sections, the amount of error involved with excavation increases when more materials, such as casing and slurry, must be introduced to the hole. Therefore, when possible, the dry method is the optimal method for construction, however, wet ground conditions generally prevent this.

2.3.2 Casing Method

When drilling will take place in both self-restraining soils and soils prone to caving, the casing method may be used. Casing is generally a steel pipe pile, as shown in Figure 2, with an outer diameter six inches greater than the required diameter of the hole (O'Neill and Reese 1999, Caltrans 1997). Casing is placed in the layer that is likely to



Figure 2 Pile casing (Goodman *et al.* 2002)

collapse or slough, and the remainder of the excavation can be carried out as with the dry method. The casing used may be permanent or temporary, however, since casing can significantly reduce skin friction, it is optimal to remove it when feasible and provide grouting. If the casing cannot be removed, grouting around the outside of the casing

will aid in retrieving some of the side resistance (e.g. Reese *et al.* 1985, Littlechild 2000). Other tests have shown that even when casing is removed there still may be a slight drop in side resistance. This drop in resistance could be attributed to the smoothing of the sides of the borehole, which reduces the friction at the soil-concrete interface (e.g. Camp *et al.* 2002). Typical design procedures by Caltrans discount any side resistance in cased areas (Caltrans 1997 and correspondence, August 2003).

Surface casing is used when the site contains weaker top soils, underwater conditions, and artesian conditions. Surface casing extends above the soil or water surface to provide a guide for the drill, ensure safety precaution for workers, and prevent debris from falling in the hole. Since casing has been shown to reduce skin friction, the soils surrounding the pile will have less effect of downdrag when shrinking or uplift when expanding. The casing method should not be used if the pile is designed to resist loads by skin friction, which may be reduced up to 90% with casing (e.g. Camp *et al.*

2000, O'Neill and Reese 1999). In this event, the wet (slurry) method is another construction choice.

2.3.3 Slurry Method

An alternative to the casing method is the slurry method. When excavations or caving soils are below the water table or too deep for drilling casing, the slurry method may be used. Due to advances in drilling machines and improved slurry mixes, the slurry method for CIDH pile construction has become increasingly popular in recent years (Caltrans 1997 and O'Neill and Reese 1999). Slurry is introduced into the excavation when the soil of concern is reached. The slurry must be contained at a level about 5-feet above the piezometric surface to maintain a pressure great enough to prevent groundwater from flushing into the excavation and collapsing the borehole. Slurries can consist of just water, but are generally composed of a bentonite and potable water mixture, termed *mineral slurry*; or a mixture of polymers and water, a *polymer slurry*. The polymer slurry is a recent advance that is becoming more common due to its higher environmental compatibility and easy re-usability over the bentonite (O'Neill and Reese 1999).

The impact of slurry on the capacity of CIDH piles depends on the type of slurry used and the amount of time it is left in the borehole. Slurry is removed from the excavation with the raising concrete column. If mineral slurries remain in the hole too long the filter cake can become very thick, which can be difficult to remove with the raising concrete. The thicker the filter cake, the more likely slurry will be trapped around the sides of the borehole or within the concrete. Slurry trapped around the sides of the CIDH pile may reduce the side resistance, and slurry within the concrete will cause weak spots or poor concrete quality. For this reason, Caltrans specifies that the filter cake (from either a mineral or polymer slurry) must be removed prior to pouring the concrete if it exceeds a certain thickness. Removal of excessive filter cake build-up can be done by circulating the slurry.

In summary of the different types of typical construction methods, the dry, casing, and slurry methods are most common. The dry method, as long as the hole is stable, has little influence on the capacity. As will be shown in Chapter 4, the casing and the slurry method have been analyzed and tested as to their impact on the axial capacity. Casing and slurry are the two materials talked about so far in the construction of CIDH piles. However, many other materials are also involved in CIDH pile construction.

2.4 Materials

The key materials used in the construction of CIDH piles are drill types, slurries, and concrete. The type of drill rig used on a project will depend on the soil conditions anticipated. Soil conditions also govern the type of slurry mix used because each mix reacts differently to different soils. The type of concrete mix used is dependent on the required design strength of the CIDH pile and the desired flow characteristics. Many different mixes exist in the market for slurries and concrete. Slurries range from freshwater to many different patented mixes and admixtures. Concrete mixes for CIDH piles are generally termed *cocktails* due to the extent of admixtures used.

2.4.1 Drilling Equipment

The most common type of drill is the drilling auger, which is shown in Figure 3 and Figure 4. For short lengths, the continuous flight auger is used. This auger has flight lengths longer than the hole to be drilled and is driven by a power unit at the top that spirals the auger into the ground. As the drilling auger advances, the soil is spun upward through the flights out the top of the hole, which then must be shoveled away. For deeper drilling, a 5- to 8-foot auger is attached to a rod called a *Kelly Bar*, which lowers the auger to the desired drilling depth. After the auger



Figure 3 Rock auger (Goodman *et al.* 2002)

has advanced its full length into the soil, the auger must be removed so that the soil cuttings can be cleaned off for further drilling (Caltrans 1997).

Drilling buckets are used when augers are not able to effectively remove the soil, such as with cohesionless soils. The buckets are equipped with cutting teeth on the bottom so that when the bucket is rotated into the ground the teeth cut through the material and the cuttings are forced into the bucket.



Figure 4 Drilling auger (Stewart *et al.* 2001)

When full, the soil is contained by rotating the bucket in the opposite direction of the drilling rotation, thus closing sliding flaps on the bottom. The bucket can then be raised to discard the excavated soil. Cleanout buckets work in the same fashion, but are used to clean out extra drill cuttings at the bottom of the hole, and to flatten the base surface (Caltrans 1997). Another method to clean out the bottom of a drill hole is to use a U-tube pressure washing system (Lin 2000).

When rock formations and cobbles are encountered core barrels may be used (see Figure 5). These barrels have teeth on the ends that core through the rock. The broken up material may then be removed by a variety of methods (Caltrans 1997).



Figure 5 Core barrel (Goodman *et al.* 2002)

2.4.2 Slurry Mixes

The three main types of slurry mixes are plain water, mineral, and polymer. Water may be used in rock formations; however, the use of water in most excavations is uncommon due to its tendency to erode the soil. Therefore, this section will focus on mineral and polymer slurries.

Bentonite slurry, also referred to as mineral slurry since bentonite is a type of clay, is made by hydrating the bentonite powder for several hours with water. Upon mixing, the hydrated bentonite-water mixture turns into a gel-like substance. This gel is composed of plate-like particles that penetrate into the outer surfaces of the borehole creating a seal, or a *mudcake*, around the borehole. Due to the thickness of mineral slurries, any particles that fall into the hole during drilling are caught in the fluid and held in suspension rather than accumulating at the bottom of the hole. This aids in bottom cleanliness since most materials are extracted along with the removal of the slurry. Removal of bentonite must be well-contained due to its potential to contaminate surrounding soils if disposed of improperly. Since bentonite takes several hours to prepare and must be contained upon removal, it is advantageous to re-use mixes by filtering out any additional materials that have collected during the drilling process (O'Neill and Reese 1999). Mineral slurry should also be carefully monitored during the drilling process. The pH, viscosity, density, and sand content are all required tests by Caltrans (Caltrans 1997).

Although bentonite slurries have been the most commonly used slurry since the 1960s, polymer slurries are now replacing the bentonite. States that enforce high environmental protection standards, such as California, have stringent policies regarding the use of bentonite slurries due to environmental concerns. Therefore polymer slurries have been on the rise. Polymers must be mixed with potable water and, unlike the bentonite, do not have to hydrate. Polymer slurry mixes are composed of long, chain-like molecules that bond to the soil around the borehole surface, creating a seal. The hydrocarbon polymer chains do not create a mudcake around the surface, but rather infiltrate the soil and depending on the soil density will create a build-up around the

surface called a *gelcake*. The soil density will determine the thickness of the gelcake. A looser soil allows greater infiltration, thus more particles build up around the borehole wall in order to penetrate the soil, and a thicker gelcake forms. A dense soil will not allow for as much infiltration, thus only a thin gelcake results. Since polymer slurries have a density that is almost equivalent to that of water it is important to keep the slurry level at least five feet above the piezometric surface.

Polymer slurries do not create a gel-like substance, unlike mineral slurries, therefore particles are not held in suspension. The excavated materials remaining in the borehole must be removed by other clean-out methods (O'Neill and Reese 1999). However, due to the fact that particles do not remain in suspension, polymer slurries are easier to re-use. Polymers are also advantageous in the fact that they are not as harmful to the environment, so disposal is more cost effective.

There are two different types of polymer mixes, natural and synthetic. Natural polymers are biodegradable and consist of starches, gums, and cellulose, to name a few. Although there are advantages to natural polymers, such as having the unique ability of remaining stable in acidic environments, they are not commonly used because they are expensive and difficult to recycle. Synthetic polymers are the most common in practice and are composed of hydrocarbons which create long, hair-like strands. Synthetic polymers have negative charges (hydrolyzed zones) that repel other particles and cause them to remain in suspension in water. However, the polymers are only partially hydrolyzed so as not to repel the soil at the sides of the CIDH pile walls where bonding is supposed to occur. Caution must be taken if synthetic polymers are exposed to hard water because the chains will clump together causing the slurry to be ineffective. The polymer mix should always be monitored by checking the pH.

Both polymer and mineral slurries must be monitored by checking the pH, density, sand content, and the viscosity. If the properties of the slurry are inadequate, chemical admixtures can be added to obtain the desired levels. Admixtures are not just unique to

slurries, as will be discussed in the next section, concrete is another mix used in CIDH pile construction that utilizes many additives.

2.4.3 Concrete Mixes

The desired behavior of concrete for CIDH pile construction is high workability, ability to easily flow through the reinforcing cage, resistance to segregation, and the ability to compact under its own weight (O'Neill and Reese 1999). The most common type of cement used in CIDH piles is normal weight Type I or Type II concrete. Typical concrete characteristics are slumps in the range of 240- to 255-mm (9.5-10 in.) and 28-day strengths of 24.1-27.6 MPa (3500-4000 psi).

Concrete mixes are generally composed of many different admixtures, the mix known as a *cocktail*. Cocktails are often specified to combine desired effects such as increasing the workability of the concrete, delaying the set time, and increasing the concrete strength, to name a few. The most common type of admixtures is pozzolans, such as fly ash and silica fume. These are used to increase the set time and improve the durability and the strength of the concrete. Increased set time is desired so that the contractor has enough time to pour the concrete and remove any casing before the concrete begins to gain significant strength. Retarders may also be used to delay set time of the concrete, however, if used in excess the concrete may take too long to set and will lose strength. Another type of admixture used in CIDH piles is expansive concrete. This type of admixture causes the concrete to expand, rather than shrink, upon hardening. The downfall to expansive admixtures is that they have the tendency to set too quickly. However, they are beneficial in CIDH pile construction because the expanding action compacts into the soil and improves the soil-concrete frictional interface.

Due to the tight spiral reinforcement spacing requirements of CIDH piles, segregation of concrete during placement poses a concern. With so many different admixtures that are desired for CIDH pile construction, another challenge is achieving a mix design with the desired properties. Therefore, a product called self-compacting

concrete (SCC) is rising in the industry as an alternative to traditional concrete mixes. SCC is much more fluid than regular concrete and is qualitatively measured by a spread test rather than a slump cone. Due to the fluid-like behavior of SCC, the concrete readily flows between tight spacing, such as spiral reinforcement, and does not require additional consolidation by vibration (Ferraris *et al.* 2000). This product was first researched by Okamura in 1986, and by 1988 the first test batch was implemented. SCC was originally termed *high performance concrete* by Okamura and Maekawa (Ouchi 1998), but this name was also introduced at the same time by Aitcin *et al.* 1989 to describe concrete with high durability due to a low water-cement ratio. Therefore, the name was changed to *self-compacting concrete*.

SCC is relatively new in the United States, and to date, SCC has not been employed much for the use in CIDH pile construction. However, its performance in building construction has been successful in satisfactorily filling complicated formwork and flowing through congested reinforcement. The success of this concrete in other projects, mainly in other countries, shows potential for advancing in CIDH pile construction.

This chapter has covered most of the topics related to the construction of CIDH piles; however, the reasons certain construction methods are employed are due to the intended design of the CIDH pile.

2.5 Design

Results obtained from many recent studies have yet to be considered in much of the current design practice. This section focuses on current CIDH pile design procedures, namely with the California Department of Transportation (Caltrans), and which areas have yet to reflect up-to-date research.

CIDH piles are mainly designed to withstand axial and lateral loads. Axial load is resisted by either the bearing capacity at the base, side resistance (skin friction), or both. Lateral loads are resisted by reinforcement within the pile, and to some degree, the soil

resistance. Skin friction can contribute significantly to the overall pile resistance; however, studies have shown that when casing is used the amount of side resistance is reduced (e.g. Bennet *et al.* 1996, O'Neill *et al.* 1999, Camp *et al.* 2000). This is discussed in greater detail in Chapter 4. Lateral resistance can be reduced due to pile defects (e.g. Petek *et al.* 2002, Sarhan *et al.* 2002). This is also discussed in greater detail in Section 4.3.

The design length of CIDH piles is dependent on the soils encountered and the anticipated loads. In-situ soil properties and the water table position play a key role in the design length of CIDH piles, as well as the required geometry and reinforcement design to resist lateral, axial, and torsional loads. As the depth of the pile increases, the design diameter will generally increase in order to keep the length to diameter ratio below thirty, as recommended in the FHWA guidelines (O'Neill and Reese 1999).

The design procedure may follow the Allowable Stress Design (ASD) or Working Stress Design (WSD) method, or the Load and Resistance Factor Design (LRFD). The latter now being the standard in the 1994 AASHTO Specifications for Highways and Bridges. Some state agencies, such as the California Department of Transportation (Caltrans), have their own set of standard specifications that may contain one or both methods of design. These methods are explained in more detail in Chapter 3.

2.6 Construction Specifications

Due to the high variability involved in the construction of CIDH piles, explicit yet flexible specifications are necessary. Specifications should include controls for an installation plan, acceptable tolerances, and expected project documentation (O'Neill and Reese 1999). In order to write appropriate specifications, it is helpful if the designer is able to adequately forecast the type of construction method to be used. Programs are being developed, such as DS² (Fisher *et al.* 1995), to aid designers in forecasting a likely construction method. This program uses a compilation of systems that contain information of past projects and contractor experience to formulate cost estimates,

construction methods, and site conditions that are likely to be encountered. Although the designer generally does not specify the type of construction method anticipated, it will have been considered and accounted for in the design process.

Specifications should also include drilling slurry tolerances and/or acceptable casing conditions. It is important to monitor the drilling slurry properties at various depths in the hole in order to know how much settlement has occurred and how much soil material is in the hole. If one location reports an extremely high amount of soil, this could indicate a cave-in, in which case immediate action would need to take place to remedy the problem.

Evidence of reinforced concrete failures during earthquakes show that past designs inadequately confined the concrete. Therefore, increased lateral reinforcement, such as spirals or hoops, are now specified in columns and CIDH piles. CIDH piles generally have spiral reinforcement, and under current codes the pitch (spacing between spirals) is specified around 76-152 mm (3-6 inches). Although this aids in containing the concrete, it also inhibits concrete flow. This can cause segregation of the concrete between the inner core and the area outside of the reinforcing cage, which can reduce the capacity of the CIDH pile. Recognizing this, Caltrans specifies a minimum of 127 mm (5 in.) for spiral pitch. Other defects that can occur within the pile are discussed in Chapter 4.

Caltrans has explicit specifications on the placement of CIDH piles with the slurry method. This is due to the fact that visual inspection is not possible when constructing with drilling slurry. First, a plan of installation must be submitted by the Contractor and approved by the Engineer. The Contractor must also test a concrete mix design prior to placement to prove it meets specifications in fluidity and penetration. Testing procedures must be specified and occur at regular intervals at the midpoint and bottom of the pile for the drilling slurry. Concrete placement is crucial, and must be done within a two-hour period.

The code by Caltrans seems to adequately cover construction specifications during the construction process; however, there are little recommendations in these codes for remediation. Methods such as post-grouting have been shown in multiple studies to increase the capacity of piles that had soft bottoms, or reduced side friction due to casing, which will be discussed more in Chapter 4. Removal of casing also has potential of creating defects in the pile, such as necking, smoothing the walls of the pile, or the casing cannot be removed, to name a few. All of these problems can be remedied by post-grouting. Use of SCC would also aid in alleviating these problems because the concrete flows easier as the casing is removed.

A general outline of information has been provided in this chapter regarding the history, design, and construction of CIDH piles. The following chapters provide more detail on CIDH pile behavior, the current design methods, and the current research for CIDH piles.

3 CIDH PILE BEHAVIOR AND DESIGN

The behavioral response of CIDH piles to axial loading is resistance in shear along the sides of the pile and bearing at the tip. Therefore, the axial design of the pile is based on the strength of the soil. Conversely, reinforcement design in a CIDH pile is to resist lateral loads. The way in which a CIDH pile is constructed will affect both lateral and axial response. Although lateral, or flexural, design is considered in the following chapters, the main focus is on axial design. This chapter describes CIDH pile resistance, how resistance is computed in design, and how innovative construction methods can optimize CIDH pile behavior.

3.1 Side Resistance

Side resistance, which includes shear friction and adhesion, is typically the first type of resistance mobilized in response to axial loading. As the pile is loaded axially and tries to displace downward, the side resistance at the pile-to-soil interface is activated. Thus, side resistance is employed under small displacements.

Side resistance occurs in both cohesive and cohesionless materials and can be calculated by a variety of methods. Cohesive materials are those which contain more than 50% fines, such as clays or silts. Soils that contain more than 30% fines will behave like a cohesive material, but are not defined as such. Cohesionless soils, also known as sands, gravel, and non-plastic silts contain particles that are large enough that they do not stick together, or have cohesive qualities.

In order to estimate the side resistance of a CIDH pile, certain site data must be obtained, such as the undrained shear strengths, the unit weights, and the position of the groundwater table. Much uncertainty is still involved in estimating the side resistance of CIDH piles due to the fact that different drilling methods will have different influences on the state of the soil around the sides of the borehole. Therefore, the value of the side resistance varies with the soil and the construction method, for example, the use of casing

will result in lower side resistance than if the dry or slurry method is employed. Empirical factors are therefore multiplied into design equations to account for the variability in side resistance. However, the factors or equations chosen for design are at the discretion of the designer or chosen code, so design values will vary by practice. The most common methods for calculating the side resistance are the α - and β -methods. Typically, the alpha-method is used to find the side resistance in clays and the beta-method is used for sands. However, some beta-methods are given for any soil in general.

3.1.1 Alpha-Method (α -Method) for Cohesive Soils

The α -method is used to calculate the side resistance in cohesive soils. The unit side resistance, or undrained cohesion, of the cohesive soil, s_u , is multiplied by an empirical adhesion factor, α , obtained from empirical charts based on the undrained cohesion. Kulhawy and Jackson (1989) give alpha values that range from 1.0 for soft clay to 0.30 for very stiff clays as shown in Figure 6, based on a range of test results.

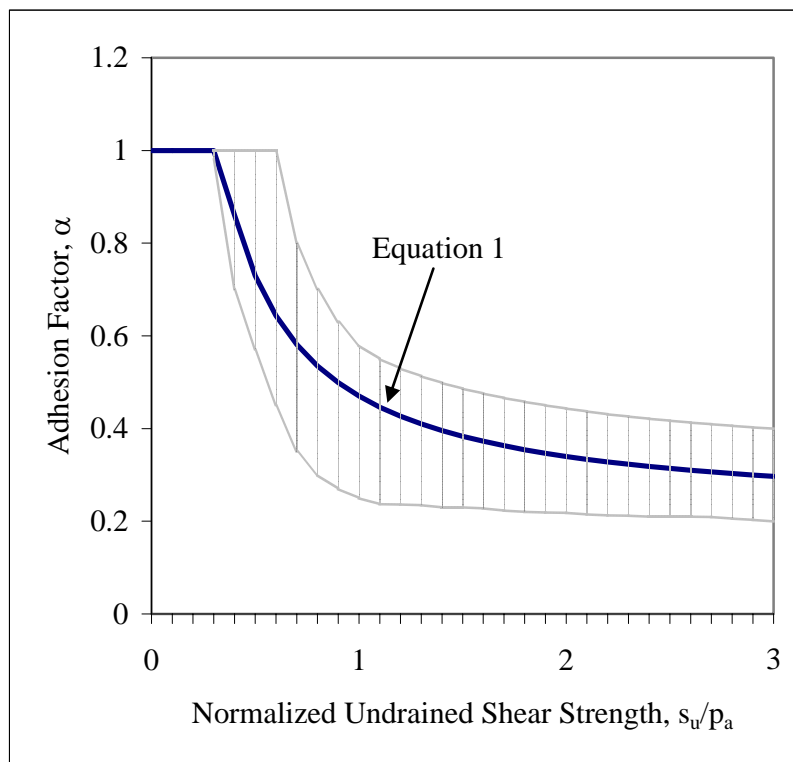


Figure 6 Variation of α with c_u/p_a based on tested results by Kulhawy and Jackson (1989)

Equation 1 is derived from the best-fit curve of tested alpha-values shown in Figure 6. Alpha is based on the undrained shear strength, s_u , and atmospheric pressure, p_a . The maximum value of alpha is limited to 1.0 ($\alpha \leq 1.0$).

$$\alpha = 0.21 + 0.26 * (p_a / s_u) \quad \text{Equation 1}$$

O'Neill and Reese (1999) recommend the use of an average alpha value of 0.55, except in the top 1.5 m (5 ft) of the CIDH pile and the bottom one-diameter length, where alpha is zero. Caltrans also follows this procedure if the dry or slurry method of construction is expected. However, if the use of casing is anticipated, the side resistance over the length of the casing will be discounted.

The total side resistance, Q_s , is equal to the total surface area in contact with the pile within each layer multiplied by its undrained shear strength, s_{ui} , and the pertaining alpha factor, α_i .

$$Q_s = (\pi * D) * \sum (\alpha_{(i)} * s_{u(i)} * L_{(i)}) \quad \text{Equation 2}$$

In Equation 2, D is the diameter of the pile and L_i is the thickness of the soil layer. Caltrans limits the value of unit side resistance in clays to 263 kilopascals [kPa] (2.75 tons/ft² [tsf]) for use in design.

Note that the alpha value plays a significant role in Equation 2 in that it reduces the resistance to almost half. As stated previously, studies have shown that alpha varies widely from a value of 1.0, recognizing the full cohesive strength of the material, down to almost a quarter of the cohesive strength. This wide range is due to the uncertainty in achieving adequate side resistance due to unexpected field conditions, such as differing construction practices and inadequate bond between the concrete and the soil. As will be discussed in Chapter 4, if the side resistance can be better assured in the field, design

values for capacity can be increased, thus reducing the geometry of the pile and creating more economic designs.

3.1.2 Beta-Method (β -Method) for Cohesionless Soils

Side resistance in sands is found using the beta-method. The method by Das (1999) is based on the at-rest earth pressure coefficient, K_o , the average effective vertical stress found at the midpoint of the soil layer, σ_{vi}' , and the friction angle, ϕ . The total side resistance in cohesionless soils is found by the following Equation 3, where the effective stress, σ_{vi}' , is multiplied by its pertaining empirical beta factor, β , given in Equation 4, and the depth of the soil layer, D . The summation of this product from each layer multiplied by the perimeter length gives the total side resistance, Q_s .

$$Q_s = \pi * D * \sum_{Li} (\beta_i * \sigma_{vi}') * \quad \text{Equation 3}$$

$$\beta = K_o * \tan \phi \quad \text{Equation 4}$$

$$K_o = 1 - \sin \phi \quad \text{Equation 5}$$

The beta-method given in O'Neill and Reese (1999) is the method most commonly used in practice. They give the following equations for finding the unit side resistance, q_s (kPa) and β , where β_i is the beta factor for the pertaining layer.

$$q_s = \beta_i * \sigma_{vi}' \quad \text{Equation 6}$$

The beta factor is a dimensionless correlation factor between the vertical effective stress, σ_{vi}' , found at the midpoint of the soil layer, and the unit side resistance, q_s . Beta is limited to a minimum of 0.25 and a maximum value of 1.20 ($0.25 \leq \beta_i \leq 1.20$) and q_s must not exceed 200 kPa (2.1 tsf) (O'Neill and Reese 1999 and Caltrans 2000).

For sands with an N-value greater than or equal to 15 ($N \geq 15$), β_i is found by the metric equation below, where N is the average SPT blow count for the soil layer, and z_i is the vertical distance from the ground surface to the middle of the soil layer, in meters.

$$\beta_i = 1.5 - 0.245 * [z_i]^{0.5} \quad \text{Equation 7}$$

If the N-value is less than 15 ($N < 15$) then the dimensionless correlation factor is scaled by a ratio of the N-value.

$$\beta_i = [N/15] * \{ 1.5 - 0.245*[z_i]^{0.5} \} \quad \text{Equation 8}$$

For gravelly sands or gravels with an N-value greater than 15, O'Neill and Reese (1999) provide the following Equation 9. However, if the N-value is less than 15, β is scaled accordingly as shown with Equation 10.

$$\beta_i = 2.0 - 0.15 * [z_i]^{0.75} \quad \text{Equation 9}$$

$$\beta_i = [N / 15]*\{1.5 - 0.245*[z_i]^{0.5}\} \quad \text{Equation 10}$$

Soil that exceeds a blow count of 50 is an *intermediate geomaterial* (IGM). The following equations apply for the side resistance of IGMs in cohesionless soils.

$$q_s = \sigma_{vi}' * K_{oi} * \tan \phi_i' \quad \text{Equation 11}$$

$$\phi_i' = \tan^{-1} * \{ [N_i / (12.3 + 20.3 * (\sigma_{vi}'/p_a))]^{0.34} \} \quad \text{Equation 12}$$

$$K_{oi} = (1 - \sin \phi_i') * [0.2 * p_a * N_i / \sigma_{vi}']^{\sin \phi_i'} \quad \text{Equation 13}$$

The blow count value, N, should be limited to 100, even if tests give a higher value. The angle of internal friction, ϕ_i' , pertains to the layer of consideration, and K_{oi} is the at-

rest earth pressure coefficient in that layer. The vertical effective stress, σ_{vi}' , is found at the midpoint of the layer.

Caltrans uses Equation 6 to find q_s and the equation for β_i similar to Equation 9 except in English units, where β_i is also limited between the values of 0.25 and 1.20 ($0.25 \leq \beta_i \leq 1.20$) and q_s must not exceed 200 kPa (2.1 tsf).

$$\beta_i = 1.5 - 0.135 * [z_i]^{0.5} \quad [\text{Caltrans, English}] \quad \text{Equation 14}$$

Due to the nature of soils, and the high amount of variability involved in trying to accurately predict soil properties, it should be noted that the equations given for side resistance, and tip resistance in the following section, are meant to give a *rough* estimate of the resistance, they should not be taken as exact predictions.

3.2 Bearing (Tip) Resistance

Tip or bearing resistance is the resistance given by the base of the pile. In order to calculate the bearing resistance of a CIDH pile, the properties at the tip of the pile must be known, such as the undrained shear strength of a cohesive material or the SPT blow count, N , for a cohesionless soil. These properties are then multiplied by an empirical bearing capacity factor and the cross-sectional area of the tip to obtain the bearing resistance. Although the tip resistance is less complex to calculate than the side resistance, it still inherits uncertainty due to construction procedures. Several methods are employed for the use of calculating the bearing capacity. Some examples are given in the following sections as presented by Das (1999) and O'Neill and Reese (1999).

3.2.1 Tip Resistance in Cohesive Soils

Bearing resistance in cohesive soils are based on the undrained cohesive strength of the soil, s_u , multiplied by a bearing capacity factor for cohesive soils, N_c , and the area of

the base, A_b . The numerical value of N_c is based on the depth-to-width ratio of the foundation and must be less than or equal to 9 ($N_c \leq 9$). If the depth to width ratio is greater than 4, which is generally the case with CIDH piles, then $N_c = 9$. Therefore, for simplicity, the bearing resistance equation for CIDH piles in clays can usually be reduced to $q_p = 9 * s_u$, as long as the undrained cohesion strength, s_u , is greater than 96 kPa.

$$Q_p = N_c * s_u * A_b \quad \text{Equation 15}$$

$$N_c = 6 * [1 + 0.2 * (L/D)] \quad \text{Equation 16}$$

According to past research, CIDH piles must displace an amount on the order of 10-20% of the diameter of the pile in order to obtain an N_c value of 9 in the field (O'Neill and Reese, 1999). This is relatively large considering some codes limit settlement to one-half inch. However, if this resistance cannot be attained without large displacements, it may be discounted in design. Therefore, as will be discussed further in Chapter 4, it would be of great benefit to ensure that the tip resistance can contribute to resistance under the same displacements required to activate the side resistance. This can be accomplished by post-grouting the bottom of the pile. Rather than changing the geometry of the pile to obtain greater surface area for increasing the side resistance, post grouting may be more cost effective so that the tip resistance can contribute to the overall capacity and reduce the amount of side resistance required.

Since excessive settlement can be an issue with CIDH piles, O'Neill and Reese recommend the above equation when displacements are limited to a maximum of one inch. The equations given above are based on the length-to-diameter ratio, L/D , since as the diameter of the pile increases, so do the displacements. Caltrans follows the same procedure as O'Neill and Reese (1999), except the maximum value of unit end bearing, Q_p/A_b , is limited to 3830 kPa (40 tsf) and displacements are limited to 12.7 mm (0.5 inches) under service loads. Ultimate displacements used to be limited to a maximum of 12.7 mm (0.5-inches); however, this requirement has eased up as long as the pile can reach the ultimate capacity (Caltrans correspondence 2003).

If settlement is unaccounted for, O'Neill and Reese (1999) also provide an equation similar to the original Q_p Equation 15 given above, except that the value, N_c , is replaced by N_c^* , which varies with the undrained cohesion rather than with the geometry of the pile. N_c^* varies from 6.5 for an undrained cohesive strength of 24 kPa (500 psf), 8.0 for $s_u = 48$ kPa, and 9.0 for $s_u \geq 96$ kPa (2000 psf). This equation is also related to the rigidity index of the soil, I_r , which is equal to the Young's soil modulus divided by three times the undrained cohesion.

$$q_{pr} \text{ [kPa]} = (4/3) * [\ln (I_r + 1)] * s_u = N_c^* * s_u \quad \text{Equation 17}$$

$$I_r = E_s / (3 * s_u) \quad \text{Equation 18}$$

Caltrans has a slightly different equation for a reduced tip resistance when the pile diameter is greater than 6.25 feet and settlements will not be accounted for in design. However, typical design methods at Caltrans follow the FHWA procedure (correspondence August 2003).

$$q_{pr} \text{ [ksf]} = \{ 2.5 / [(a * B_t)/12 + (2.5 * b)] \} * q_p \quad \text{Equation 19}$$

$$a = 0.0071 + 0.0021 * (L/D) \quad \text{Equation 20}$$

$$b = 0.45 * (s_u)^{0.5} \quad \text{Equation 21}$$

Where Equation 20 must be less than 0.015 ($a \leq 0.015$) and Equation 21 cannot be less than 0.5 but must also not exceed 0.015 ($0.5 \leq b \leq 0.015$). The reduced tip resistance, q_{pr} , has the same limit as the normal tip resistance, q_p , of 3830 kPa (40 tons/ft²).

3.2.2 Tip Resistance in Cohesionless Soils

When designing for cohesionless soil conditions under the axial loading of a CIDH pile, soil investigations must determine what the density of the soil is, usually by a standard penetration test (SPT). The load-bearing capacity is then calculated based on the SPT blow count, N . Blow counts are the number of times it takes for a dropped hammer to penetrate one foot into the soil, which directly relates to the bearing resistance. However, since the CIDH pile is a stationary object that bears on the soil in a less dynamic manner than a dropped hammer, the blow count value can be increased by a specified amount to obtain the estimated bearing capacity. According to Caltrans, soil is considered to be *competent* when the N -value is greater than or equal to 20 for upper layers, and 30 for lower layers. This means that the soil is adequate enough to withstand axial loads without remediation of the soil. Soil is considered *poor* when the N -value is less than 10, and the soil is too weak to withstand axial loading. When the value is between 10 and 20, the soil is classified as *marginal*, and additional investigation is recommended (Caltrans 1997).

According to O'Neill and Reese (1999), the soil is classified as *cohesionless* when the blow count is less than or equal to 50, and the tip resistance can be found by Equation 22 and Equation 23. If greater than 50, the material is an IGM.

$$q_p = 0.60 * N \text{ (tsf)} \qquad \text{Equation 22}$$

$$q_p = 57.5 * N \text{ (kPa)} \qquad \text{Equation 23}$$

This procedure is fairly simple in application and thus should be used as an estimate of the tip resistance and not taken an exact value. Caltrans uses this equation for cohesionless soils with N -values less than 75, and q_p is limited to a maximum value of 3830 kPa (40 tsf).

For IGMs the following Equation 24 is recommended by O'Neill and Reese (1999). Other equations for reduced base resistance for IGMs can be found in the 1999 FHWA Manual for Drilled Shafts.

$$q_p = 0.59 * [N * (p_a / \sigma_{vb}')]^{0.8} * \sigma_{vb}' \text{ (kPa)} \quad \text{Equation 24}$$

As with the side resistance IGM equation, N should be limited to 100. The atmospheric pressure, p_a , in the SI system is 101 kPa, and the vertical effective stress, σ_{vb}' , is the value calculated at the elevation at the base of the pile, in kilopascals (O'Neill and Reese 1999).

Similar to calculating the bearing capacity in clays, displacement limits may also be taken into account when calculating the bearing resistance in sands. Das (1998) recommends reducing the above equation to q_{pr} when the pile diameter, D, exceeds 50 inches. Caltrans also uses this reduction Equation 25.

$$q_{pr} = [50 / D \text{ (in.)}] * q_p \quad \text{Equation 25}$$

The tip resistance may also be calculated using the effective stress at the base of the pile multiplied by a bearing capacity factor, N_q , which is difficult to obtain in the case of CIDH piles because the original N_q factors were based on piles, which are driven, and CIDH piles are not. Therefore, N_q values are lower than what is used in calculations for bearing capacities of piles. Several researchers have provided values for N_q for CIDH piles; however, these values tend to vary by a great amount, so experience and good engineering judgment must be utilized. The weight of the CIDH pile is subtracted out of this equation by assuming that the CIDH pile weight is approximately equal to the soil it has replaced.

$$Q_{p(\text{net})} = A_b * \sigma_{vb}' * (N_q - 1) \quad \text{Equation 26}$$

Values for N_q can be found in tables provided in textbooks under methods for Vesic, Meyerhof, and Terzaghi, to name a few (e.g. Das 1999).

In general, tip capacity is mobilized at displacements that far exceed the displacements required to activate side resistance (Osterberg 2000). This can be attributed to the construction of the pile. Disturbed or loose soil at the tip of the pile, due to excavation or drilling fluid deposits, must compact before it will provide resistance. This requires several inches of displacement. If this sediment could be compacted beforehand, this required displacement is eliminated and axial capacity can be mobilized to resist loads in unison with the side resistance (e.g. Osterberg 2000, Walter *et al.* 2000, Littlechild *et al.* 2000, Dapp *et al.* 2002, Mullins *et al.* 2000). For example, Caltrans will only recognize full tip capacity to be contributing after a displacement equal to 5% of the pile diameter has occurred, and typically, tip resistance is completely discounted due to the possibility of a soft bottom occurring. Cleanout methods, such as pressure washing with U-tubes (Lin, 2000), and post-grouting methods can aid in preventing soft bottoms. Studies concerning post-grouting have proven to be very effective in reducing displacements and increasing the axial capacity, as will be further discussed in Chapter 4.

The methods covered so far are for the axial design of CIDH piles, which does not take into account the reinforcement design. CIDH piles are also designed structurally in order to withstand flexural (lateral) and axial loads. Although lateral behavior is not the focus of this research study, a brief description of the structural design of CIDH piles is warranted in order to provide an overall outlook of CIDH pile behavior.

3.3 Structural Design (Axial and Lateral Resistance)

The structural design of CIDH piles is typically based on p-y curve data. P-y curves model the soil as a set of springs, varying in stiffness, that are attached to the pile, thus accounting for the soil resisting lateral loads in conjunction with the pile resistance. Axial and bending moments are plotted on an interaction diagram that is computed using a computer program such as LPILE or COM624, and the reinforcement is designed accordingly (O'Neill and Reese 1999).

The length of a CIDH pile is generally not based on structural requirements, but rather on the amount of surface area required to obtain the desired amount of axial resistance. Therefore, there is a depth at which the lateral loading applied at the top of the pile is no longer felt. This point occurs at the *depth to fixity* from the top of the pile. According to Caltrans, this length is typically taken as 10 to 15 times the diameter (Caltrans correspondence, 2003). Therefore, the upper portion of the pile is designed for lateral loading, and the required reinforcement generally extends the length of the pile, for ease of construction.

Some design methods choose to ignore the soil contribution on a preliminary basis, and then re-check the design based on p-y curve data for the design of the top portion of the pile. This is conservative, and recognizing this, O'Neill and Reese (1999) indicate that further research is needed. The amount of reinforcement could be decreased outside of the critical region of the upper portion of the pile; however, for shorter piles it is generally easier to have a consistent reinforcing schedule throughout the length of the pile. In addition, current design methodology in AASHTO (1994) ensures a consistent spiral pitch throughout the length of the pile. Caltrans indicates in their specifications that outside of the critical region for lateral loading, the CIDH pile may be designed as an axial member (Caltrans 2000).

Currently, computer programs for p-y curves are fairly limited as to the type of soils that can be input. Therefore, further research on soil-interaction with CIDH piles and upgraded computer programs would aid in advancing CIDH pile design.

There are several methods that exist in calculating the load demand. The design procedure may follow the Allowable Stress Design (ASD) or Working Stress Design (WSD) method, or the Load and Resistance Factor Design (LRFD). The latter now being the standard in the 1994 AASHTO Specifications for Highways and Bridges. Foundation design, such as side and bearing resistance of CIDH piles, is based on the ASD method, whereas structural design, such as the lateral resistance of a CIDH pile is designed using the LRFD approach. Some state agencies, such as Caltrans, have its own set of standard

specifications that contains both methods of design. Caltrans is currently incorporating LRFD into their design practice; however, the WSD approach is still in use (Caltrans correspondence, 2003).

3.3.1 Allowable Stress Design (ASD) Method

The ASD method finds the required loading on an element or structure. The design capacity must then exceed this loading multiplied by a factor of safety. This approach is most common in calculating the axial resistance of the soil for a CIDH pile. The side resistance and the tip resistance is computed and added together. This sum is then divided by a factor of safety to obtain the allowable axial loading of the CIDH pile. If the required loading calculated in the analysis of the structure exceeds the allowable value, the CIDH pile geometry may need to be changed, or other methods, such as post-grouting may be considered to increase the side and bearing resistance. Caltrans uses the ASD for foundation applications.

Typical factors of safety in the ASD vary by state and industry. The FHWA recommends factors of safety from 2.3 to 3.5 depending on the expected control over construction of the CIDH pile. The less the control, the more the factor of safety must increase. Caltrans assigns a factor of safety of 2.0 in the design of the axial capacity, which includes both side and tip resistance, assuming that the level of quality control in the field is normal. If normal control cannot be assured, Caltrans specifies increasing the factor of safety (Caltrans, 2000).

3.3.2 Load and Resistance Factor Design (LRFD)

The LRFD approach is a rational method based on observed behavior. Each individual applied loading, such as dead or live load, is multiplied by an appropriate factor, generally greater than 1, for that specific loading. The sum of each factored load is the nominal, or ideal, loading. The structure or element is then designed to a capacity that is the nominal loading divided by a resistance factor that is less than one. Caltrans is currently incorporating the LRFD approach for most structural designs.

In high seismic areas, capacity design is the design method of choice because the method of failure is controlled by the designer. The capacity design method designs for failure modes at predetermined locations, or *plastic hinges*. The member in which a plastic hinge formation is desired under say, earthquake loading, will be designed for the LRFD ideal loading conditions, or the nominal loading divided by an appropriate resistance factor less than one. Adjoining members where failure is not to occur will be designed based on an increase to the nominal load by applying an overstrength factor. This ensures that critical members in a structure are stronger than the location where the plastic hinge is desired, therefore forcing the failure in areas that can be easily assessed and repaired.

Typically, in a CIDH pile design, the applied load is determined from the LRFD approach. The CIDH pile capacity is then designed with an additional factor of safety in order to force the plastic hinge above ground, e.g. in a column. Caltrans typically uses a factor of 1.25 for piles that are to force the plastic hinge in the column (Caltrans 1997). This is advantageous in order to easily assess and repair any damage after an earthquake.

3.4 Testing Methods

To ensure that a CIDH pile was constructed without major defects, non-destructive evaluation (NDE) procedures should be performed. Different NDE testing procedures are able to report on the soundness of concrete and possible existence of voids or flaws in the CIDH pile. The typical testing procedures that will be covered in this report include gamma-gamma logging (GGL), impulse response methods, and cross-hole sonic logging (CSL).

3.4.1 Gamma-Gamma Logging (GGL)

Caltrans currently utilizes the gamma-gamma log (GGL) method, or gamma ray scattering, to test the integrity of CIDH piles. This is done by lowering a probe through

an inspection tube in the pile, which is also known as a *downhole method*. As the probe lowers, a nuclear sensor on the probe sends out radio waves, which pass through the surrounding material and are received by a detector located on the upper portion of the probe. The number of signals received, or the scatter count, is compared to a standard count that was performed on the same concrete material. The comparison indicates the relative denseness of the material. If the concrete is sound, the scatter count will be equal to, or lower than the standard material.

Caltrans requires all CIDH piles constructed in wet conditions (e.g. under the slurry method or beneath the groundwater table) to be tested by GGL; however, there are some disadvantages to this form of testing. The GGL method is limited to a range of only 51 to 102 mm (2-4 inches) around the perimeter of the pile, which is small when considering most CIDH piles are 1 to 3 m (3 to 10 feet) in diameter and the access tubes for the nuclear probes are spaced approximately 1 m (3 ft) apart. Therefore, GGL is used as a preliminary test, and if an anomaly is detected, CSL is carried out to see how far the anomaly has extended into the core of the pile.



Figure 7 Gamma-gamma log testing (Caltrans 2002)

The nuclear probe sends out gamma radiation, which must be kept to small emissions in order to protect against harm. Another downfall to this method is that the test results are skewed by close proximity to steel, thus the tubes must be placed in specific locations around the reinforcing cage. Research on other testing methods, such as impulse response and crosshole sonic logging (CSL), and the results are presented in Chapter 4. Descriptions of these two methods are provided in the following sections.

3.4.2 Impulse Response Methods

The impulse response methods, also known as sonic echo, or impact hammer can be used to test already cast-in-place piles. A sensor is attached to the top of the pile to record the arrival of ultrasonic waves. A rubber headed hammer, or similar device, is used to impact the top of the pile, thereby sending transient, longitudinal wave motions through the concrete. When these waves reach an interface of different density or material (e.g. an anomaly, or the bottom of the pile) a wave is reflected. The sensor records when the impact at the top of the pile was made, and when the reflected signals are received. The difference in time indicates particle velocity and depth to the interface. The known depth to the base of a pile and the average time it takes for the wave to travel that distance and back to the receiver can be used to calculate the average particle velocity through the concrete. Different authors report different ranges of velocity for sound concrete, such as 3500 to 4300 meters/second (Finno *et al.* 2002). If the vibratory waves hit a defect the waves will return to the sensor prematurely, or before the expected reflection from the bottom of the pile. Using the average particle velocity, the depth to the anomaly can then be found. If the velocity versus time indicates a distance to the bottom of the pile then no defect was hit with that particular wave (Finno 2002).

Impulse response tests are fairly easy and inexpensive to set up; however, analysis of the data requires experience. The analysis of the data may not always be clear, and sometimes anomalies may be detected where there is none. The data is read by applying different numerical filtering methods to the raw data, and reading the graphical results of the filtered, smoothed data. Where the graph indicates an “abrupt” change in signal indicates a change in the pile, either in cross-section or material density. Therefore, if a more accurate, but more expensive, method is desired, cross-hole sonic logging does not require as much technicality in reading the results, and provides a better visual representation of the CIDH pile.

3.4.3 Cross-hole Sonic Logging (CSL)

Cross-hole sonic logging (CSL) is another downhole technique that is somewhat similar to the gamma ray scattering method. Probes are lowered into water-filled PVC pipe or coreholes that extend the length of the pile. The probes send and receive

ultrasonic waves that pass through the material in between. The signal strength and the velocity information of these waves are reported to a computer from the sensors to provide a type of map, giving a visual representation of different cross-sections within the pile. This method, which uses ultrasonic waves, is safer than using radio waves, and gives a detailed view of the pile within the reinforcing cage. However, CSL cannot see outside of the reinforcing cage. Since GGL only reports on the concrete around the perimeter of the pile, an effective testing strategy, as carried out by Caltrans is to use CSL in conjunction with GGL.

Tubes are placed at specific locations around the perimeter of the pile to obtain the desired cross-sections. If PVC pipe is used rather than coreholes, it is important to ensure good bond between the tube and the concrete. This can be aided by wetting the PVC pipes before pouring concrete. CSL can also report on the quality of underwater CIDH piles by hooking PVC tubes to the outer sides of the CIDH pile. Testing results on these methods and other design uncertainties are presented in Chapter 4.

This chapter has presented the current standards pertaining to the design of CIDH piles. In order to check the accuracy of these methods, research by others will be summarized and their results compared to what the design calculations given in this chapter would compute.

This page is intentionally blank.

4 CASE HISTORIES AND RESEARCH

CIDH pile research began in the 1960s, but the recent increase in popularity of these deep foundations reveal that there are still many variables in the design and construction process that have yet to be standardized. Questions still arise as to how construction methods influence the behavior of CIDH piles, such as if bottom cleanliness affects bearing capacity, or how much skin friction is reduced due to permanent and temporary casing.

This chapter presents brief descriptions and summarized results from various case studies presented by others on CIDH piles. The information provided is based on key information from each case study. However, in order to maintain the focus of this research, only the most pertaining details from each case study are included in these sections, the original references are provided for additional information. Where applicable, the design methods discussed in Chapter 3 are used to calculate a predicted design value based on the soil data given in the report. If the soil properties are provided, these values are used in the calculations. Otherwise, the applicable unit weights from Appendix B are substituted. The design values are then compared to the test results from the case study to assess the applicability of the design methods. Therefore, the effects of different construction methods are addressed, as well as the accuracy of design methods to predict the axial capacity for various situations. Trends of effects and design methods are discussed further in Chapter 5.

The ultimate goal of design is to optimize capacity, therefore, research is conducted on what influences side, bearing, and lateral resistance, as well as the largest cause of pile defects, and how pile integrity can be assured. This chapter covers some of the major research conducted to date, on CIDH pile performance due to different construction methods. CIDH pile construction studies that show potential for improvement in practice are related to effects on tip and side resistance, optimizing post-construction testing and remediation, and improved materials.

4.1 Construction Method Effects on Capacity

As construction methods and inspection improve, the consistency of successful CIDH pile construction will increase. The design equations given in Chapter 3 try to account for the uncertainty that can occur in the field, which may be over-conservative for new methods of construction. Table 1 shows the focus of each case study that will be presented in this section and Table 2 follows with a brief summary.

Table 1 Case study checklist for differing methods of construction, see Table 2 for summaries

Construction Method Case Studies			References for Sections 4.1.1 - 4.1.5				
			<i>Camp et al. 2002</i>	<i>Finno et al. 2002</i>	<i>Reese et al. 1985</i>	<i>Petek et al. 2002</i>	<i>Sarhan et al. 2002</i>
Construction Method:	Dry		X			X	X
	Slurry		X		X		
	Casing	Temporary	X	X	X	X	X
		Permanent	X		X		
	Planned Anomalies			X		X	X
Soil Type:	Cohesive		X	X	X	X	X
	Cohesionless				X		
Reported on:	Axial Capacity	Tip	X	X	X	X	
		Side	X	X	X	X	
	Lateral Capacity						X
	Bottom Cleanliness		X				
	Settlement		X				

Table 2 Case study summaries on construction effects on capacity

Test Reference	Description	Results
Camp <i>et al.</i> 2002 [Section 4.1.1]	Piles 1.8 to 2.4 meters (6 to 8 feet) in diameter were constructed under different construction methods to compare the effects on axial capacity.	-Casing reduces skin friction -Bottom cleanliness shows no impact on axial capacity [Numerical results presented in Table 3]
Finno <i>et al.</i> 2002, Iskander <i>et al.</i> [Section 4.1.2]	Researched the impact of anomaly size on axial capacity for 0.9-m (3-ft) diameter piles.	-Soft clay layer may not provide much resistance [Numerical results presented in Table 5]
Reese <i>et al.</i> 1985 [Section 4.1.3]	Compared the effects of casing on axial capacity for 0.9-1.2 m (3-4 ft) diameter piles.	-Permanent casing reduced side resistance [Numerical results presented in Table 7]
Petek <i>et al.</i> 2002 [Section 4.1.4]	Researched the impact of anomaly location on axial capacity using computer modeling in PLAXIS.	-Anomalies in bottom of pile do not affect capacity -Piles in soft soils not affected by anomalies [Numerical results presented in Table 8]
Sarhan <i>et al.</i> 2002 (2 Studies) [Section 4.1.5]	Study 1: Analyzed the type of defect effect on lateral capacity. Study 2: Researched minor flaws in critical regions of the pile and effect on lateral capacity	-15% Cross-Sectional area defects can cause 30% reduction in lateral capacity [Numerical results presented in Table 9]

As summarized in Table 2 and described in more detail in the following sections, these studies report on a variety of construction variables, such as the use of casing and slurry, anomalies within the pile, bottom cleanliness, and large diameter piles. A brief introduction to each of these construction issues is discussed in the following paragraphs.

One major cause of concern is casing, which can significantly reduce side resistance of a CIDH pile (e.g. O'Neill and Reese 1999, Littlechild 2000). Depending on the types of soils involved, the majority of CIDH pile capacity may be found in side resistance; therefore, casing can have detrimental effects on the desired behavior of the foundation. However, there are many instances where casing must be used. When the casing is temporary, and is able to be withdrawn during concrete placement, most of the side resistance is recovered, although studies have also indicated that it may not be as high as if casing were not used at all (e.g. Camp 2002, Reese 1985).

When drilling slurry is used, the main concern is whether the filter cake reduces capacity by lessening the bond at the soil-concrete interface. However, as long as the filter cake is not excessive, studies have found that this is not an issue (e.g. Camp *et al.* 2002, O'Neill and Reese 1999). Only when an excessive *mudcake* develops in the case of mineral slurries, does a reduction in side resistance occur. However, measures can easily be taken to ensure that thick mudcakes are removed prior to concrete placement by agitating or circulating the drilling slurry. It has been noted that polymer slurries, which are becoming the standard in most states, may show increased side resistance over time due to the reaction between the polymers and the concrete (O'Neill and Reese 1999). Polymer slurries do not generally produce a filter cake thick enough to pose many problems. For more detailed information on drilling slurries, refer to Chapter 2.

Bottom cleanliness is also an issue to be addressed. Cleanout methods involve several choices, such as pressure washing systems and cleanout buckets, but inevitably, some sediment is left in the bottom of the hole. Although “soft bottoms”, due to the presence of excessive loose materials, has not shown a significant reduction in capacity, it can increase the ultimate displacements experienced by the pile.

The first case study presented in Section 4.1.1, by Camp *et al.* (2002), covers most of these issues relating to the effects of different construction methods on the axial capacity of CIDH piles.

4.1.1 Case Study by Camp, Brown, and Mayne (2002)

This case study by Camp *et al.* (2002) is one of the few published papers on large diameter CIDH piles. Since this case study is relatively significant in this research study, a description of the load testing procedure is provided in addition to the general data. Results were reported on final failure conditions for the tip and side resistance, settlement, and the amount of sediment at the bottom of the hole. Construction procedures included the dry, slurry, and casing methods. Slurry types included bentonite, polymer, and freshwater. Casing was driven through upper layers of loose sands and soft clays, with a vibratory hammer, into stiff clay. The 1.8-meter (6-ft) diameter CIDH piles were constructed with a drilling auger, whereas the 2.4-meter (8-ft) CIDH piles were excavated with a digging bucket. The following Table 3 presents a summary of results on twelve CIDH piles that ranged from 1.8- to 2.4-meters (6-8 feet) in diameter and 23.2- to 48.2-m (76-158 ft) in length. Casing lengths range from 16.8 to 23.3 meters (55 – 76 ft) in length, which extends into the bearing clay layer, but not the whole length of the pile. For additional information on casing and what is not provided in the following section, refer to Camp *et al.* (2002).

Table 3 Numerical test results (Camp *et al.* 2002), see Table 1

Construction Method	Final Failure Conditions (Estimated from graphs)		Back-Calculated Side Resistance, kPa (tsf) (Average value from data)		Bottom Cleanliness
	Settlement, mm (in.)	Unit End Resistance, kPa (tsf)	Cased Section	Uncased	Sediment Thickness, mm (in.) min/max/avg
Bentonite Slurry L = 48.2 m (158 ft) D = 2.4 m (8 ft)	108 (4.25)	3800 (39.7)	30 (0.31)	173 (1.8)	12 / 26 / 19 (0.5 / 1.0 / 0.7)
Polymer Slurry 1 L = 48 m (157 ft) D = 2.4 m (8 ft)	84 (3.31)	3100 (32.4)	65 (0.68)	210 (2.2)	11 / 25 / 32 (0.4 / 1.4 / 0.9)
Polymer Slurry 2 L = 33.5 m (110 ft) D = 2.4 m (8 ft)	72 (2.83)	2500 (26.1)	100 (1.0)	172 (1.8)	5 / 35 / 17 (0.2 / 1.4 / 0.7)
Polymer Slurry 3 L = 48.2 m (158 ft) D = 2.4 m (8 ft)	115 (4.53)	3600 (37.6)	--	168 (1.7)	20 / 40 / 30 (0.8 / 1.6 / 1.2)
Polymer Slurry 4 L = 34.3 m (113 ft) D = 2.4 m (8 ft)	72 (2.83)	2000 (20.9)	--	192 (2.0)	0 / 30 / 16 (0.0 / 1.2 / 0.6)
Dry 1 L = 33.5 m (110 ft) D = 2.4 m (8 ft)	90 (3.54)	2900 (30.3)	50 (0.52)	192 (2.0)	9 / 38 / 19 (0.4 / 1.5 / 0.7)
Dry 2 L = 33.5 m (110 ft) D = 2.4 m (8 ft)	--	--	--	--	8 / 30 / 16 (0.3 / 1.2 / 0.6)
Dry 3 L = 33.1 m (109 ft) D = 1.8 m (6 ft)	81 (3.19)	2400 (25.1)	--	239 (2.5)	5 / 26 / 11 (0.2 / 1.0 / 0.4)
Dry 4 L = 23.2 m (76 ft) D = 2.4 m (8 ft)	--	--	--	--	6 / 25 / 12 (0.2 / 1.0 / 0.5)
Dry 5 L = 48.2 m (158 ft) D = 2.4 m (8 ft)	118 (4.63)	2800 (29.2)	--	165 (1.7)	5 / 21 / 11 (0.2 / 0.8 / 0.4)
Dry 6 L = 35.1 m (115 ft) D = 1.8 m (6 ft)	63 (2.48)	3100 (32.4)	--	--	6 / 41 / 16 (0.2 / 1.6 / 0.6)
Freshwater L = 48 m (157 ft) D = 2.4 m (8 ft)	144 (5.67)	4000 (41.8)	--	200 (2.1)	25 / 52 / 37 (1.0 / 2.0 / 1.5)

The CIDH piles presented in Table 3 were constructed in soils that were either very loose to loose sands or very soft to soft clay for the upper 12 to 17 meters, and the base of the CIDH piles bear in stiff clay/silt (classified as CM/CH), called *Cooper Marl*. The Cooper Marl was reported to have undrained cohesion strengths, s_u , ranging from 140 kPa to 240 kPa (1.5–2.5 tsf), whereas the upper clay layer ranged from 16 kPa to 23 kPa (0.17–0.24 tsf) and the sand layers had N-values around 15. The CIDH piles in this test were instrumented only within the Cooper Marl. Camp concluded in a following study that the Cooper Marl had unique properties in its strength (Camp *et al.* 2002, [2]).

4.1.1.1 Testing Procedure

The CIDH pile reinforcing cages were instrumented with vibrating wire and resistance type strain gages prior to placement. The instrumentation was provided in the sections of the pile within the Cooper Marl. Load testing was carried out with Osterberg Cell testing and Statnamic testing. Osterberberg cells are two parallel plates that are placed in the cross section of the pile. The area between the two plates is pressurized, which pushes upward on the portion of the pile above the cell, and downward on the lower portion of the pile. Statnamic testing applies an axial load at the top of the pile. Failure was defined when *plunging* occurred, which is where the top or the bottom of the pile displaces significantly relative to small increases in load. The maximum and minimum load-displacement curves are provided in Figure 8.

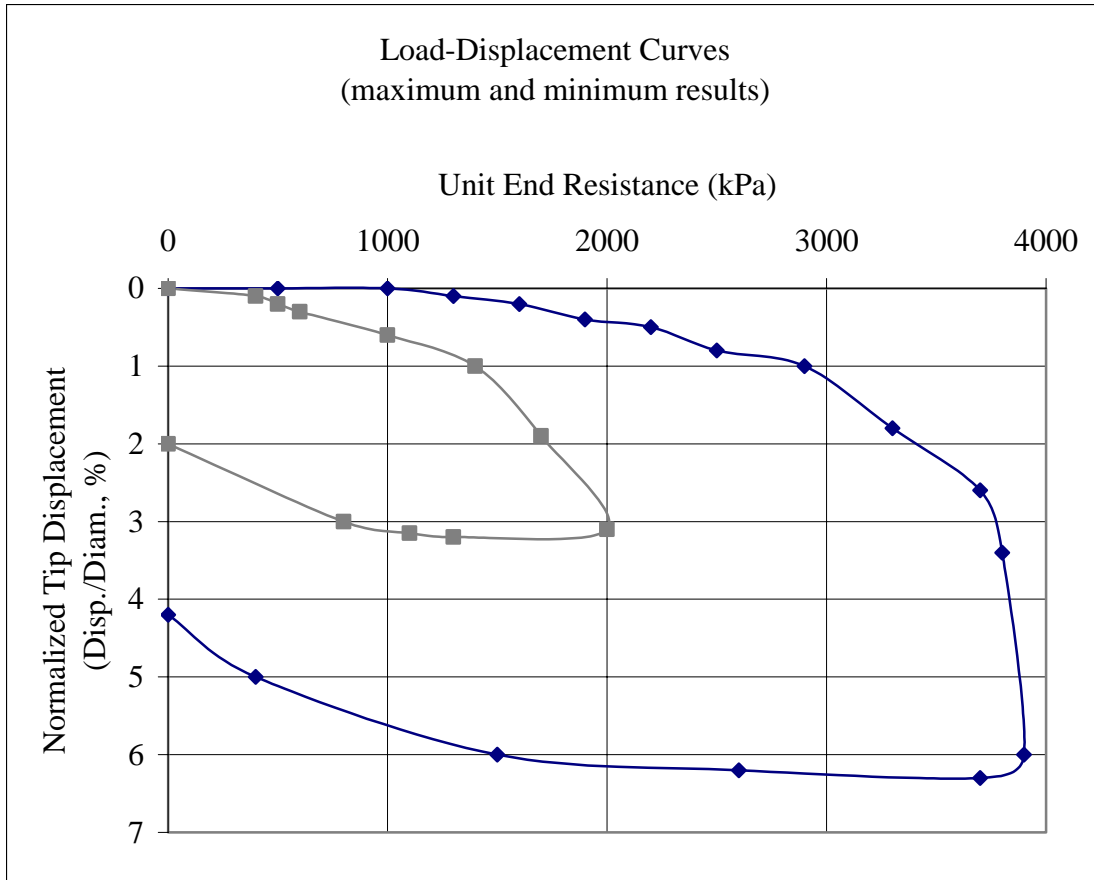


Figure 8 Load-displacement curves for the minimum shallow-depth value and maximum deep-depth value (Camp *et al.* 2000)

Note that the maximum tip displacement in Figure 8 reaches 6% of the pile diameter, which is for a 2.4-m (8-ft) diameter CIDH pile. Design failure conditions can be limited to 4% of the diameter (Dapp *et al.* 2002), and service displacements may be limited to 13 mm (0.5-inches) (Caltrans correspondence 2003). Therefore, if the failure criterion is limited by displacements the full tip resistance may not be activated.

4.1.1.2 Discussion of Results

Numerous construction methods, such as dry, wet, and casing were tested by Camp *et al.* to find the resulting effects on side resistance, tip resistance, and displacements. The numerical results in Table 3 show that side resistance along the permanent casing sections of the pile decreased considerably, whereas uncased areas maintained satisfactory side resistance. Table 3 also shows that the dry and wet methods of construction result in similar capacities. The real marked difference in resistance is shown in the cased areas of CIDH piles. Since the use of casing cannot always be avoided in the field, Section 4.2 discusses methods that have been successful in alleviating this problem.

The numbers in Table 3 were checked using the soil properties given in this report and the design equations presented in Chapter 3, these results are shown in Table 4. The N_c value used to calculate the tip resistance can easily be defined as 9.0 since the length to diameter ratio is much greater than 4. Therefore the tip resistances of the CIDH piles are expected to be on the order of 1260 kPa to 2160 kPa (13.2 tsf to 22.6 tsf) [see Appendix A].

Table 4 Design values vs. tested results from Table 3 (Camp *et al.*)

Type of Axial Resistance	Design Estimate	Tested Value
Tip Resistance, kPa (tsf)	1260 – 2160 (13.2 – 22.6)	2000 – 4000 (20.9 – 41.8)
Side Resistance in Cooper Marl, kPa (tsf)	77 – 132 (0.80 – 1.4)	165 – 200 (1.7 – 2.1)

Table 4 compares the computed design values to the tested values in Table 3. As can be seen in Table 4, the maximum computed design tip resistance corresponds to the minimum tested value, also see Figure 25 in Appendix C.

Tested values of side resistance in the pile were calculated from the strain gage results. The side resistance is estimated based on typical soil properties with the beta- and alpha-methods. The alpha-method is used to calculate the side resistance for the Cooper Marl using the given undrained cohesion strength and the assumed value of $\alpha = 0.55$ by O'Neill and Reese (1999). The beta-method is used to find side resistance in the sands using estimated moist unit weights to calculate the vertical effective stress and multiplying that by a calculated value of β following the methods given by O'Neill and Reese (1999). The design calculations for the upper layers, comprised of low density sand or soft clay, show that little resistance is expected in these layers. The computed side resistance for the upper layers range from 10-50 kPa (0.10-0.52 tsf), whereas the Cooper Marl, where the piles were instrumented, has a computed design side resistance between 77-132 kPa (0.80-1.4 tsf), see Appendix A for sample design calculations. Note that the uncased portions of every tested pile reported higher side resistance than the design equations compute, which is shown in Figure 29 in Appendix C. On the other hand, the cased areas of the pile reported side resistances lower than the design equations, as shown in Figure 30 in Appendix C.

Camp *et al.* also looked at the bottom cleanliness of the pile, sediment depths are given in Table 3. A 13-mm (0.5-in.) sediment depth limit was set for over 50% of the area, and no more than 38-mm (1.5-in.) anywhere else. These limits were found to be fairly stringent and difficult to accomplish; out of the 12 piles tested, only three were able to fully meet this requirement. However, in comparing the sediment depths to the tested tip capacity and settlement obtained, no noticeable correlation is apparent; see Figure 16 and Figure 17 in Chapter 5. Therefore, bottom cleanliness may not have as significant of an impact on the capacity of CIDH piles. In terms of displacement, it should be noted that these piles were loaded to failure, as shown in Figure 8, which resulted in larger displacements than what is generally allowed in design. Chapter 5 addresses the issue of bottom cleanliness further as to its affect on the activation of full axial capacity. Section 4.2 addresses post-grouting, which may eliminate bottom cleanliness concerns and settlement issues. Caltrans typically neglects end bearing in design, especially in wet

conditions, therefore limits are set at the discretion of the inspector as to what is excessive in sediment depth.

Based on the results in this study, design calculations seem to underestimate the capacity of these large diameter CIDH piles. Capacity did not show significant decreases with regards to the wet and dry methods of construction or bottom cleanliness, as is further discussed in Chapter 5. Casing, however, did show a reduction in capacity. This is also shown in the case study by Reese *et al.* (2002).

4.1.2 Case Study by Reese, Owens, and Hoy (1985)

Another study related to pile construction methods was conducted by Reese *et al.* (1985) who tested three different piles and analyzed the change in capacity when casing was left in place. Out of the three piles tested, Piles 1 and 3 were instrumented with Mustran cells along the length of the pile to measure axial strain, Pile 2 was not instrumented. Failure was defined when plunging occurred. The numerical results are summarized in Table 5; however, for further information not covered in this section refer to Reese *et al.* (1985).

Table 5 Numerical test results (Reese *et al.* 1985), see Table 1

Testing Description	Diameter, m (ft)	Length, m (ft)	Load at Failure, kN (tons)	Final Tip Resistance, kN (tons)
Test Pile 1* – Temporary Casing, 16m	1.2 (4)	18.3 (60)	4404 (495)	498 (56)
Test Pile 2** – Temporary and Permanent Casing	0.9 (3)	19.8 (65)	721 (81)	--
Test pile 3* – Permanent Casing	0.9 (3)	19.8 (60)	1859 (209)	231 (26)

* Instrumented piles

**Pile not instrumented

The CIDH piles were located in soils consisting of a loose to firm sand/soft clay mixture for the top 6.1 m (20 ft), soft to medium clay to 9.1 m (30 ft), a very dense sand layer for the next 3 m (10 ft), and soft to medium silty clay (varved clay) as the bearing stratum. The soil property given in the report is for the varved clay, an undrained cohesive strength, $s_u = 38$ kPa (0.4 tsf).

The first CIDH pile listed in the table was constructed with temporary 16-meter (52-foot) long casing and augering the soil out of the middle. The remaining length was excavated with slurry. As the concrete was poured, the casing was removed. This pile serves as the control pile. The second pile was constructed with a temporary 1219-mm (48-inch) diameter casing that was driven to 15 m (50 ft). The inner 914 mm (36 in.) was excavated with slurry, and a permanent 914-mm (36-in) diameter casing was placed inside the first casing and the concrete poured. Upon removal of the outer temporary casing the soil moved inward, indicating a void space between the pile and soil, thus side resistance is expected to be low. The third pile used surface casing for the upper 3 m (10 ft), and was excavated with the slurry method for the remaining depth with a permanent 914-mm (36-in) casing placed down to 12 m (40 ft).

As seen in Table 5, side resistance dropped dramatically when casing was left in place. The calculated unit tip resistance, following the alpha-method is approximately 350 kPa, which for the respective 1.2-m (4-ft) and 0.9-m (3-ft) piles are 400 kN (45 tons) and 222 kN (25 tons). Since these piles differ in size, it may be easier to compare the unit side resistances. Therefore the tip and back calculated side resistances are also shown in kilopascals in Table 6. Test pile 2 was not instrumented, so specific tested side and bearing resistance values are not given for this pile.

The tested tip resistance at failure for the first and third test piles was 498 kN (56 tons) and 231 kN (26 tons), respectively. Both are very close to the calculated design values, as shown in Table 6, indicating that according to the information given in this report, the design calculation procedures for finding tip resistances were fairly accurate for these soil conditions.

Table 6 Design values vs. tested results from Table 5 (Reese *et al.*)

Axial Resistance		1.2-m (4-ft) Diameter		0.9-m (3- ft) Diameter		
		Predicted	Tested	Predicted	Tested	
			Pile 1		Pile 2	Pile 3
Tip Resistance, <i>kPa (tsf)</i> kN (tons)		350 (3.6)	440 (4.6)	350 (3.6)	--	363 (3.8)
		400 (45)	498 (56)	220 (25)	--	231 (26)
Side Resistance, <i>kPa (tsf)</i> kN (tons)	Clay	21 (0.21)	Back-Calculated: 221 <i>kPa</i> (2.3 <i>tsf</i>)	21 (0.21)	Back-Calculated: 45 <i>kPa</i> (0.5 <i>tsf</i>)	Back-Calculated: 147 <i>kPa</i> (1.5 <i>tsf</i>)
		990 (110)		850 (95)		
	IGM	275, 200 <i>limit</i> (2.8,2.1 <i>limit</i>)		275, 200 <i>limit</i> (2.8,2.1 <i>limit</i>)		
		2260 (250)		1700 (191)		
Total Capacity, kN (tons)		3650 (410)	4404 (495)	2770 (310)	721 (81)	1859 (209)

To back-calculate the tested side resistance of test pile 1, the tested tip resistance is subtracted from the tested total resistance to give a derived side resistance of 3906 kN (439 tons). Dividing this value by the effective area of Pile 1, which is the total surface area minus the upper 1.5 m (5 ft) and lower pile diameter surface area lengths, gives a unit resistance of 221 kPa (2.3 tsf). If pile 2 is assumed to have a tip resistance close to the design value, as was the case with piles 1 and 3, then the side resistance is back-calculated as 45 kPa (0.5 tsf). Pile 3 has a unit side resistance of 147 kPa.

The report indicates that the majority of the side resistance occurred in the 3-m (10-ft) layer of dense to very dense silty sand between the depths of 9-12 m (30-40 ft). SPT values in this layer were as high as 175 blows per 0.3 m (1 ft), which classifies this

material as an IGM according to Reese and O'Neill (1999). Following the procedure for O'Neill and Reese (1999), the side resistance is computed as 271 kPa (2.9 tsf) [see Appendix A], which takes into account the limiting N-value of 100. Note that Caltrans limits the side resistance to 200 kPa (2 tsf), therefore Table 6 reports a value of 200 kPa (2 tsf) for the limit.

The remaining effective length of the pile outside the 3-m (10-ft) sand layer is assumed to have a cohesive strength similar to the bearing layer of 38 kPa (400 tsf). Following the alpha-method, the side resistance is 21 kPa. For the 1.2-m (4-ft) and 0.9-m (3-ft) diameter CIDH piles, the total side resistance is 950 kN and 814 kN, respectively. Therefore, summing tip and side resistance gives a total capacity of 3650 kN and 2770 kN, again respectively. These results are shown in Table 6.

The design methods used in calculating the predicted values match closely what was found in the field. Test pile 1 exceeded the design values, whereas test piles 2 and 3, as expected due to the way in which they were constructed, did not meet the design values. This study is continued in Section 4.2.1 by looking at the post-grouting of piles 2 and 3.

The case studies by Camp *et al.* and Reese *et al.* looked at the effects of actual construction methods affecting pile capacity. The following studies by Finno *et al.* (2002), Petek *et al.* (2002) and Sarhan *et al.* (2002) look at the effects on pile capacity when construction methods cause anomalies to occur in the pile, such as cave-ins or void spaces. Finno *et al.* briefly looked at the axial capacity of two CIDH piles, one constructed with anomalies and the other without.

4.1.3 Case Study by Finno, Chao, Gassman, and Zhou (2002)

Finno *et al.* (2002) researched the effects of different sized anomalies on the axial capacity of four CIDH piles at the National Geotechnical Experimentation Site in Amherst, Massachusetts. The axial capacity of two of these CIDH piles is reported here. One pile was constructed with anomalies that included neckings (reductions in cross-

sectional area), voids, and inclusions. The voids and inclusions were intended to range from 5-40% of the cross-sectional area. The other pile was constructed with no anomalies. Temporary casing was used to construct each pile. For additional information on this study, refer to Finno *et al.* (2002).

The main focus of this study was to test the non-destructive evaluation method, impulse response, and is further discussed in Section 4.3.1. However, a brief description of the study and load test results is presented here to introduce the effects of anomalies on pile capacity. The two 15-m (50-ft) long, 0.9-m (3-ft) diameter CIDH piles were constructed in clay, the upper layer consisting of 5 meters (16.4 ft) of overconsolidated stiff sandy silt, underlain by 37 m (121.4 ft) of soft varved clay. The undrained cohesion strengths for the stiff silt and soft clay were 300 kPa (3.1 tsf) and 30 kPa (0.31 tsf), respectively.

Failure was defined when plunging occurred. The defective pile failed at an axial load of 1060 kN (119 tons), whereas the control pile had an ultimate capacity of 1200 kN (135 tons), a difference of 13%. This implies that if anomalies of minimal size were to occur during the construction of a pile, the capacity would not be largely affected. This study is looked at further in Section 4.4 to analyze how accurately the NDE methods of impulse response and CSL could identify the planned anomalies.

Since the CIDH piles are in clay, the side resistance design values are estimated using the alpha-method. The stiff clay is calculated to contribute 1166 kN (131 tons), or 165 kPa (1.7 tsf), and the soft clay is computed to resist 513 kN (57.7 tons), or 16.5 kPa (0.17 tsf). The base resistance, with an N_c value of 9, is 172 kN (19 tons), or 270 kPa (2.82 tsf). Table 7 compares these design values to what was tested.

Table 7 Design values vs. tested results by Finno *et al.* (2002)

Resistance	Tested Values of Total Axial Load, kN (tons)	Computed Design Values, kN (tons)	
		Side Resistance in Stiff Clay Only	Total Resistance
Resistance, kN (tons)	1060-1200 (119-135)	1166 (131)	1850 (208)

Note that the design calculations give a total axial resistance, including side and tip resistance, as 1850 kN (208 tons), as shown in Table 7. However, neither pile met the calculated total design capacity. This could indicate that the soft clay did not contribute as much in side resistance. If this soft clay layer is neglected in any contribution to side and bearing capacity, the total capacity reduces to 1166 kN (131 tons). This value is a closer match to what was tested; however, in design this layer may have been accounted for. The anomalies reduced pile capacity by about 12%. The reason for such a small decrease may be attributed to the piles being in soft clay and the soil having a greater effect on the failure. This is further discussed by Petek *et al.* (2002).

The following case study by Petek *et al.* (2002) looked more in-depth at the effects of anomalies on the axial capacity. However, the study by Finno *et al.* was reported with field testing results, whereas Petek *et al.* modeled the piles with the computer program, PLAXIS.

4.1.4 Case Study by Petek, Felice, and Holtz (2002)

Petek *et al.* (2002) looked at the effects on axial capacity of CIDH piles, modeled by the computer program, PLAXIS, when defects occurred in the concrete due to construction. The main focus of this study was to see how much the axial capacity was affected by defects that were not identified by NDE testing. The piles were analyzed using PLAXIS, and then checked against actual field testing results to calibrate the model. Numerical results for the computer modeling done by Petek *et al.* are summarized in Table 8. Refer to Petek *et al.* for further testing results and information.

Table 8 Numerical modeling results from PLAXIS (Petek *et al.* 2002)

Soil Type	Defect Size	Location of defect from top of 15 m (50 ft) long Pile, m (ft)	Load at Failure, kN (tons)	Capacity Reduction (%)
Soft	None	--	840 (94.4)	--
	50% (Void)	2 (6.56)	877 (99)	-4
	97%	2 (6.56)	820 (92)	2
	98%	2 (6.56)	560 (63)	33
	1-m (3.28-ft) weak concrete layer (WCL)	7.5 (24.6)	864 (97)	~0
	1-m (3.28-ft) WCL	13 (42.6)	880 (99)	-2
Medium Stiff	None	--	3250 (365)	--
	92%	2 (6.56)	2230 (251)	31
	92%	7.5 (24.6)	3220 (362)	1
	92%	13 (42.6)	3140 (353)	3
	0.6-1 m (2-3.28 ft) WCL	2 (6.56)	2440 – 2960 (274 – 333)	25 – 9
	0.6-1 m (2-3.28 ft) WCL	7.5 (24.6)	3290 (370)	~0
Very Stiff	None	--	6460 (726)	--
	85%	2 (6.56)	4638 (521)	28
	85%	7.5 (24.6)	6260 (704)	3
	85%	13 (42.6)	6280 (706)	3
	0.6-1 m (2-3.28 ft) WCL	2 (6.56)	3930 – 3030 (442 – 341)	40 – 53
	0.6-1 m (2-3.28 ft) WCL	7.5 (24.6)	6030 – 5200 (678 – 584)	7 - 20
	0.6-1 m (2-3.28 ft) WCL	13 (42.6)	6480 (728)	~0

Since this was not a field study, these results are not checked with design calculations. However, this data is provided to give an idea how pile defects can affect the axial capacity. The study found that CIDH piles located in weak cohesive soils were

not significantly affected axially by defects located at any location within the pile. However, if the pile is constructed in stronger soil, the CIDH pile must withstand greater loads and therefore defects in the top portion of the pile did affect the axial capacity. Defects in the bottom of the CIDH pile did not show significant reduction in capacity (<5%). Further discussion on this is discussed in Section 5.3, along with the following case study by Sarhan *et al.* (2002) who also studied the effect of minor anomalies.

4.1.5 Case Study by Sarhan, Tabsh, and O'Neill (2002)

Not only do concrete defects affect axial capacity based on location and size, but they also have noticeable affects on the lateral resistance, as found by Sarhan *et al.* (2002). Although it is beyond the scope of this research to give an in-depth report on lateral design, it is worth mentioning how construction flaws can impact the lateral capacity of the pile as well.

Sarhan *et al.* looked at the impact of *minor flaws*, which were defined as being less than a 15% reduction in cross-sectional area and one-diameter in depth, that were not detected by NDE methods in critical regions of the pile. Tests were performed on small-scale and full-scale specimens to analyze the reduction in capacity with several different forms of defects. The second study by Sarhan *et al.* then used the results of these tests to calibrate computer models in the program, PCACOL, to analyze other types of defects. A brief summary of results is presented in Table 9, however for information on all the data refer to Sarhan *et al.* (2002).

Table 9 Numerical modeling results on lateral capacity (Sarhan *et al.* 2002)

Type of Defect	Approximate % Reduction	Continued Study: % Reduction due to full-scale PCACOL modeling
None	--	--
15% Void located outside rebar cage	17	13
15% Void extending from outside rebar cage into concrete core	32 (small scale), 27 (full scale)	27
Increased spiral spacing (from 25.8 mm (1-in) to 50.8 mm (2-in))	13	N/A
Cage offset by 12.7 mm (0.5-in)	14	5
Increased spiral spacing with cage offset by 12.7 mm (0.5-in)	17	N/A
Corrosion of rebar to 44% original steel area due to 15 % void extending into core on the compression side.	24	N/A
Corrosion of rebar to 44% original steel area due to 15 % void extending into core, plus cage offset by 12.7 mm (0.5-in) on the compression side.	24	35

Defects that were located in critical portions of the pile led to significant reductions in capacity, in some cases more than 30%. The type of defect also made a difference on the influence of capacity. Several types of flaws were analyzed in both studies, namely different void locations within the pile cross-section, corrosion of the reinforcing steel, cage offsets, and reduction in concrete strength.

Defects extending from the core of the pile to the outer perimeter expose the reinforcing steel and corrosion becomes an issue. After time, the exposed steel will corrode and eventually lose substantial strength. This is a case where one defect leads to another, therefore the studies also included looking at multiple defects occurring at once. The worst-case scenario was a cage offset that caused a void extending into the core of the pile, therefore exposing reinforcing steel and causing corrosion in a critical flexural location. This produced a 35% reduction in lateral moment capacity, and if extreme

corrosion was considered flexural capacity was further reduced to 47%. Examples of several numerical results for loss in capacity due to flaws are presented in Table 9.

In conclusion to the studies presented by Sarhan and Petek, it may be recommended to focus on critical areas within the pile during NDE testing procedures. Further discussion on these results is provided in Section 5.3.

This section gave several examples of case histories that show how different construction methods can influence the capacity. In summary, several issues may be noted. The case studies by Camp *et al.* (2002) and Reese *et al.* (1985) showed notable reductions in side resistance. Finno *et al.*, Petek *et al.*, and Sarhan *et al.* showed that the impact of anomalies on capacity is dependent on its location and size within the pile, as well as the soil type the pile is located in. Camp *et al.* reported on numerous affects, such as bottom cleanliness and pile size. Bottom cleanliness may not have the expected effect on axial capacity as previously believed, and the capacity of large diameter CIDH piles may be underestimated since almost every tested value exceeded design values, with the exception of cased areas. Tables and figures relating these analyses are presented in Chapter 5.

Each case history so far has reported on issues in construction that may affect capacity. Therefore, the following Section 4.2 addresses post-grouting, a method that may help alleviate these construction challenges due to casing, anomalies, and bottom cleanliness.

4.2 Post-Grouting

As shown by the case histories in Section 4.1 by Camp *et al.* and Reese *et al.*, side resistance in CIDH piles is dramatically reduced when casing is used. Acknowledging this, post-grouting is an option taken to restore the frictional resistance lost due to casing. Post-grouting is a pressurized process that injects grout, a water-cement mixture, through tubes to the area of concern. The tube or apparatus used for grouting may be within or

outside of the pile. If it is within the pile, the concrete surrounding the tube must be cracked open by either pressure washing with water or injecting the grout itself under high pressure. This is done after the concrete has set, but before it has gained significant strength. Grouting will then take place when the concrete is close to the design strength.

The two types of grouting methods are permeation grouting and compaction grouting. Permeation grouting infiltrates the soil voids with a highly fluid grout that readily flows into the soil. This process is highly dependent on the ability to make the grout of extremely low viscosity (very fluid). The application of this method is reasonable in sands, where particle and void spaces are larger; however, in clays this method is difficult, if not impossible, to apply without some form of soil mixing. Compaction grouting, on the other hand, uses a highly viscous (i.e. thick) grout that is pressure injected into the space between the base or sides of the pile and the soil. As the grout expands, the surrounding soil is compacted and densified. Compaction grouting is generally the method used for post-grouting.

Tables 10 and 11 report several studies that have been conducted on post-grouting the tips and sides of CIDH piles. The following sections report on each of these studies and the effects on capacity.

Table 10 Case study checklist for post-grouting CIDH piles

Post-Grouting Case Studies			References for Sections 4.2.1 - 4.2.4			
			Reese <i>et al.</i> 1985	Littlechild <i>et al.</i> 2000	Dapp and Mullins 2002	Brusey 2002
Construction Method:	Dry				N/A	
	Slurry		X			
	Casing	Temporary	X	X		X
		Permanent	X			
Soil Type:	Cohesive		X			
	Cohesionless		X	X	X	X
Post-Grouting Report:	Axial Capacity	Tip			X	X
		Side	X	X	X	X
	Settlement		X			X

Table 11 Case study summaries on post-grouting

Test Reference	Description	Results
Reese et al. 1985 [Section 4.2.1]	Piles post-grouted from the case history presented in Table 2.	-Post-grouting significantly increases side resistance [Numerical results presented in Tables 12-13]
Littlechild et al. 2000 [Section 4.2.2]	Side resistance compared for sands of various densities.	-High density sands have naturally high side resistance and show minimal improvement with post-grouting -Side resistance in low density sands improve with post-grouting [Numerical results presented in Tables 14-15]
Dapp and Mullins 2002 [Section 4.2.3]	Post-grouted the tips of CIDH piles in cohesionless soils	-Post-grouting increased the tip capacity by 2 to 8 times [Numerical results presented in Tables 16-17]
Brusey 2000 [Section 4.2.4]	Compared non-grouted CIDH piles with piles post-grouted at the tips and sides	-Post-grouting increased total capacity [Numerical results are presented in Tables 18-19]

4.2.1 Case Study by Reese *et al.* (1985), (Cont'd from 4.1.3)

The first study presented in Tables 10 and 11, by Reese *et al.* (1985), expands off the case study presented in Section 4.1.2 by also looking at the impact of post-grouting the cased areas. The results presented in Table 12 are in addition to the information provided in Section 4.1.2.

Table 12 Numerical Results for Post-Grouting (Reese *et al.* 1985), see Table 5 and Table 11

Testing Description	Load at Failure, kN (tons)		Settlement, mm (in.)	
	Non-grouted	Post-Grouted	Non-grouted	Post-Grouted
Test Pile 1	4404 (495)	--	49 (1.94)	--
Test Pile 2 – Temporary and Permanent Casing	721 (81)	3319 (373)	43 (1.69)	40 (1.58)
Test Pile 3 – Permanent Casing	1859 (209)	3772 (424)	31 (1.23)	48 (1.88)

Recall from Section 4.1.2 that the piles are located in soft to medium clay layers, and a 3-m (10-ft) thick dense sand layer. The soil properties and construction methods are described in more detail in Section 4.1.2, and are found in Reese *et al.* 1985.

The significant increase in side resistance due to the application of post-grouting is evident in Table 12. The total resistance of test pile 2 increased by more than four times, and test pile 3 more than doubled.

Table 13 Design values vs. tested results from Table 12, see also Table 6 (Reese *et al.*)

Axial Resistance	Non-Grouted	Post-Grouted 0.9-m (3- ft) Diameter		
	Tested	Predicted	Tested	
	Pile 1		Pile 2	Pile 3
Total Capacity, kN (tons)	4404 (495)	2770 (310)	3319 (373)	3772 (424)
Back-Calculated Unit Side Resistance, kPa (tsf) (excludes upper 1.5m (5-ft) and lower diameter length)	221 (2.3)	200, controlled by design limits (2.1)	306 (3.2)	350 (3.6)

As mentioned in Section 4.1.2, the values in the table above were predicted using the alpha-method for the clays and the beta-method for the IGM layer. Both of the tested values for the post-grouted piles are close to the design calculation values. The side resistance of test pile 2 can be back-calculated if the design value for tip resistance, 222 kN, is assumed. This assumption seems applicable since piles 1 and 3 were both close to design values for tip resistance. Therefore, the side resistance of pile 2 is estimated to be 3096 kN (348 tons), or 306 kPa (0.65 tsf). Note that the unit side resistance of test pile 1, which was tested without permanent casing, is approximately 221 kPa (2.3 tsf) as calculated in Section 4.1.2. If this value represents the control value for side resistance, then test pile 2, after post-grouting, exceeded full resistance. Noticing the fact that test pile 2 was constructed very poorly, this is a good indication that post-grouting can remedy even the worst situations. Test pile 3 increased from a side resistance of 147 kPa (1.5 tsf) to a side resistance of 350 kPa (3.6 tsf) after post-grouting, which even exceeds the control value.

Piles 2 and 3 both showed significant increases in side resistance due to post-grouting, and even exceeded test pile 1 in side resistance. The predicted design values for the IGM for these piles, following the method given by O'Neill and Reese (1999), is very close to the post-grouted values. Further discussion on this case study is presented in Chapter 5.

Reese *et al.* post-grouted CIDH piles with the majority of the length in clays, which improved resistance. Littlechild *et al.* (2002) looked at post-grouting CIDH piles located in sands of varying density.

4.2.2 Case Study by Littlechild, Plumbridge, Hill, and Lee (2000)

Littlechild *et al.* (2000) also reported on the increase in side resistance of CIDH piles due to post grouting. As summarized in Table 11 and numerically shown in Table 14, Littlechild *et al.* tested 10 piles, 7 of which were post-grouted. The piles were instrumented with vibrating wire strain gages and the displacements were monitored by dial gages. Total failure load was considered when the displacement exceeded 0.075 mm (0.003 in) for one load increment, or a maximum of 10% of the diameter, which is fairly large relative to the other case studies. Only one pile reached the 10%*D failure condition. For further information refer to Littlechild *et al.* (2000).

Table 14 Numerical test results (Littlechild *et al.* 2000), see Table 11

Concrete Pile Type		N-Value	Side Resistance kPa (tsf)
Non-Grouted	Rectangular 230x635 mm (9x25 in.) Pile	160	220 (2.3)
	Rectangular 230x635 mm (9x25 in.) Pile	55	72 (0.75)
	1.2-m (4-ft) Diameter Pile	40	53 (0.55)
Grouted	230x635 Pile, L = 51 m (167 ft), Grouted from 39-51 m (128-167 ft)	55	134 (1.4)
	230x635 Pile, L = 38.1 m (125 ft), Grouted from 22-38.1 m (72-125 ft)	40	144 (1.5)
	230x635 Pile, L = 38.1 m (125 ft), Grouted from 22-38.1 m (72-125 ft)	95	206 (2.15)
	1.2-m Diameter Pile, L = 53 m (174 ft), Grouted from 22-53 m (72-174 ft)	32	115 (1.2)
	1.2-m Diameter Pile, L = 53 m (174 ft), Grouted from 22-53 m (72-174 ft)	125	211 (2.2)
	1.2-m Diameter Pile, L = 32 m (105 ft), Grouted from 14-32 m (46-105 ft)	34	192 (2.0)
	1.2-m Diameter Pile, L = 30 m (98 ft), Grouted from 20-30 m (66-98 ft)	130	172 (1.8)

The soils in this test were composed of sand fill in the upper layers, alluvial sand down to a depth of approximately 30 meters (100 feet), and highly decomposed weathered granite extended to bedrock. This decomposed weathered granite ranged in N-values from a cohesionless soil, 32-55, to an IGM, 95-160.

Although these results are for rectangular and smaller diameter piles, the impact of grouting on side resistance is still evident. Littlechild *et al.* noted in this study that the piles located in soil with high N-values (classified as IGMs by O'Neill and Reese) did not benefit as much from post-grouting because side resistance was already high to begin with. The most improvement in side resistance was found in lower density soils where

the side resistance was initially low. Post-grouting more than doubled the side resistance of CIDH piles in soils with N-values between 30 and 60.

Table 15 Design values vs. tested results from Table 14 (Littlechild *et al.*)

N-Value	Side Resistance, kPa (tsf)		
	Predicted Design Value	Tested Value	
		Non-Grouted	Grouted
N < 55, “cohesionless” kPa (tsf)	72 (1.5)	53-72 (0.55-0.75)	115-192 (1.2-2.0)
N > 50, “IGM” kPa (tsf)	330 (Limit = 200) (3.4) (Caltrans limit = 2 tsf)	220 (2.3)	172-211 (1.8-2.2)

Using the beta-method recommended by O’Neill and Reese (1999), the estimated unit side resistance for the piles is approximately 72 kPa (0.75 tsf) for cohesionless soils and 330 kPa (3.4 tsf) for IGMs. Note that for the IGMs, Caltrans limits this value to 200 kPa (2 tsf), which in this case seems to be an adequate limit. The cohesionless soil data corresponds well with the test results from the non-grouted piles; however, the post-grouted piles exceeded this capacity two- to three-fold. The tested IGM values, on the other hand, are less than the design calculations, without the limit, for both the non-grouted and post-grouted piles.

Needless to say, this study shows the benefit of post-grouting in weathered granite and granular soils that are classified by O’Neill and Reese as *cohesionless*. The method to compute side resistance in IGM over-estimates the capacity; however, the limit set by Caltrans matches well with the tested results. Further discussion on this case study is continued in Chapter 5.

The two case histories covered so far by Reese *et al.* and Littlechild *et al.* have shown the benefits of post-grouting the sides of CIDH piles, but post-grouting can also be applied to the base for improved axial resistance. The last two case histories in Table 11 summarize the research performed by Dapp *et al.* (2002) and Brusey (2000), who found

that post-grouting the tips of CIDH piles eliminates soft bottoms and increases the total bearing capacity.

4.2.3 Case Study by Dapp and Mullins (2002)

Typical construction methods inevitably leave some amount of sediment at the base, preventing mobilization of tip resistance until after the pile has displaced enough to densify the loose material. The displacement required for this to happen generally exceeds the amount of displacement needed to fully activate side resistance. Thus, if the base of the pile is encompassed in compact material, loads can be resisted under little displacement and act collectively with side resistance. Dapp and Mullins (2002) researched post-grouting the tips of CIDH piles, 0.6 meters in diameter and 15 meters long, to determine if post-grouting reduced the amount of displacement needed for full axial capacity to be activated. Piles were instrumented at distances 0.46 m (1.5 ft) and 3.2 m (10.5 ft) up from the base of the pile. Statnamic testing was taken to a plunging failure. To observe the effects of elastic pile shortening, displacements were measured at the top and at the base of the pile. However, the elastic shortening of the pile was insignificant. Table 16 shows a summary of results from these tests. For more in-depth information refer to Dapp and Mullins (2002).

Table 16 Numerical test results (Dapp & Mullins 2002), see Tables 10-11 for summary

Type of Pressure Grouting for 0.6-m (2-ft) diameter, 4.6-m (15-ft) long CIDH piles	Site 1		Site 2	
	Total Load, kN (tons)	Tip Load – back calc'd, kN (tons)	Total Load, kN (tons)	Tip Load – back calc'd, kN (tons)
No Grout	961 (108)	98 (11)	890 (100)	62 (7)
Flat-Jack, Release Pressure	1094 (123)	347 (39)	--	--
Flat-Jack, Hold Pressure	1210 (136)	365 (41)	1290 (145)	463 (52)
Sleeve Port with Plate	1379 (155)	507 (57)	1397 (157)	587 (66)
Sleeve Port, no Plate	1450 (163)	569 (64)	--	--

The CIDH piles in the case study by Dapp *et al.* (2002) were located on two different sites. Site 1 was reported to have shelly sands at the tip elevation and Site 2 had a bearing layer of silty silica sand. Soil properties, other than N-values, were not explicitly given in the report. However, in order to check the data in Table 16, the given SPT N-values ranging from 2 to 10 and general soil properties in Appendix B for loose to medium silty sand were used to estimate the tip resistances that might be calculated in design, following the methods given in Chapter 3 by O'Neill and Reese (1999) [see Appendix A].

As shown in Table 16, four different post-grouting procedures were tested on two separate sites, and these were compared to a non-grouted pile on each site. The tests were conducted in cohesionless soils. Mullins reported that although post-grouting can be beneficial in all soil types, it makes the greatest impact in sands. This is due to the fact that clays will consolidate (i.e. settle with time), and thus do not compact as well as sands.

Note that in Table 16, two grouting mechanism types are mentioned, the Flat Jack and the Sleeve Port. The Flat-Jack device is a steel plate that is wrapped in a rubber membrane. The grout flows out of the plate and expands in the membrane, thus preventing grout loss into the soil. The Flat-Jack can either pressurize the grout during the curing process, or have the ability to flow back into the pile. Both methods were tested. The Sleeve Port is based on a similar concept, but is a smaller perforated pipe, rather than a plate, enclosed in a rubber tube. A steel plate can be placed above the pipe to provide a flat bearing surface for the pile. The Sleeve Port was tested with and without the steel plate. As can be observed from the data, the Sleeve Port method gave higher results than the Flat Jack on both sites. However, both methods far exceeded the control pile with no grouting by 7 to 9 times the tip capacity, and increased the overall resistance approximately 50%.

Table 17 Design values vs. tested results from Table 16 (Dapp *et al.*)

Type of Resistance	Calculated Design Estimates	Tested Result Range	
		Non-grouted	Grouted
Tip Resistance, kN (tons)	35 – 170 (4 – 19)	62 – 98 (7 – 11)	347 – 587 (39 – 66)
Side Resistance, kN (tons)	40 – 260 (4 – 30)	--	--
Total Resistance, kN (tons)	70 – 425 (8 – 48)	890 – 961 (100 – 108)	1094 – 1450 (123 – 163)

Since groundwater information was not provided in the report, both dry and wet conditions were considered in estimating the design resistances. The tip capacity was estimated to be in the range of 35 to 170 kN (4 to 19 tons), which, as can be seen in Table 17, the piles without grout fall within this range, but the post-grouted piles far exceed this. Therefore, once again, the methods to compute the tip resistance are fairly accurate for sands, but post-grouting increases this capacity dramatically.

Note that the design calculations for side resistance, using the beta method, are far below what was tested in the field. The final axial capacity values are under half as much

as what was tested. However, the soil properties, such as the unit weights of the soil were assumed to be typical values [see Appendix B], therefore the soil estimates may have underestimated the unit weights. Otherwise, the method for computing side resistance in cohesionless soils, i.e. the beta value, might be too conservative for loose sands.

This research by Dapp and Mullins (2002) was funded by the Florida Department of Transportation (FDOT). It is of interest to note that the favorable results of these tests prompted FDOT to incorporate post-grouting into their code.

4.2.4 Case Study by Brusey (2000)

Another recent case study pertaining to the post-grouting of CIDH piles was tested by Brusey (2000), who looked at post-grouting the tips and the sides of CIDH piles. Since both the sides and the tip resistance were reported with post-grouting this study is described in more detail, with a testing procedure given. CIDH piles that were 0.91 to 1.2 meters (3 to 4 ft) in diameter by 13.7 to 18.3 meters (45 to 60 ft) in length were constructed with temporary casing. The installation of the temporary casing was by a vibratory method and an oscillatory method described later. The final axial capacity at failure and the corresponding settlement were reported. These results are summarized in Table 18. For additional information in this section, refer to Brusey.

Table 18 Numerical test results for post-grouting (Brusey 2000), see Tables 10-11

Testing Description		Total Load at Failure, kN (tons)	Settlement, mm (in.)
Non-Grouted (DS-1, DS-2, and DS-3)	Temporary casing to 18.3 m (60 ft) L = 18.3 m (60 ft) D = 0.91 m (3 ft)	3443 (387)	37 (1.4)
	Temporary casing to 18.3 m (60 ft) L = 18.3 m (60 ft) D = 0.91 m (3 ft)	3381 (380)	37 (1.4)
	Temporary casing to 16.8 m (55 ft) L = 18.3 m (60 ft) D = 1.2 m (4 ft)	4413 (496)	49 (1.9)
Post-Grouted (DSG-1 and DSG-4)	Temporary casing to 13.7 m (45 ft) L = 13.7 m (45 ft) D = 1 m (3.25 ft)	6228 (>700)	19 (0.75)
	Temporary casing to 16.8 m (55 ft) L = 16.8 m (55 ft) D = 1.1 m (3.5 ft)	8897 (>1000)	46 (1.8)

The soils on this site consisted of an upper layer of hydraulic sand fill from 3 – 4.6 meters (10-15 feet), underlain by highly compressible organic tidal marsh for 3 meters (10 feet), and a bearing stratum of fine to medium glacial outwash sand of varying density for about 30 meters (100 feet).

The piles were installed using two different construction techniques. The non-grouted piles were installed using the vibratory method, where the casing was advanced to depth using a vibratory hammer. This procedure worked well for the 0.9-m (3-ft) casing, but problems were encountered with the 1.2-m (4-ft) diameter casings. This method was favorable due to the rapidity in which the casings were installed, but for larger diameter casings, a larger vibratory hammer may have to be used (Brusey 2000). The casings were meant to be temporary, but one 1.2-m (4-ft) pile casing could not be removed with the vibratory hammer, therefore only the total axial capacity was given for this pile. The grouted piles were installed using the oscillatory method with double walled casing. The reinforcement cage was placed with grout tubes attached, and the casing was removed after concrete placement. Although the process was slower with the

oscillatory method, no problems were encountered. After the concrete set for 24 hours, the piles were grouted by pumping water through the grout tubes until the concrete fractured and grout could be administered. The lower 5 to 6.5 meters (16 to 21 feet) of the piles were grouted. The bases of the piles were then grouted by a mini-jack device. To test the adequacy of the grouted sides, a 1.5-mm (0.6-in) limit was set on the amount of uplift caused by grouting the base. This limit was never exceeded, thus adequate perimeter grouting was assumed. In addition, each pile was tested by GGL and impulse response methods to ensure pile integrity.

4.2.4.1 Testing Procedure

The piles were tested statically, with failure defined as reaching a displacement of 4% of the diameter. However, the tests were carried out past this point to obtain load displacement curves which are shown in Figure 9. Displacements were recorded at the top of the pile.

It should be noted that the second non-grouted pile in Table 18, DS-2, is not reported in the load-displacement curve in Figure 9 because it was load tested with a different procedure, the flat jack load cell, which is similar to the Osterberg cell test method described in the case study by Camp *et al.* (2002) but was constructed by the contractor. In order not to mix the results of different test procedures, the static load tests are reported since it was the main test procedure. It is evident in Figure 9 that post grouting increased the capacity and reduced displacements. The largest non-grouted displacement occurred at about 12% of the pile diameter, for DS-1. The largest grouted pile displacement was only 3.5% of the pile diameter. Recall from Camp *et al.* (2002) that large diameter pile displacements at failure were slightly greater than 6% of the pile diameter. The reduction in displacement shown by Brusey may be attributed to adequate compaction of the soil beneath the tip from post-grouting, therefore full axial capacity was utilized under less displacement.

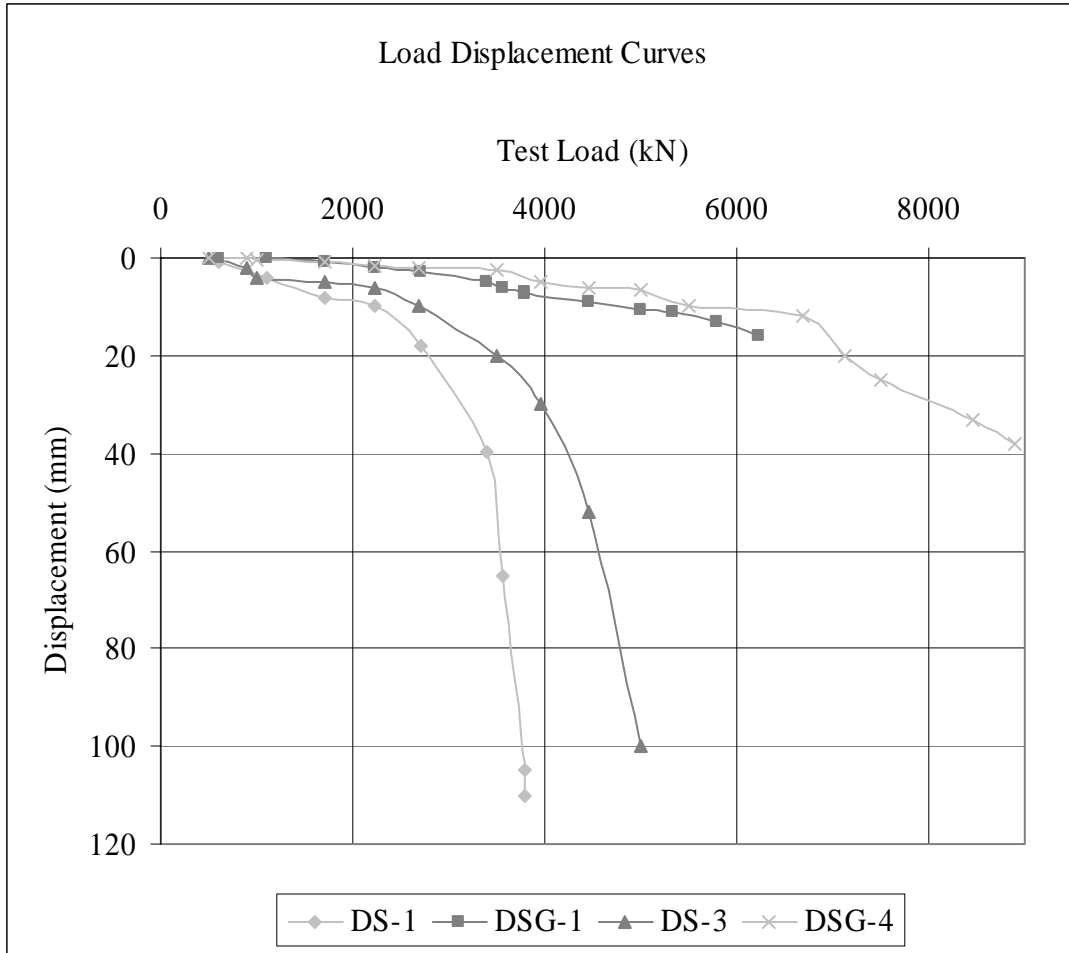


Figure 9 Load displacement curves for non-grouted (DS) and post-grouted (DSG) piles (Brusey 2000)

4.2.4.2 Discussion of Results

As shown by the results in Table 18 and Figure 9, post-grouting the base and lower perimeter of the CIDH piles greatly increased the overall capacity.

Table 19 Design estimates vs. tested results from Table 18 (Brusey 2000)

Type of Resistance	Calculated Design Estimates	Tested Result Range	
		Non-grouted	Grouted
Tip Resistance, kN (tons)	2330 – 3180 (260 – 360)	--	--
Side Resistance, kN (tons)	2580 – 2600 (290 – 290)	--	--
Total Resistance, kN (tons)	4910 – 5780 (550 – 650)	3440 – 4410 (387 – 496)	6230 – 8900 (>700 – >1000)

The report indicated that the N-values obtained on-site were representative of these soils; however, no actual N-values were given. Therefore, typical estimated soil properties and methods by Terzaghi and Vesic (Das 1999) were used to compare design values with the tested values shown in Table 18. The calculated tip resistances were in the range of 2330 to 3180 kN (260 to 360 tons) [see Appendix A]. CIDH piles in cohesionless soils are generally designed for end bearing; however, if side resistance is calculated for the grouted area of the pile, (the upper layers consisted of fill and tidal marsh and may not be considered a reliable source of skin friction) the total capacity is 4910 to 5780 kN (550 to 650 tons), which is slightly above the tested capacities but below the grouted pile ranges. Post-grouting brought the capacities of these piles to exceed what might have been calculated in a preliminary design that includes side resistance. This may be of interest since side resistance is generally discounted in cohesionless soils. Also take note that the values of failure for the non-grouted piles are taken at a limited displacement of 4% times the diameter. The post-grouted piles did not reach this value, and although the testing continued for the non-grouted piles past the failure limit, they never reached the capacity of the grouted piles. Thus, both tip and side resistances were improved.

The author also noted the relatively low cost of post-grouting with the mini-jack device. The cost to post-grout exceeded the cost of the same size CIDH pile by 30%. However, note that the post-grouted piles were shorter than the non-grouted piles and exceeded the capacity of the non-grouted pile by 2 to 3 times.

Although only four post-grouting case histories are covered in detail in this report, others exist with similar results. However, it should be noted that research is still limited on large diameter post-grouted piles. It is apparent that casing reduces the side resistance of CIDH piles, and post-grouting significantly increases capacity. Therefore, in cases where poor side resistance is anticipated, from either casing or soil conditions, an easy and cost-effective remedy is achieved by post-grouting. Post-grouting can also seal defects found in the pile, such as voids due to concrete segregation and inadequate pours. Chapter 5 compares the case histories presented in this section in more detail.

Another issue with CIDH piles is to know when pile remediation, such as post-grouting, need to occur. Since CIDH piles are below ground, visual inspection of the pile integrity is not possible. Therefore, in order to know if defects or flaws have occurred, adequate testing procedures are needed.

4.3 Test Methods

Tables 20 and 21 show several studies that have been conducted on different methods of testing. Non-destructive testing methods test the integrity of the pile, after construction, without disturbing the soil or the pile itself. The main methods focused on in this section are crosshole sonic logging, gamma ray testing, and impulse response. Summaries are presented in this section to provide an overview of trends. For more information on soil data and testing please refer to the specific reference.

Crosshole sonic logging (CSL) requires preparation during the construction of the CIDH pile. Tubes are placed at specific locations around the perimeter of the pile in order to feed a sensor device through. Sensors and probes are lowered through water-filled tubes in specified locations around the perimeter of the pile to send and receive signals. Two tubes are utilized at one time, one with an ultrasonic wave emitter, and the other with a detector. The strength and speed of the ultrasonic signal that is received by the sensor indicates the quality of the concrete. CSL can also report the quality of

underwater CIDH piles by hooking PVC tubes to the outer sides of the CIDH pile. CSL is described in greater detail in Section 3.4.3.

The impulse response method, also known as the sonic echo or the impact hammer method, can be used to test already cast-in-place piles. A sensor is attached to the top of the pile. A rubber headed hammer, or other similar device, is used to impact the top of the pile, which sends transient, longitudinal wave motion through the concrete (Caltrans 1997). Further detail on this method is provided in Section 3.4.2.

Table 20 Case study checklist for testing procedures

Reference	Testing Procedure		
	Impulse Response	Cross-hole Sonic Log	Gamma-Gamma Log
Finno <i>et al.</i> 2002	X		
Robinson <i>et al.</i> 2002		X	
Branagan <i>et al.</i> 2000		X	
Caltrans (correspondence)		X	X

Table 21 Summaries of case studies on testing methods

Test Reference	Description	Results
Finno <i>et al.</i> 2002	Tested the impulse response method on its ability to identify known anomalies. [Continued from Table 1]	Adequately identified anomalies in the upper portion of pile but not the lower portion.
Robinson <i>et al.</i> 2002	Reported on the same CIDH pile as Finno <i>et al.</i> (2002) with cross-hole sonic log (CSL) testing.	Anomalies were clearly identified.
Branagan <i>et al.</i> 2000	Used CSL to test the integrity of CIDH piles for a vehicular bridge.	Anomalies were identified and confirmed by coring.
Caltrans correspondence	Has evaluated several Non-Destructive Testing (NDT) methods to set acceptance criteria for CIDH piles.	Uses gamma-gamma log testing as the primary test and CSL testing if anomalies are discovered.

Caltrans currently requires the gamma-gamma log test procedure, also called gamma ray scattering, as a primary test for CIDH piles constructed in wet conditions. Wet conditions include excavations beneath the water table and slurry methods of construction. Gamma-gamma logging uses a probe that is lowered into pre-set tubes within the pile. One end of the probe has a radioactive source that sends out signals several inches into the surrounding concrete, the signal is then collected at the other end of the probe where a detector is located. The data obtained by the detector is called a *scatter count*. The lower the scatter count is, compared to the scatter count for a known concrete specimen, indicates the denseness of the concrete. The lower the scatter count is in relation to the standard, the denser the concrete. Further explanation of this method is described in Section 3.4.1. The following sections discuss the case studies that are summarized in Tables 20 and 21.

4.3.1 Case Study by Finno *et al.* (2002), Cont'd

The first case history discussed in Table 21 shows the progress of the impact hammer/sonic echo/impulse response method, referred to hereafter as impulse response. As described in Section 4.1.1, the test piles were constructed at the NGES Amherst site in soil consisting of upper layers of fill and stiff, sandy silt, underlain by soft clay. Three test piles were constructed with anomalies in known locations. The impact-hammer method was then tested on its ability to identify the locations of these anomalies. Finno *et al.* (2002) reported on two piles in this study, the control pile with no anomalies, and a pile with six anomalies. The sonic echo testing was not able to identify each anomaly, especially those located in the lower portion of the pile. The wave velocities were also not able to discern between anomalies located in close proximity of each other.

4.3.2 Case Study by Robinson, Rausche, Garland, and Ealy (2002)

The pile that consisted of six anomalies was also tested using cross-hole sonic logging (CSL), and was reported by Robinson *et al.* (2002). Unlike the sonic echo procedure, CSL was able to identify the anomalies well. However, the two other CIDH piles that were to be tested by CSL had blocked access tubes, thus the tests could not be

carried out in this reported study. Robinson also reported on CSL results at the NGES in Auburn, Alabama for CIDH piles constructed with anomalies. Each anomaly was detected, as well as other anomalies not planned for. Cross-sectional velocity time readings give an actual visual representation of the pile over the entire length.

4.3.3 Case Study by Branagan, Vanderpool, Murvosh, Klein (2002)

CSL also proved to be successful, as discussed in the third case history of Table 4.3, preventing a potential failure in the foundation of the Overton, Nevada Muddy River vehicular bridge. Piles on this bridge were tested by CSL and were found to be unsatisfactory. Further testing by coring confirmed the CSL results which led to remediation of the defects by the contractor and design engineer (Branagan *et al* 2000).

Cross-hole sonic logging is a popular testing method because it is able to report on the core cross-section of the pile. However it cannot report on the concrete cover as GGL can.

4.3.4 Case Study by Caltrans (2003)

Gamma-gamma log testing does not send signals between tubes, but rather operates with a single probe that has a sender and a receiver location at either end. The probe has a nuclear source that emits gamma waves which travel several inches before being collected by a receiver located at the top of the same probe. Tests are conducted in one tube at a time so the data does not get crossed. Gamma-gamma logging tests the integrity of the concrete immediately surrounding the PVC tube which includes the area around the reinforcing cage and concrete cover. If poor concrete quality is reported, follow-up testing is performed. Since GGL cannot report on the whole cross-section of the pile, Caltrans uses CSL to further investigate anomalies.

NDE methods may not always catch every flaw in a CIDH pile, which generally means they are small or in the lower portion of the CIDH pile (as shown with impulse response testing), but this may not be detrimental to the capacity. As previously

discussed, minor flaws will not have as great of an impact on axial capacity, but may affect lateral capacity if in a critical location (e.g. Petek *et al.* 2002, Sarhan *et al.* 2002). Further discussion of NDE methods is presented in Chapter 5.

Pile defects normally stem from an inadequate concrete fill that may be the result of several reasons. One is that the concrete is not able to readily flow through reinforcement. Another may be blockage of the concrete due to inclusions, such as sloughing because drilling slurry, or casing removal allows sediment to fall in the hole in the concrete. The introduction of innovative materials, such as improved drilling slurries and self-compacting concrete, has greatly helped in alleviating these problems.

4.4 Self-Compacting Concrete

The concrete mix design of self-compacting concrete (SCC) has been used in many other countries with excellent success, but the trend has yet to migrate to the United States. Table 22 reports on an international workshop that focused on the uses of SCC and its effectiveness in multiple structures for a wide range of projects. However, this section will not go into detail on case studies since there has not been significant research or reports on the use of SCC in CIDH piles. Although SCC has yet to be used much in the construction of CIDH piles, the success of this product in the construction of other structures is very promising in its ability to ease the difficulty of concrete placement in CIDH piles.

Table 22 Self-Compacting Concrete Case Histories

Reference	Description
Int'l Workshop on SCC 1998	Tests conducted for complicated building designs. SCC proved successful in almost all cases, with no segregation, and all void spaces filled. No reports given on the use of SCC in CIDH piles.

SCC was mainly tested on large-scale projects that would have required extremely high costs in labor and concrete placement if regular concrete were to be used. The application of SCC eliminated the requirement of using compacting machines, and in some cases the concrete was even pumped from the batch plant to the site, eliminating additional labor and transportation. Other projects utilized this product when complicated formwork made the use of regular concrete virtually impossible. Due to the high density of reinforcement in some areas, concrete segregation and inadequate fills were almost inevitable. The application of SCC was successful in each case.

The downfall to using SCC is that it is relatively expensive due to lack of material accessibility for a standard mix design. When a batch plant is called upon to make SCC, it needs to call in new materials and go through several test batches to ensure a proper

mix. If a batch plant is not experienced in this, or if the materials are not readily available, this will cause a considerable increase in cost. That is why SCC has only been truly cost-effective on large-scale projects when the reduction in construction time and labor was significant enough to justify the high price of using SCC.

In regards to CIDH pile construction, there has been concern over the increasing requirements for confinement reinforcement. The amount of spacing that is left between reinforcing bars is relatively small, and due to the fact that CIDH piles cannot easily be visually inspected as concrete is being poured, leaves much room for error. Therefore, it seems without question SCC would be a highly beneficial product for the construction of CIDH piles.

This chapter presented numerous case studies and the tested results on capacity. The effects of construction methods within each study were discussed as well as comparing the design equation predictions to the actual tested values. Chapter 5 follows up on this by showing the trends between these case studies. Construction method effects will be discussed further as well as design equation predictions.

5 DISCUSSION ON DESIGN vs. RESEARCH

Compared to the design of other structures, explicit code specifications for CIDH piles are still being developed for the first time. General conclusions on the behavior of CIDH piles can only be drawn after multiple field tests have been conducted. Therefore, CIDH pile testing and analysis has been a large focus in the last couple decades in order to set up codes and design models. However, as with any design code, advances in industry and current progress in testing require ongoing updates for code specifications. As can be concluded from the current design methodology presented in Chapter 3 regarding CIDH piles and the most recent information from the testing reported in Chapter 4, some design and construction methods should evolve, others warrant more research, while some still prove to be satisfactory. This chapter will compare and discuss the case histories and design methods from Chapters 3 and 4.

5.1 Comparisons of Construction Methods and Predictions

Numerous case studies were presented in Chapter 4 along with the predicted estimates from the design equations in Chapter 3. Plots of the numerical data from the case studies in Chapter 4 are provided in Appendix C. Some figures from Appendix C will also be included in this chapter for easy reference. Calculations for the design predictions are included in Appendix A. The following figures provide graphical comparisons of the numerical data provided in Chapter 4. Figure 10 shows the results from case studies that provided information on the tip resistance.

5.1.1 Tip Resistance

In measuring the tip resistance, cohesionless soils depend on the measured N-values, and cohesive soils are dependent on the undrained cohesive strength. Both of which are multiplied by a constant correlation factor.

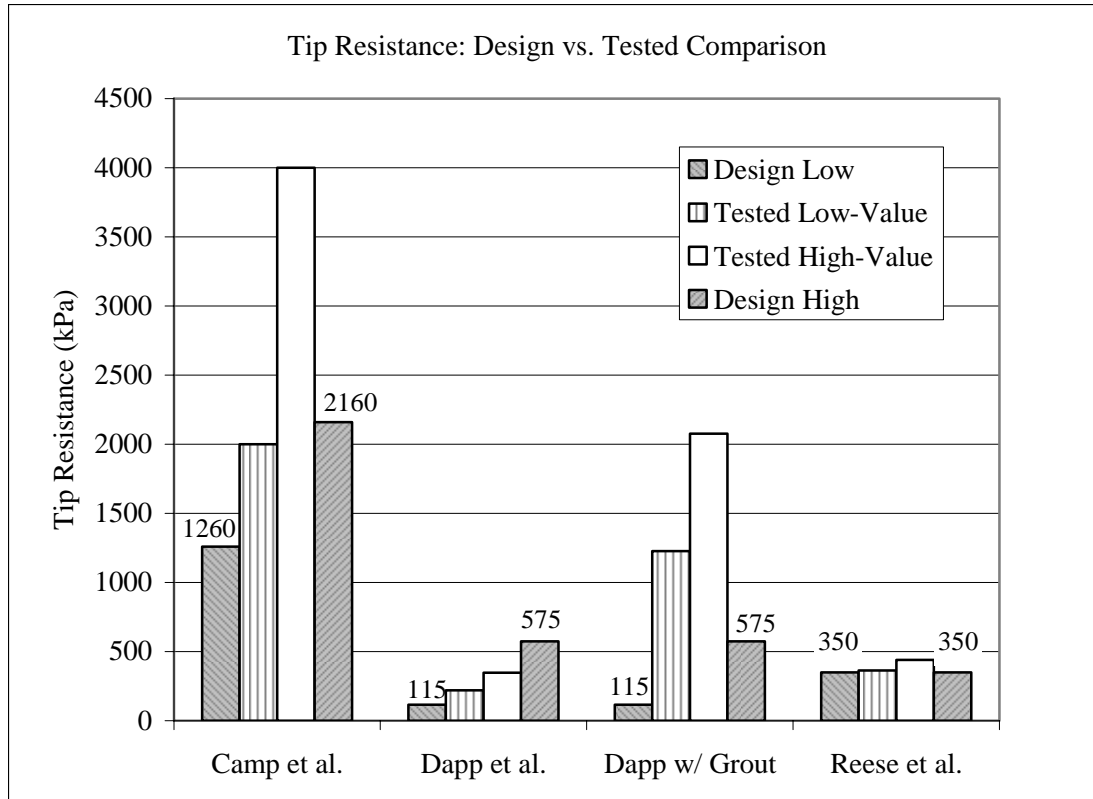


Figure 10 Comparison of case histories for tip resistance between tested- and design-values (Camp *et al.* 2002, Dapp *et al.* 2002, Reese *et al.* 1985)

Design calculations for tip capacities in clays and sands matched closely to what was obtained in the field. Figure 10 shows that tip resistances were fairly close within design ranges except in the study by Dapp *et al.* after post-grouting and for Camp *et al.* with the tested high-value, which both exceeded design values. The lower end design value for Camp *et al.* fell within the design range. Recall from Chapter 4 that these studies utilized all the typical methods of construction, slurry, dry, and casing.

These results indicate that the empirical factors are giving a relatively close comparison of what is expected in the field under *typical* construction methods. However, with post-grouting and large diameter piles, the tip resistance is underestimated for the given studies. Both the non-grouted and post-grouted tip resistance results by Dapp *et al.* are presented in Figure 10 in order to show the increase in tip capacity due to post-grouting. The failure criterion for both Camp *et al.* and Dapp *et al.* was a plunging

affect. Note that the design predictions are the same in both the non-grouted and post-grouted cases because design equations do not yet account for this method. Post-grouting is also shown to improve the side resistance, as shown in Figure 11 in Section 5.1.2, which reports on the tested and predicted values of side resistance from Chapter 4.

5.1.2 Side Resistance

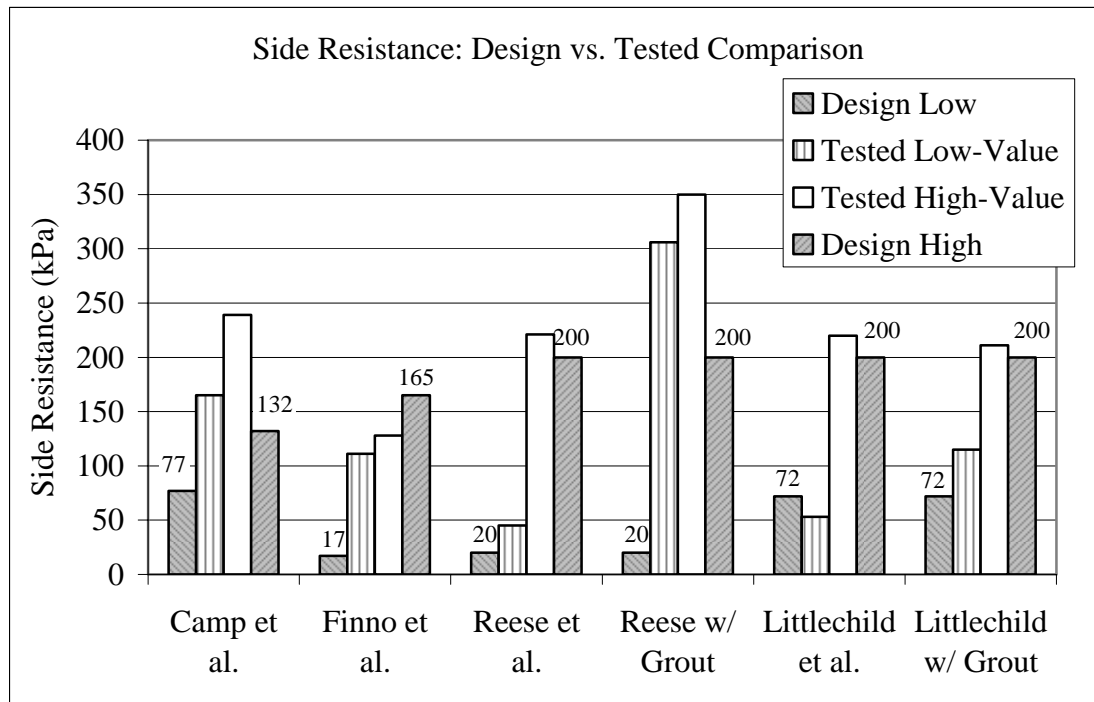


Figure 11 Comparison of case histories between design- and tested-values for side resistance (Camp *et al.* 2002, Finno *et al.* 2002, Reese *et al.* 1985, Littlechild *et al.* 2000)

Design predictions for the side resistance seem within reasonable limits of what is tested in the field, as shown in Figure 11. However, as discussed with tip resistance, the values by Camp *et al.* exceed the design capacity range as well as post-grouting. Recall that the study by Littlechild *et al.* was tipped in sands with varying densities. The high design values are for piles that were located in IGM. The IGM was strong enough that post-grouting did not aid in side resistance. However, the lower design value showed improvement with post-grouting. The study by Reese *et al.* showed a definite

improvement in side resistance, which was expected since the original low test-value piles were constructed with both permanent and temporary casing.

The study by Camp *et al.* is of special interest because it is the only published study that reports on large diameter CIDH piles, 1.8 to 2.4 meters (6 to 8 feet) in diameter. And considering this, both the tip resistance and the side resistance exceeded design values in Figure 10 and Figure 11. To further illustrate this point, Figure 12 and Figure 13 show the individual results for the side resistances and the tip resistances, respectively.

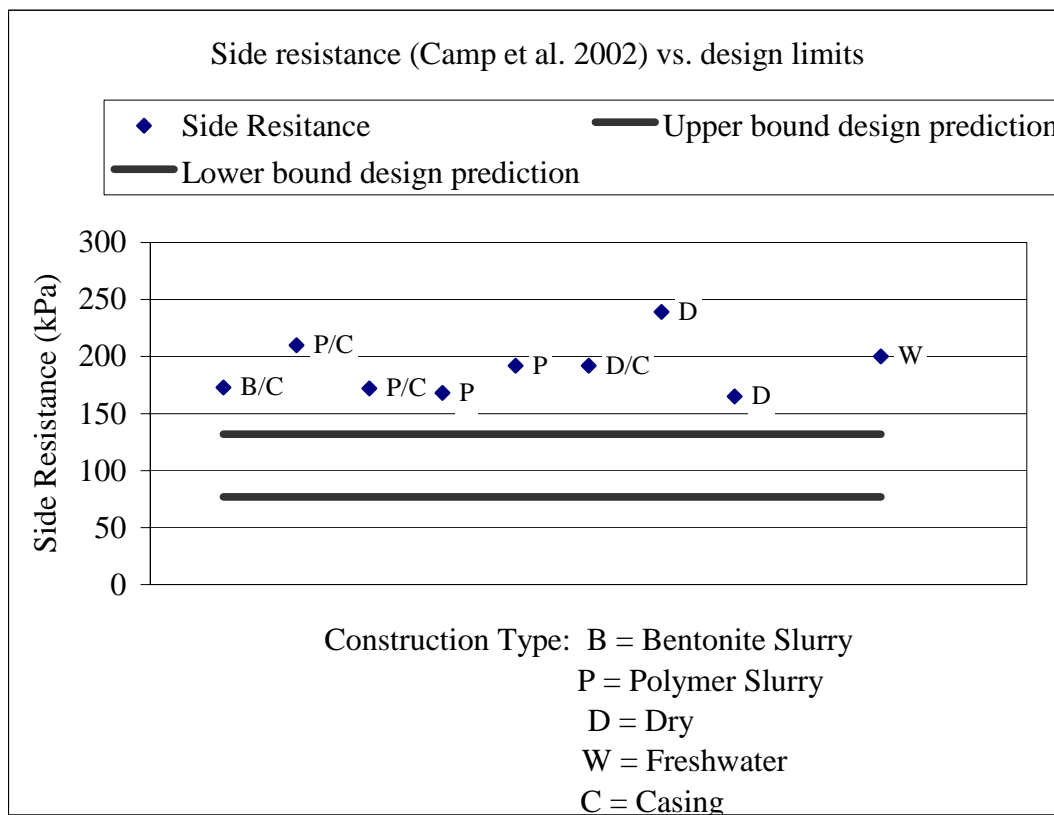


Figure 12 Tested side resistance values in portions of the pile without casing for Camp *et al.* (2002)

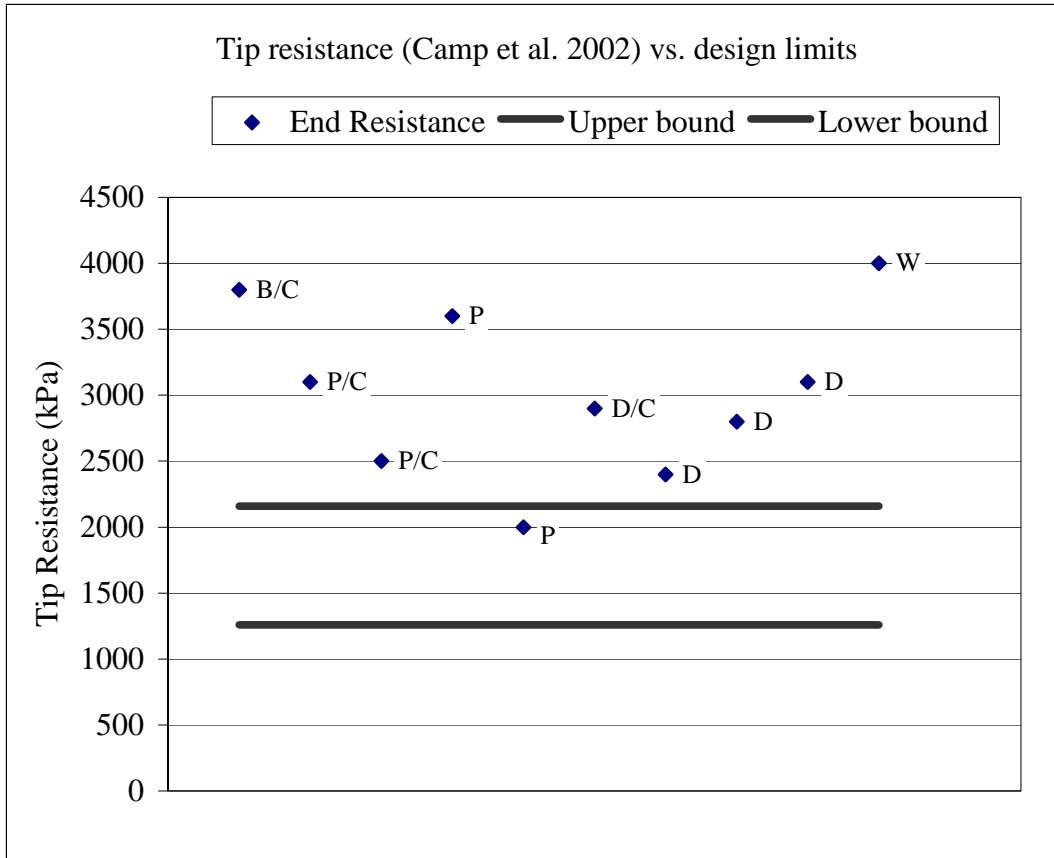


Figure 13 Tested tip resistances for Camp *et al.* (2002)

Note that almost every value exceeds the design predictions. This could be due solely to the fact that the piles are located in stiff Cooper Marl clay, which was noted to have extraordinarily stiff properties (Camp *et al.* 2002), or because displacements were not limited thus full tip capacities could be achieved. In either case, further testing of large diameter CIDH piles may be able to provide better information as to their applicability with current design methods.

Cased piles reported lower side resistance than non-cased areas in both the studies by Camp *et al.* and Reese *et al.* as shown in Figure 14. Note that the values given for Camp *et al.* are less than the design values for both the low-end and high-end values. However, for Reese *et al.* the low-end value actually exceeds the low design prediction.

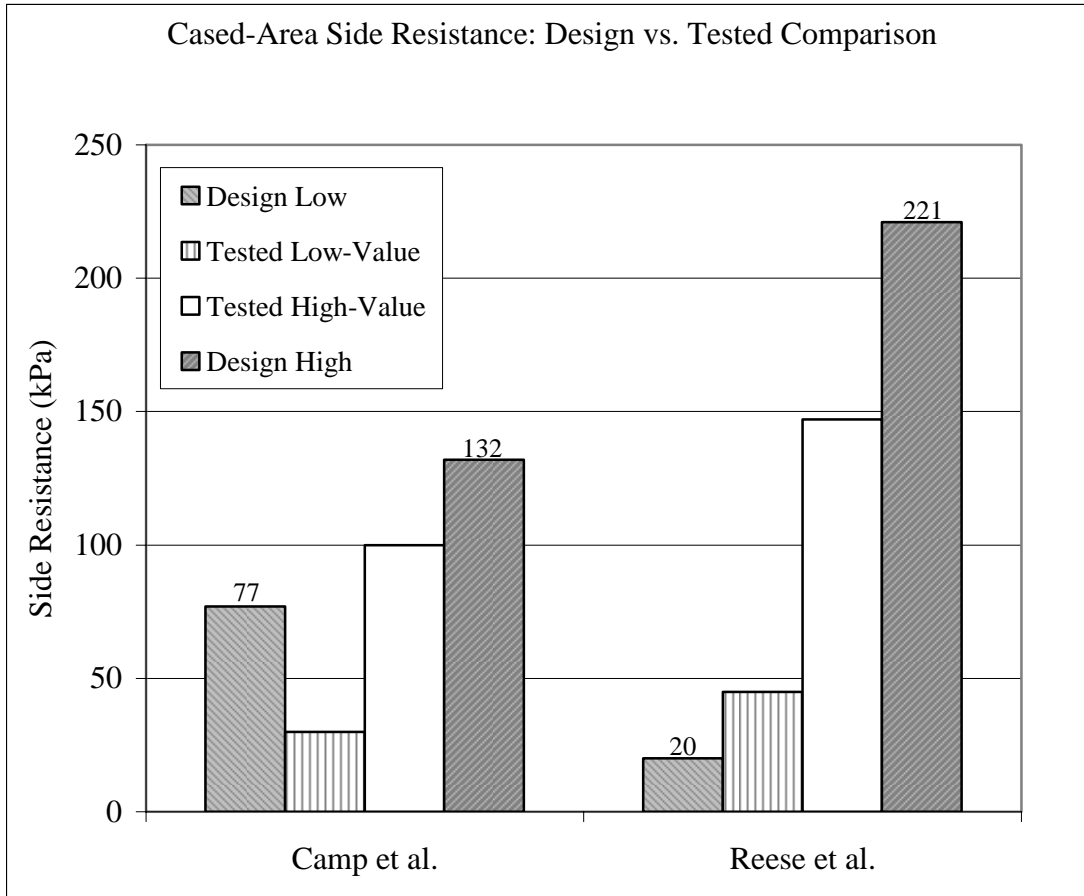


Figure 14 Side resistances reported for the cased areas of CIDH piles compared to design predictions (Camp *et al.* 2002, Reese *et al.* 1986)

According to the results presented in Figure 14, it is evident that side resistance does still exist with cased areas in CIDH piles. However, as noted in Chapter 3 for the design method followed by Caltrans for side resistance, cased areas of the CIDH pile are generally discounted in contributing any side resistance. These results indicate that some side resistance could be accounted for. The design assumption that the side resistance goes to zero with casing is conservative, but without further information, it is difficult to say just how much of the cased side resistance is reliable.

Both sections on tip and side resistance reported that typical construction methods meet standard design estimates, but differ in areas of post-grouting and large diameter piles. Similar results are found in Section 5.1.3, which reports on the total axial capacity comparisons that are shown in Figure 15.

5.1.3 Total Axial Capacity

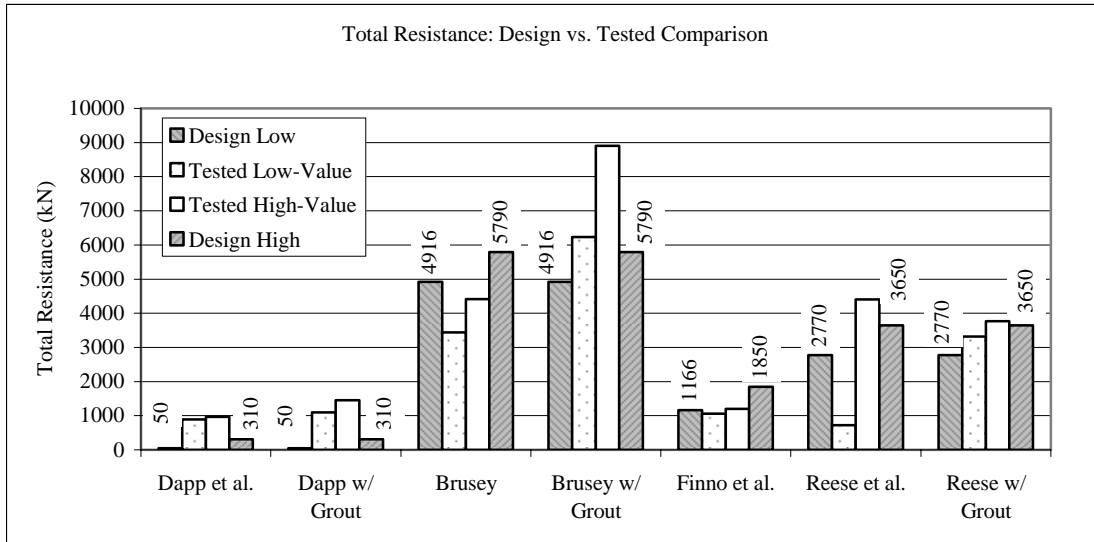


Figure 15 Comparison of case histories between design- and tested-values for the total resistance (Dapp *et al.* 2002, Brusey 2000, Finno *et al.* 2002, and Reese *et al.* 1985)

Following the same trend as before, post-grouting significantly increases the total axial capacity. The initial tests performed by Brusey (2000) did not meet the design predictions; however, after post-grouting both design values were exceeded. Recall from Chapter 4 that typical soil properties had to be assumed for the study by Brusey.

The validity of using typical soil properties in this report is that this is what may be used in actual preliminary designs. Accurate and detailed site specific soil data is not always readily available for every job, although it is recommended to obtain as much information as possible.

In conclusion of this section, design equations seem to adequately predict the axial resistance of CIDH piles under typical construction procedures. However, in regards to post-grouting and large diameter CIDH piles, changes in design are warranted. Large diameter CIDH piles are rising in the industry, thus further testing and research would benefit design methods. Post-grouting has received more attention in testing than large diameter piles, and shows great potential for improved confidence in CIDH pile

construction. In terms of how typical construction methods affect the axial capacity of CIDH piles, the use of permanent casing is the only method that shows a marked decrease in capacity. However, further testing may aid design methods in regards to casing, because as shown by Camp *et al.* and Reese *et al.*, not all side resistance is lost. These case studies also showed that the side resistance in cased areas was recovered with the application post-grouting.

Post-grouting seems to aid in all areas of CIDH pile construction. If casing cannot be removed, the side resistance can be recovered by post-grouting. If flaws are found in the pile, the voids may be filled with grout. If bottom cleanliness or excessive displacements are a concern, post-grouting the tip has shown to be effective because the material at the tip is pre-compacted, thus full tip capacity can be achieved under less displacement. When this full axial capacity is achieved, it exceeds the design prediction. Bottom cleanliness is a large concern in the construction of CIDH piles, and generally, tip resistance will be discounted because of it.

5.2 Bottom Cleanliness

Ensuring a minimum amount of sediment at the bottom of the borehole is often difficult. Adequate bottom cleanliness, therefore, is not expected by the designer and the tip resistance will often be discounted. However, the case study by Camp *et al.* (2002) constructed piles with slurry, and although the bottom cleanliness standard was not always met, the axial capacity did not significantly decrease. A plot of the data in Figure 16 compares the average sediment depth to the ultimate end bearing capacity tested by Camp *et al.* As can be observed in Figure 16, cases with thicker average sediment resulted in higher bearing capacity. This may be attributed to the fact that the piles were not limited by displacements, thus all the sediment was compacted and full tip capacity could be achieved. Therefore, if sediment can be compacted ahead of time, this capacity can be reached and even exceeded, as was shown in the case studies.

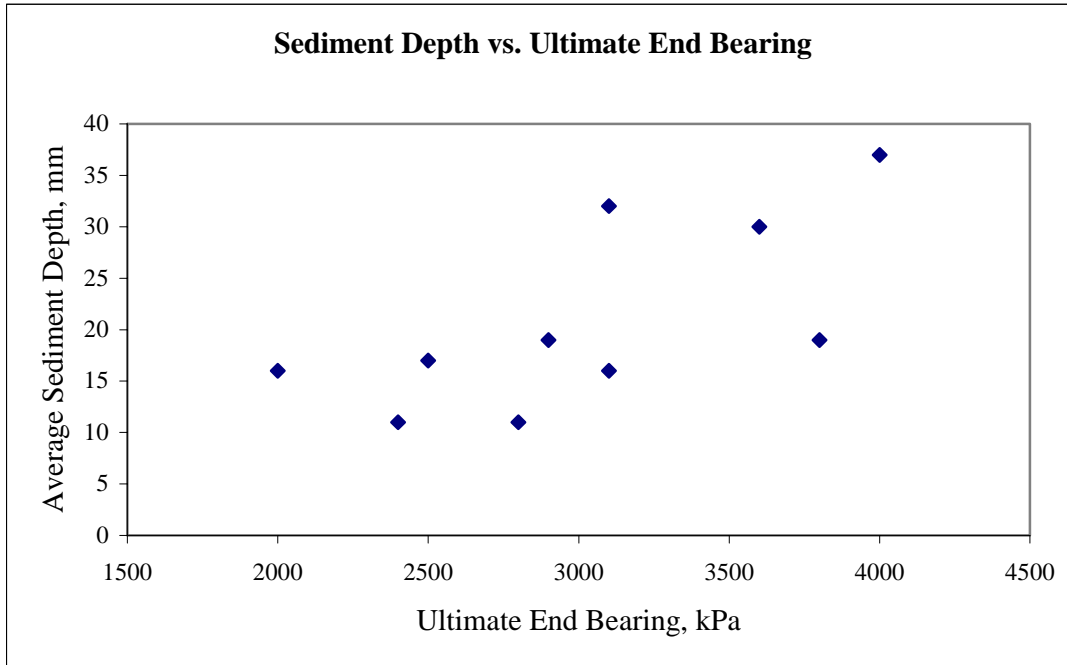


Figure 16 Average reported sediment depth vs. ultimate end-bearing from the case study by Camp *et al.* (2002)

Figure 16 shows that the average sediment depth was kept fairly constant, around 10-15 mm; however, the maximum end-bearing capacities occurred when sediment depths were greatest. This may be attributed to the pile having to displace more in order to utilize its full tip capacity. To check this, plots of the ultimate settlement versus the sediment depth, shown in Figure 17, and the ultimate load versus the ultimate settlement, in Figure 18, are compared.

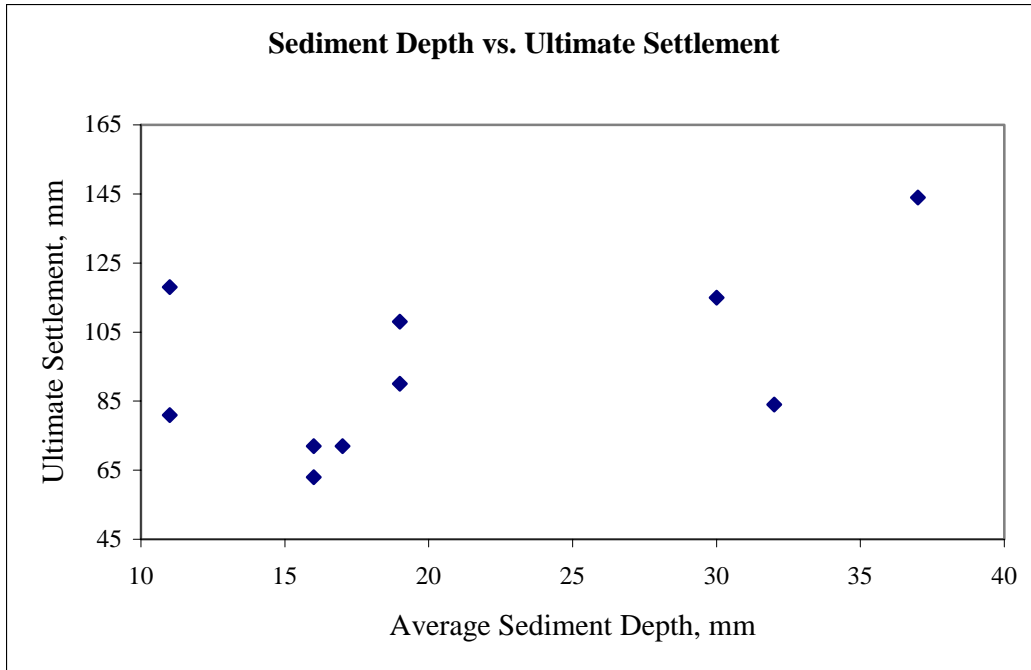


Figure 17 Comparison of the ultimate settlement to the average sediment depths as reported by Camp *et al.* (2002)

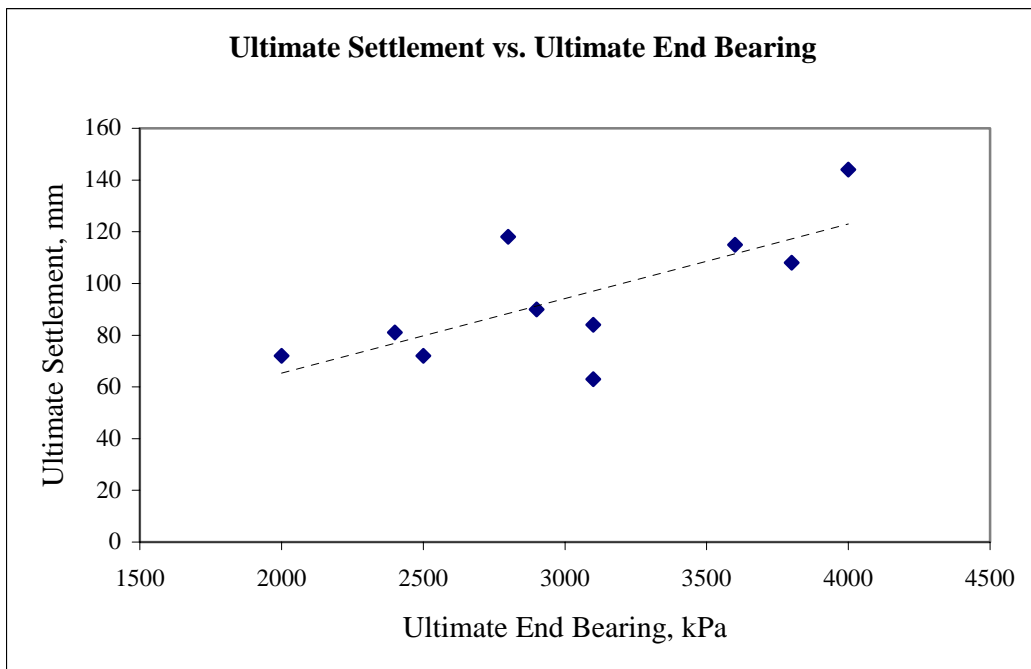


Figure 18 Comparison of the ultimate settlement to the end-bearing resistance as reported by Camp *et al.* (2002)

In reviewing Figure 17 and Figure 18 it may be concluded that the settlement increases as the end-bearing resistance increases. However, the affect of the sediment depth on the ultimate settlement does not show much correlation. This indicates that the soil itself at the base, regardless of sediment has to compact a specific amount. Therefore, in order to reduce displacements, compaction of this material would be beneficial, which can be attained through post-grouting. Further research on this subject is warranted since tip capacity can greatly contribute to the overall axial capacity of the pile. The application of post-grouting at the tip may be able to compact the sediment at the bottom of the pile and eliminate concern of this problem as well. Designers may soon be able to account for both the tip and the side resistance acting together.

5.3 Anomaly Effects and Non-Destructive Testing

The effects of NDE methods not detecting anomalies was the focus of several case histories in Section 4.1. As shown by Petek *et al.* (2002), the axial capacity of the pile is more dependent on the side and tip resistance obtained with the soil. If an anomaly occurs at the bottom of the pile within the concrete, the lateral capacity of the pile is not affected, because lateral loads are generally transferred in the upper portion of the pile. Anomalies in the bottom of the pile did not significantly decrease axial capacity. Therefore, anomalies in the top of the pile are the most important to find. Also, as found by Finno *et al.*, the axial capacity did not vary much between the pile with anomalies and the one constructed without. Petek *et al.* (2002) also recognized that defects occurring in piles located in weak soils did not affect the capacity as much as piles with defects in stiff soils as shown in Figure 19 and Figure 20. These figures also show that defects located in the lower portions of the pile have little effect on capacity, regardless of the soil type.

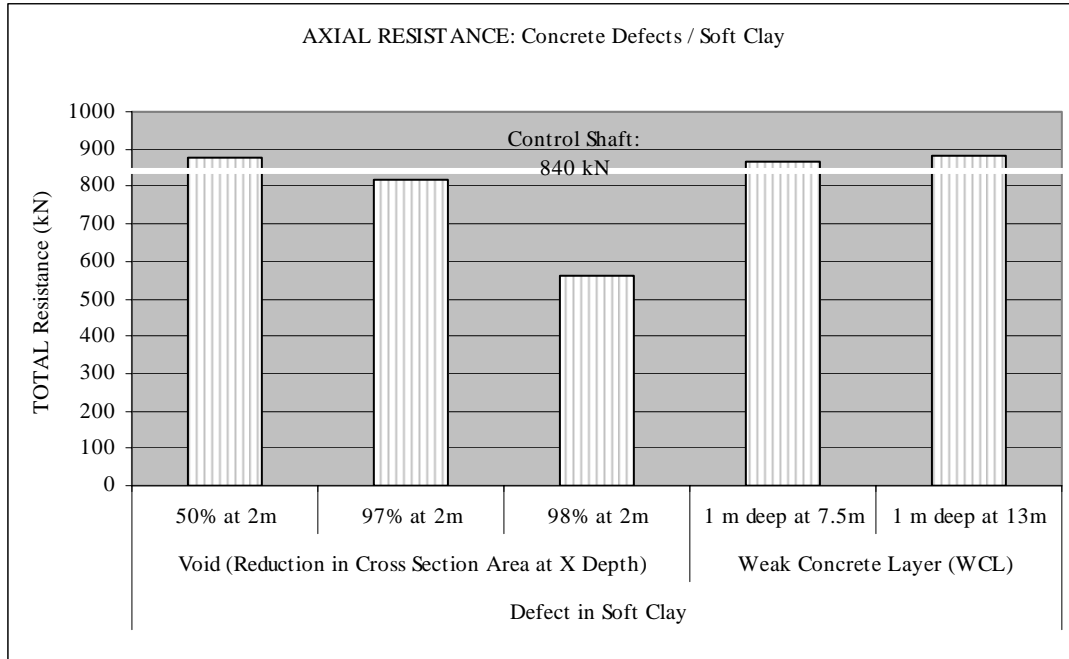


Figure 19 Axial capacity effects from defects in pile located in soft clay (Petek *et al.* 2002)

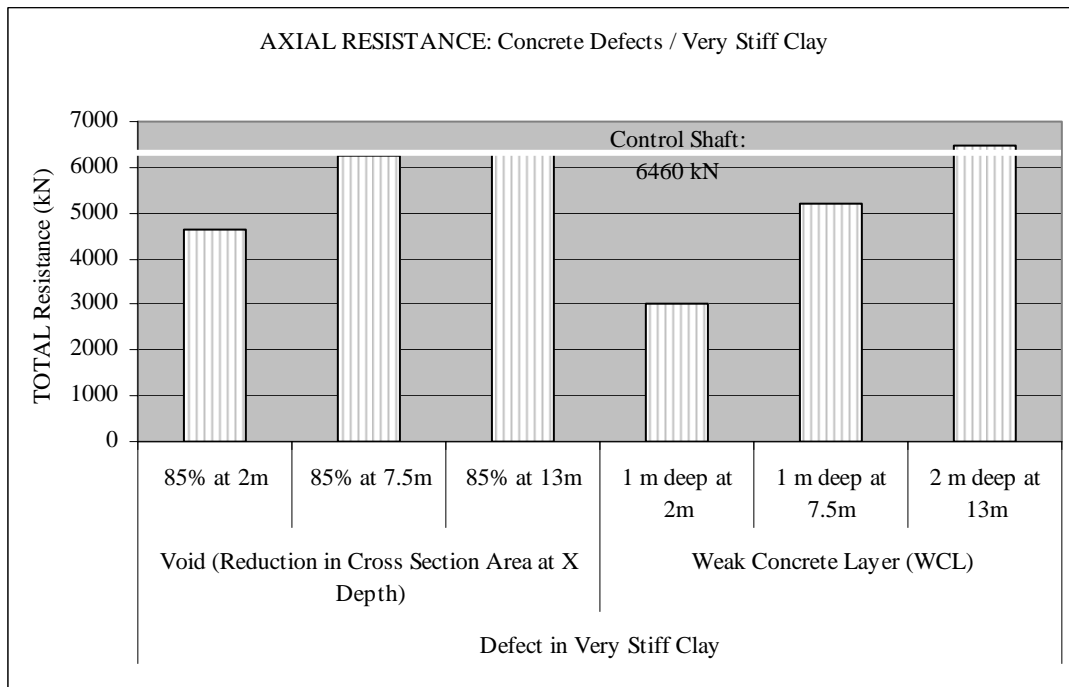


Figure 20 Axial capacity effects from defects in pile located in very stiff clay (Petek *et al.* 2002)

The CIDH piles on the NGES site were located in soft clay, which as shown in Figure 19, the failure of the clay occurs before the concrete; therefore, the anomalies in the concrete had less affect in controlling the ultimate capacity.

Studies by Petek *et al.* (2002) and Sarhan *et al.* (2002) researched the affect of different sized anomalies on the axial and lateral behavior of CIDH piles. The general conclusions were that a reduction in cross-section of 30% would cause a noticeable difference in lateral capacity. However, this size of defect would most likely be detected by NDE methods. Another factor to consider is if the flaw extends to the edge of the pile, thus exposing the reinforcing bars. In this case, corrosion becomes an issue (Sarhan *et al.* 2002). If the defect occurs in a critical location in the pile where lateral resistance is high, the loss of strength in the rebar due to corrosion could be detrimental. Sarhan *et al.* defined a minor flaw as one being less than 15% the cross-sectional area. This size of anomaly can reduce the capacity significantly if corrosion occurs.

The most effective NDE methods were the CSL testing coupled with gamma-gamma log testing. These two tests performed together report on the entire cross-section of the pile. The impact hammer method was not as effective in finding anomalies.

In consideration of both case studies over anomaly effects and NDE methods, further researched should be performed on the effect of anomalies. If NDE methods detect a flaw in the pile, it is at the discretion of the designer as to what action is to be taken regarding the anomaly. Further research would provide a better reference as to how much an anomaly, depending on size and location, will affect the capacity. Anomalies that are shown to have negligible effect on the capacity can then be disregarded, eliminating additional repair costs.

The cause of these anomalies is often attributed to poor concrete quality, due to segregation or voids. The introduction of consistent, good quality concrete mixes that have the desired quality for CIDH piles would be beneficial in construction. Therefore, research and testing on the use of SCC is recommended.

5.4 Self-Compacting Concrete

As discussed briefly in Chapter 4, SCC is a product that has been very successful in the application of structures. Due to the fact that concrete mixes in CIDH pile construction must be as fluid as possible and able to compact adequately under its own weight, further research on the use of SCC in CIDH piles would be of great benefit to aid in construction.

Due to the high seismic activity in California, specifications require much by way of reinforcing in joints and columns. Therefore, it is common practice to specify a highly fluid concrete, as is also the case with CIDH piles. In the 1997 Caltrans Foundation Manual, the Concrete Compressive Strength and Consistency Requirements state, “the concrete must also have a high fluidity in order to flow through the rebar cage, compact and consolidate under its own weight without the use of vibration, and to deliver high lateral stresses on the sides of the drilled hole in order to keep the drilled hole from collapsing...” This requirement is more or less the definition of SCC; however, this product has yet to be used much in CIDH pile construction. Caltrans specifies many admixtures in their concrete mixes, but mix designs change with each project. These unique concrete mixes not only increase cost, but also cause unexpected results to occur such as increased set time and lowered strength gain. Thus, if a specific mix design were consistently used on projects, the cost of these mixes would decrease and the product could be administered with more confidence. Research on this product would be beneficial for all construction applications.

The comparisons presented in this chapter provide information on the axial design of CIDH piles, construction procedures and their effects, bottom cleanliness, and SCC. It was shown that design methods seem fairly accurate for typical construction methods; however, new developments such as large diameter piles and post-grouting may need a modified method of design. Areas where decreases in resistance were expected, such as the use of casing and soft bottoms, were confirmed with casing but not with bottom

cleanliness. SCC is also mentioned as a topic that needs more research. Chapter 6 makes recommendations based on these conclusions.

This page is intentionally blank.

6 RECOMMENDATIONS

CIDH piles are a relatively new foundation type and improvements to their construction are very rapid. Although there is still much to learn about CIDH piles, the recent developments in CIDH pile construction should be made known so that the industry can progress. The topics in this report are presented with the hope of providing insight for future research topics and potential changes in practice. Provided below are recommendations, based on the comparisons in this study between the actual design methods employed in practice and recent tested developments, that may benefit and advance the industry surrounding CIDH piles.

1. Further research on post-grouting is recommended because it was shown to benefit axial capacity in each pertaining case. The loss of side resistance in cased sections, the issue of bottom cleanliness, displacements, and the disregard of tip resistance in design are all areas that post-grouting benefits. Further research on post-grouting is also recommended in regards to the most efficient grouting method.
2. Further research is also recommended on large diameter CIDH piles. Large diameter CIDH pile testing information is limited, and as shown in the comparisons of chapter 5, current design procedures do not accurately predict the capacity obtained in the field. Since large diameter CIDH piles are increasing in popularity for deep foundations, further research may be warranted in order to better predict their behavior.
3. Methods of calculating the side resistance should also be researched for large diameter piles, permanent casing, and for post-grouting. The current design methodologies adequately match what is shown in testing for typical construction procedures, however, this is not the case otherwise. Large diameter CIDH piles are underestimated in capacity, as well as piles that are

post-grouted. In terms of casing, side resistance is eliminated when it is used; however, the side resistance in a cased area does not go to zero.

4. The use of self-compacting concrete on CIDH piles is a good construction application and research topic. This concrete mix has been used on a variety of structural projects and eased the difficulty of construction, thus its performance in CIDH pile construction is of interest.

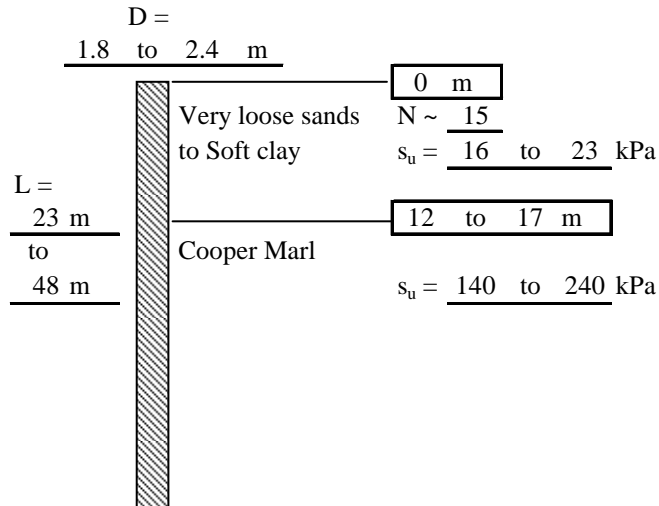
In regards to this research, much gratitude would like to be expressed to the California Department of Transportation for their support and contributions.

APPENDIX A

Sample calculations for Chapter 4:

1.) Camp *et al.* (2002)

Given:



Assumptions: Sand Unit Weight = 17.5 kN/m³
 SPT N-Value = 15
 Water Table Location: 0 m

Calculations:

TIP: $q_p = Q_p / A_b = N_c * s_u$ [Eqn. 15]

Minimum L/D = 13 ≥ 4, therefore N_c = 9

$q_{p,min} = 9 * 140 = \underline{\underline{1260}}$ kPa

$q_{p,max} = 9 * 240 = \underline{\underline{2160}}$ kPa

SIDE: Cooper Marl:

$q_s = Q_s / A_s = \alpha * s_u$ [Eqn. 16]

$\alpha = 0.55$

$q_{s,min} = 0.55 * 140 = \underline{\underline{77}}$ kPa

$q_{s,max} = 0.55 * 240 = \underline{\underline{132}}$ kPa

Upper Layer: Clay:

$$q_{s,\min} = 0.55 * 16 = \underline{\underline{9}} \text{ kPa}$$

$$q_{s,\max} = 0.55 * 23 = \underline{\underline{13}} \text{ kPa}$$

Upper Layer: Sand:

$$q_s = Q_s / A_s = \beta * \sigma'_v \quad [\text{Eqn. 6}]$$

$$\beta = 1.5 - 0.245 * (z_i)^{0.5} \quad (N < 50) \quad [\text{Eqn. 7}]$$

$$z_{i,\min} = 12 / 2 = 6 \text{ m}$$

$$z_{i,\max} = 17 / 2 = 8.5 \text{ m}$$

$$\beta_{i,\min} = \frac{1.5 - 0.245 * (6)^{0.5}}{1} = \underline{\underline{0.9}}$$

$$\beta_{i,\max} = \frac{1.5 - 0.245 * (8.5)^{0.5}}{1} = \underline{\underline{0.8}}$$

$$\sigma'_{v,\min} = \gamma' * z_i = (17.5 - 9.8) * 6 = \underline{\underline{46}} \text{ kPa}$$

$$\sigma'_{v,\max} = \gamma' * z_i = (17.5 - 9.8) * 8.5 = \underline{\underline{65}} \text{ kPa}$$

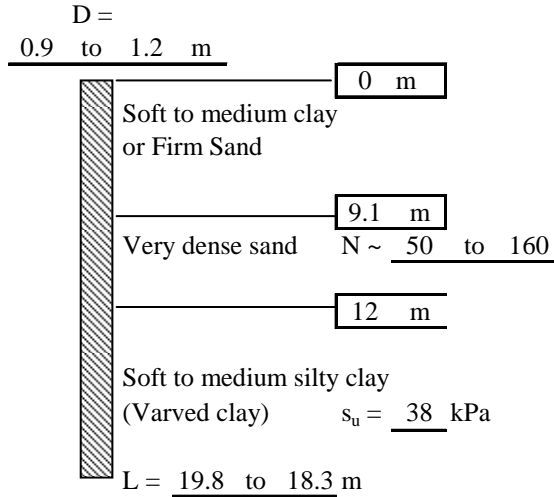
$$q_{s,\min} = 0.90 * 46 = \underline{\underline{42}} \text{ kPa}$$

$$q_{s,\max} = 0.79 * 65 = \underline{\underline{51}} \text{ kPa}$$

Conclusions: Use side resistance values calculated for Cooper Marl since this is where the shafts were instrumented.

2.) Reese *et al.* (1985)

Given:



Assumptions:

Sand Unit Weight = 21.0 kN/m³

Clay Unit Weight = 11.5 kN/m⁴

SPT N-Value = 100

Water Table Location: 0 m

Upper layer, $s_u = 38$ kPa

Atmospheric Pressure, $p_a = 101$ kPa

- In computing side resistance, the upper 1.5 m and lower D length does not contribute

Calculations:

TIP: $q_p = Q_p / A_b = N_c * s_u$ [Eqn. 15]

Minimum L/D = 22 \geq 4, therefore $N_c = 9$

$q_p = 9 * 38 = 342$ kPa

$A_{b, \min} = \pi / 4 * (0.9)^2 = 0.636$ m²

$A_{b, \max} = \pi / 4 * (1.2)^2 = 1.13$ m²

$Q_{p, \min} = 0.636 * 342 = 218$ kN

$Q_{p, \max} = 1.131 * 342 = 387$ kN

SIDE: Soft to Medium Clay

$q_s = Q_s / A_s = \alpha * s_u$ [Eqn. 16]

$\alpha = 0.55$

$$q_s = 0.55 * 38 = \underline{\underline{20.9}} \text{ kPa}$$

$$L_{e, \min} = 19.8 - 0.9 - 1.5 - (12 - 9.1) = \underline{\underline{14.4}} \text{ m}$$

$$L_{e, \min} = 18.3 - 1.2 - 1.5 - (12 - 9.1) = \underline{\underline{12.6}} \text{ m}$$

$$A_{s, \min} = \pi * (0.9) * (14.4) = \underline{\underline{40.7}} \text{ m}^2$$

$$A_{s, \max} = \pi * (1.2) * (12.6) = \underline{\underline{47.5}} \text{ m}^2$$

$$Q_{s, \min} = 20.9 * 40.7 = \underline{\underline{851}} \text{ kN}$$

$$Q_{s, \max} = 20.9 * 47.5 = \underline{\underline{993}} \text{ kN}$$

Stiff Sand layer

$$q_s = Q_s / A_s = \beta * \sigma_v' \leq \underline{\underline{200}} \text{ kPa} \quad [\text{Eqn. 6}]$$

$$\begin{aligned} \sigma_{vi}' = \Sigma \gamma' * z_i &= (11.5 - 9.8) * (9.1) + (21.0 - 9.8) * (12.1 - 9.1) / 2 \\ &= \underline{\underline{32}} \text{ kPa} \end{aligned}$$

$$\beta = K_o * \tan \phi_i' \quad (N > 50) \quad [\text{Eqn. 10-12}]$$

$$\begin{aligned} \phi_i' &= \tan^{-1} (N / [12.3 + 20.3 * (\sigma_{vi}' / p_a)])^{0.34} \\ &= \underline{\underline{1.06}} \end{aligned} \quad [\text{Eqn. 11}]$$

$$\begin{aligned} K_o &= (1 - \sin \phi_i') * (0.2 * p_a * N / \sigma_{vi}')^{\sin \phi_i'} \\ &= \underline{\underline{4.75}} \end{aligned} \quad [\text{Eqn. 12}]$$

$$q_s = 4.75 * \tan(1.06) * 32 = 271 \text{ kPa} > \underline{\underline{200}} \text{ kPa}$$

$$A_{s, \min} = \pi * (0.9) * (12.1 - 9.1) = \underline{\underline{8.5}} \text{ m}^2$$

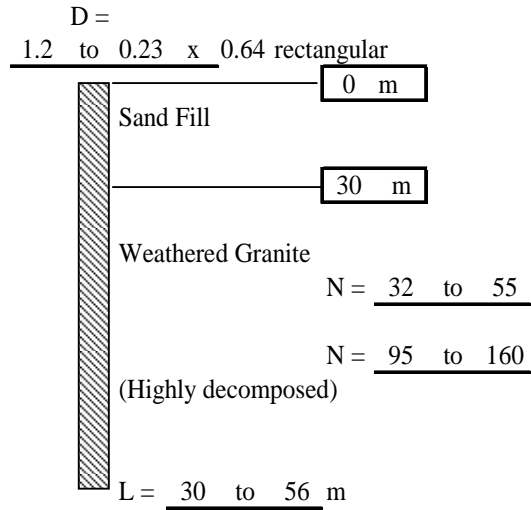
$$A_{s, \max} = \pi * (1.2) * (12.1 - 9.1) = \underline{\underline{11.3}} \text{ m}^2$$

$$Q_{s, \min} = 200 * 8.5 = \underline{\underline{1696}} \text{ kN}$$

$$Q_{s, \max} = 200 * 11.3 = \underline{\underline{2262}} \text{ kN}$$

3.) Littlechild *et al.* (2000)

Given:



Assumptions:

Sand Unit Weight = 19.0 kN/m³

Water Table Location: 0 m

IGM, N = 100

Atmospheric Pressure, p_a = 101 kPa

Calculations:

SIDE: Loose Sands (N<55):

$$q_s = Q_s / A_s = \beta * \sigma_v' \quad [\text{Eqn. 6}]$$

$$\beta = 1.5 - 0.245 * (z_i)^{0.5} \quad (N < 50) \quad [\text{Eqn. 7}]$$

$$z_{i, \min} = 30 / 2 = 15 \text{ m}$$

$$z_{i, \max} = 56 / 2 = 28 \text{ m}$$

$$\beta_{i, (\min, z)} = 1.5 - 0.245 * (15)^{0.5} = 0.6$$

$$\beta_{i, (\max, z)} = 1.5 - 0.245 * (28.0)^{0.5} = 0.2 < 0.25$$

$$\sigma_{v, \min}' = \gamma' * z_i = (19.0 - 9.8) * 15 = 138 \text{ kPa}$$

$$\sigma_{v, \max}' = \gamma' * z_i = (19.0 - 9.8) * 28 = 258 \text{ kPa}$$

$$q_{s, \min} = 0.55 * 138 = 76 \text{ kPa}$$

$$q_{s, \max} = 0.25 * 258 = 64 \text{ kPa}$$

Dense Sands (N>55):

$$q_s = Q_s / A_s = \beta * \sigma_v' \leq \underline{200 \text{ kPa}} \quad [\text{Eqn. 6}]$$

$$\beta = K_o * \tan \phi_i' \quad (N>50) \quad [\text{Eqn. 10-12}]$$

$$\phi_i' = \tan^{-1} (N / [12.3 + 20.3 * (\sigma_{vi}' / p_a)])^{0.34} \quad [\text{Eqn. 11}]$$

$$K_o = (1 - \sin \phi_i') * (0.2 * p_a * N / \sigma_{vi}')^{\sin \phi_i'} \quad [\text{Eqn. 12}]$$

$$\phi_{i', (\text{min}, z)} = \underline{0.94}$$

$$\phi_{i', (\text{max}, z)} = \underline{0.86}$$

$$K_{o, (\text{min}, z)} = \underline{1.68}$$

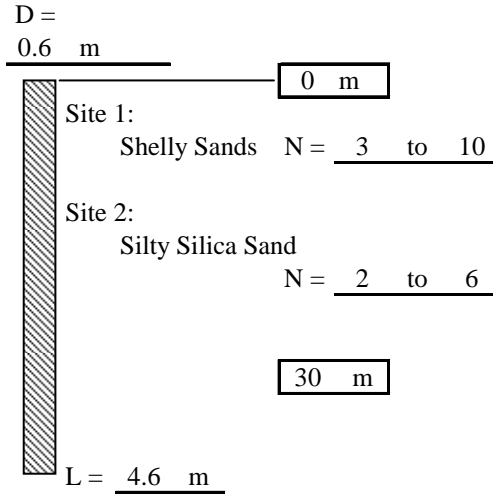
$$K_{o, (\text{max}, z)} = \underline{1.15}$$

$$q_{s, \text{min}} = 138 * \tan (0.94) * 1.68 = 317 \text{ kPa} > \underline{\underline{200 \text{ kPa}}}$$

$$q_{s, \text{max}} = 258 * \tan (0.86) * 1.15 = 345 \text{ kPa} > \underline{\underline{200 \text{ kPa}}}$$

4.) Dapp *et al.* (2002)

Given:



Assumptions:

Sand Unit Weight = 17.5 kN/m³

Water Table Location: 0 m and > 4.6 m

Calculations:

TIP: $q_p = 57.5 * N$ (kPa) [Eqn. 22]

$$q_{p, \min} = 57.5 * 2 = 115 \text{ kPa}$$

$$q_{p, \max} = 57.5 * 10 = 575 \text{ kPa}$$

$$A_b = \pi / 4 * 0.6^2 = 0.28 \text{ m}^2$$

$$Q_{p, \min} = 115 * 0.28 = 33 \text{ kN}$$

$$Q_{p, \max} = 575 * 0.28 = 163 \text{ kN}$$

SIDE: $q_s = Q_s / A_s = \beta * \sigma_v'$ [Eqn. 6]

$$\beta = (N / 15) * (1.5 - 0.245 * (z_i)^{0.5}) \quad (N < 15) \quad \text{[Eqn. 8]}$$

$$\beta_{i, (\min, z)} = (2/15) * (1.5 - 0.245 * (4.6 / 2)^{0.5}) = 0.15 < 0.25$$

$$\beta_{i, (\min, z)} = (10/15) * (1.5 - 0.245 * (4.6 / 2)^{0.5}) = 0.75$$

$$\sigma_{v', \min} = \gamma' * z_i = (17.5 - 9.8) * 2.3 = 17.7 \text{ kPa}$$

$$\sigma_{v', \max} = \gamma * z_i = (17.5) * 2.3 = 40 \text{ kPa}$$

$$q_{s,\min} = 17.7 * 0.25 = \underline{\underline{4.4 \text{ kPa}}}$$

$$q_{s,\max} = 40.3 * 0.75 = \underline{\underline{30.3 \text{ kPa}}}$$

$$A_s = \pi * 0.6 * 4.6 = \underline{\underline{8.7 \text{ m}^2}}$$

$$Q_{s,\min} = 4 * 8.67 = \underline{\underline{38 \text{ kN}}}$$

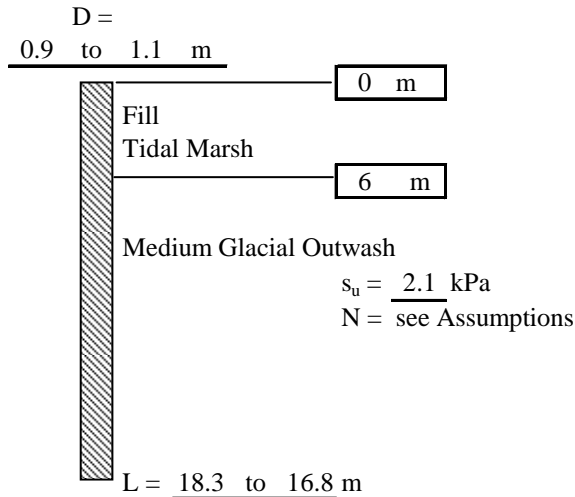
$$Q_{s,\max} = 30 * 8.67 = \underline{\underline{263 \text{ kN}}}$$

$$Q_{u,\min} = 33 + 38 = \underline{\underline{71 \text{ kN}}}$$

$$Q_{u,\max} = 163 * 263 = \underline{\underline{425 \text{ kN}}}$$

5.) Brusey (2000)

Given:



Assumptions:

Fill Unit Weight = 19.0 kN/m³

Glacial Outwash = 21.0 kN/m³

Water Table Location: 0 m

$N_q =$ 20 (Meyerhof and Vesic average)

- Assume N-values within a typical range ($15 < N < 50$)

- Assumes top layers and bottom D length do not contribute to side resistance

Calculations:

TIP: $q_p = Q_p/A_b = \sigma_{vi}' * (N_q - 1)$ [Eqn. 26]

$\sigma_{vb,PG}' = \Sigma \gamma' * z_i = (19.0 - 9.8) * (6) + (21.0 - 9.8) * (16.8 - 6.0)$
 $=$ 176 kPa POST-GROUTED SHAFT

$\sigma_{vb,NG}' = \Sigma \gamma' * z_i = (19.0 - 9.8) * (6) + (21.0 - 9.8) * (18.3 - 6.0)$
 $=$ 193 kPa NON-GROUTED

$q_{p,PG} = 176 * (20 - 1) =$ 3347 kPa

$q_{p,NG} = 193 * (20 - 1) =$ 3666 kPa

$A_{b,PG} = \pi / 4 * 1.1^2 =$ 1 m² POST-GROUTED

$A_{b,NG} = \pi / 4 * 0.9^2 =$ 0.6 m² NON-GROUTED

$$Q_{p,PG} = 3347 * 1 = \underline{\underline{3181 \text{ kN}}}$$

$$Q_{p,NG} = 3666 * 0.6 = \underline{\underline{2332 \text{ kN}}}$$

$$\text{SIDE: } q_s = Q_s / A_s = \beta * \sigma_{vi}' \quad [\text{Eqn. 6}]$$

$$\beta = 1.5 - 0.245 * (z_i)^{0.5} \quad (N < 50) \quad [\text{Eqn. 7}]$$

$$\begin{aligned} \sigma_{vi,PG}' &= \Sigma \gamma' * z_i = (19.0 - 9.8) * (6) + (21.0 - 9.8) * (16.8 - 6.0) / 2 \\ &= \underline{116 \text{ kPa}} \quad \text{POST-GROUTED SHAFT} \end{aligned}$$

$$\begin{aligned} \sigma_{vi,NG}' &= \Sigma \gamma' * z_i = (19.0 - 9.8) * (6) + (21.0 - 9.8) * (18.3 - 6.0) / 2 \\ &= \underline{124 \text{ kPa}} \quad \text{NON-GROUTED SHAFT} \end{aligned}$$

$$z_{i,PG} = 6 + (16.8 - 6) / 2 = 11 \text{ m}$$

$$z_{i,NG} = 6 + (18.3 - 6) / 2 = 12 \text{ m}$$

$$\beta_{i,(PG)} = 1.5 - 0.245 * (11)^{0.5} = \underline{0.7}$$

$$\beta_{i,(NG)} = 1.5 - 0.245 * (12.2)^{0.5} = \underline{0.6}$$

$$q_{s,PG} = 116 * 0.7 = \underline{78 \text{ kPa}}$$

$$q_{s,NG} = 124 * 0.6 = \underline{80 \text{ kPa}}$$

$$A_{PG} = \pi * 1.1 * (16.8 - 6 - 1.1) = \underline{34 \text{ m}^2}$$

$$A_{NG} = \pi * 0.9 * (18.3 - 6 - 0.9) = \underline{32 \text{ m}^2}$$

$$Q_{s,PG} = 78 * 34 = \underline{\underline{2609 \text{ kN}}}$$

$$Q_{s,NG} = 80 * 32 = \underline{\underline{2584 \text{ kN}}}$$

TOTAL:

$$Q_{u,PG} = 3181 + 2609 = \underline{\underline{5790 \text{ kN}}}$$

$$Q_{u,NG} = 2332 + 2584 = \underline{\underline{4916 \text{ kN}}}$$

APPENDIX B

TYPICAL UNIT WEIGHTS (Assumed below water table), (Coduto 1999)

SC Clayey Sand	17.5-21 kN/m ³ (110-135 pcf)
SP/SW Poorly graded/Well graded Sand	19-21 kN/ m ³ (120-135 pcf)
CL/CH Low/High Plasticity Clay	11.5-20.5 kN/ m ³ (75-130 pcf)
Water	9.8 kN/ m ³ (62.4 pcf)

This page is intentionally blank.

APPENDIX C

The proceeding figures are plots of the numerical results and design predictions presented in Chapter 4. The first set of plots compare the total axial resistance of tested and design values. The following key pertains to the figures presented in this appendix.

KEY	
D	DRY METHOD
C	CASING METHOD
C/T	TEMPORARY CASING
C/P	PERMANENT CASING
PG	POST-GROUTING
P	POLYMER SLURRY
B	BENTONITE SLURRY

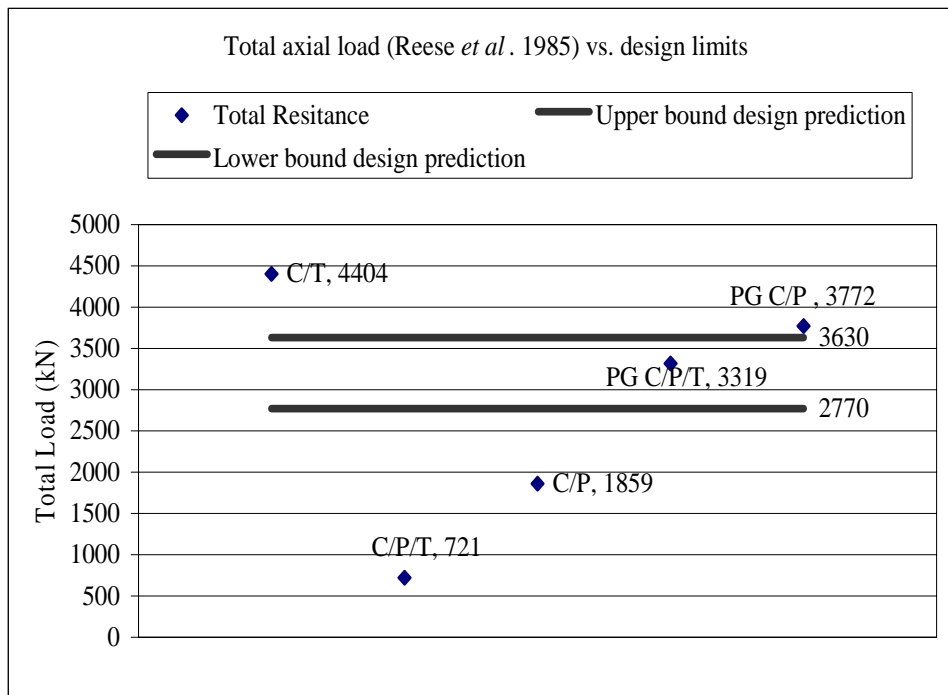


Figure 21 Total axial load versus design limits (Reese *et al.* 1985)

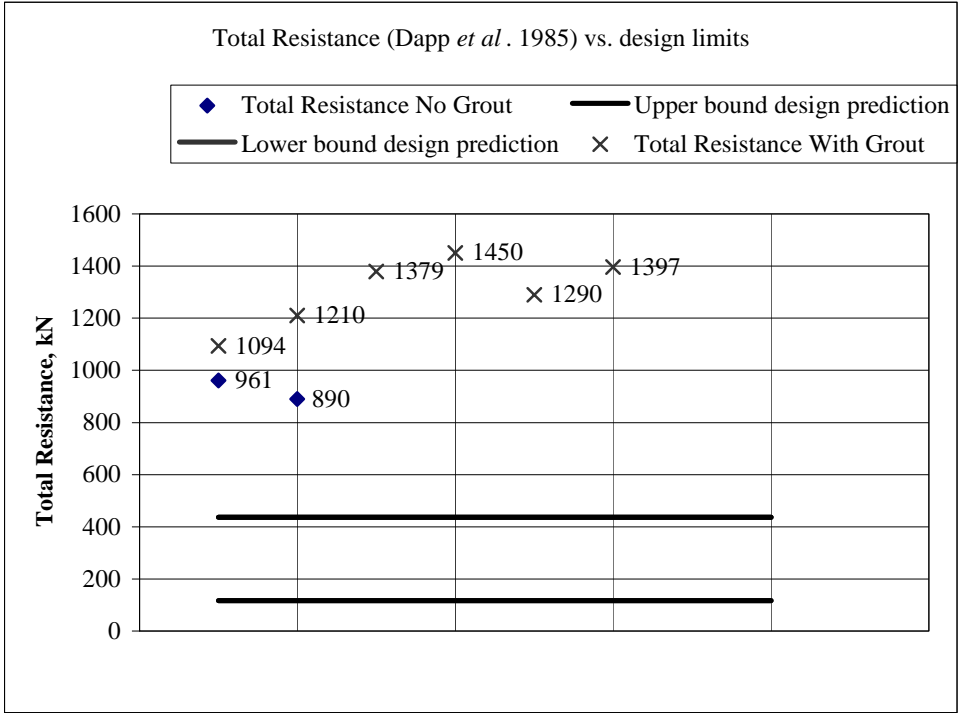


Figure 22 Total axial load versus design limits (Dapp *et al.* 2002)

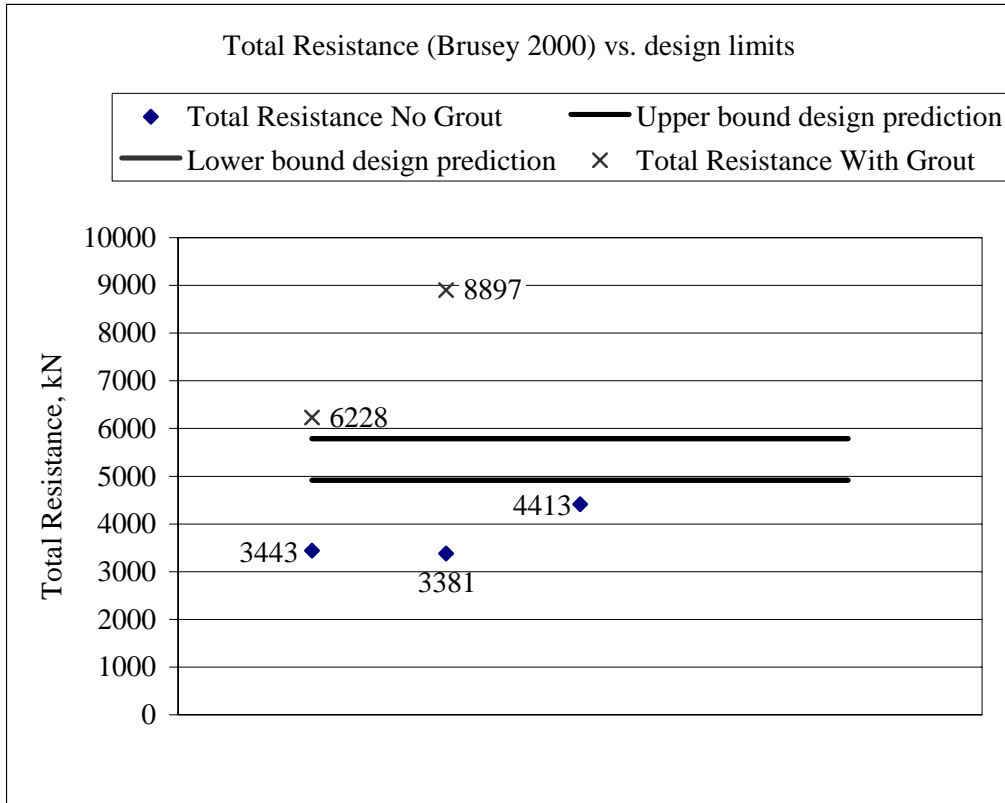


Figure 23 Total axial load versus design limits (Brusey *et al.* 2000)

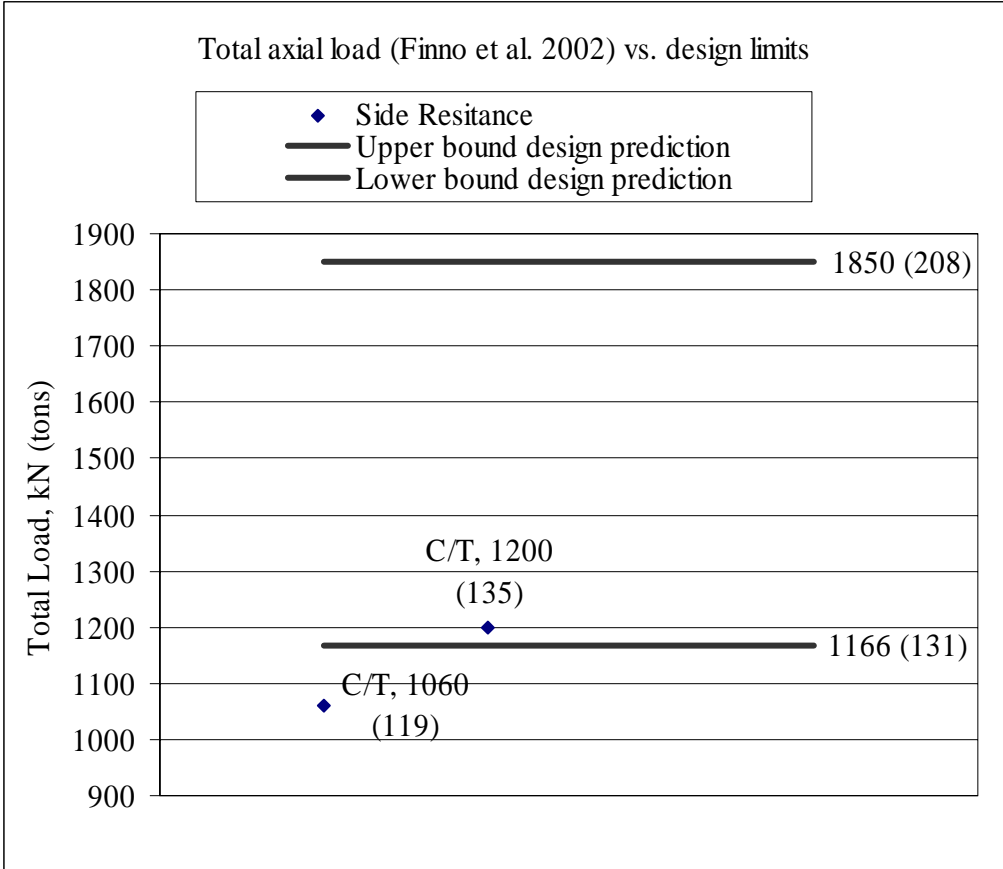


Figure 24 Total axial load versus design limits (Finno *et al.* 2002)

The following figures present the results on tip resistance for tested and design values.

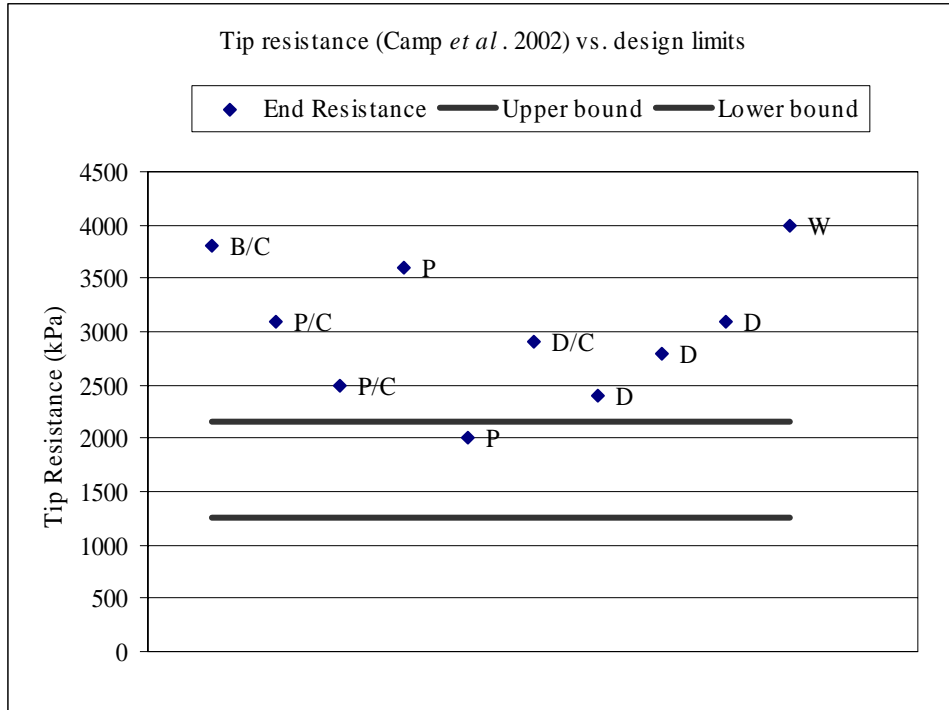


Figure 25 Tested tip resistance versus design limits (Camp et al. 2002)

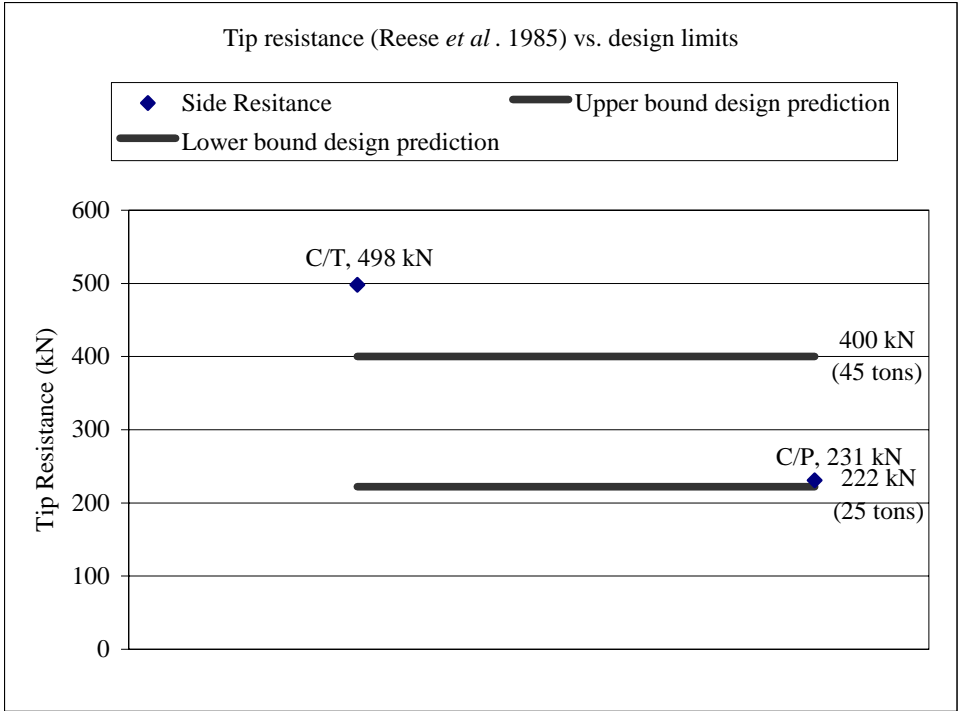


Figure 26 Tested tip resistance versus design limits (Reese *et al.* 1985)

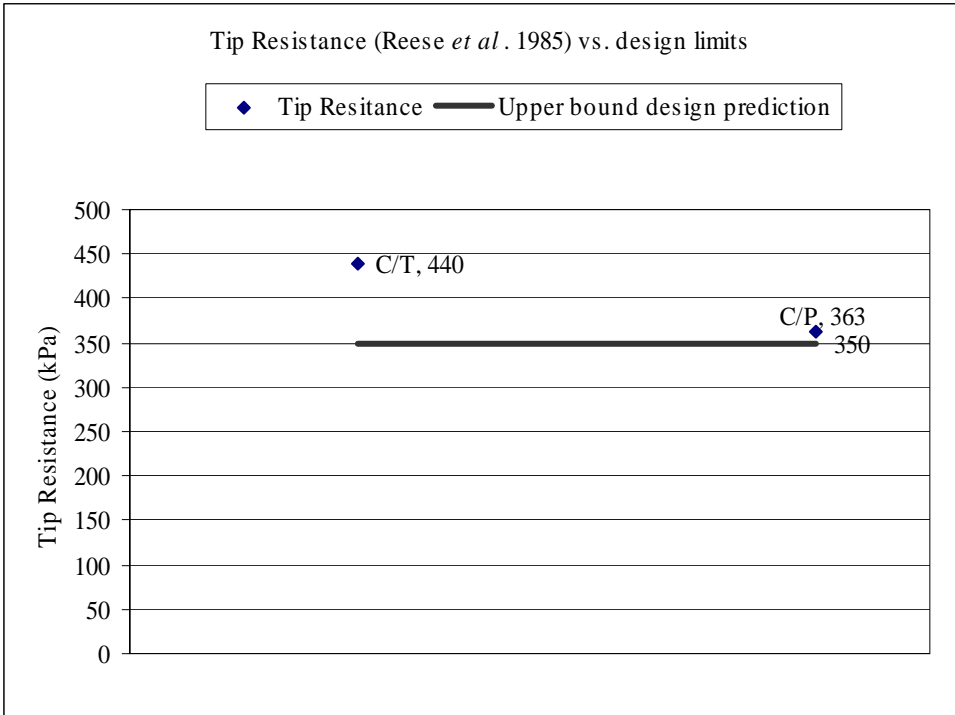


Figure 27 Tested tip resistance versus design limits (Reese *et al.* 1985)

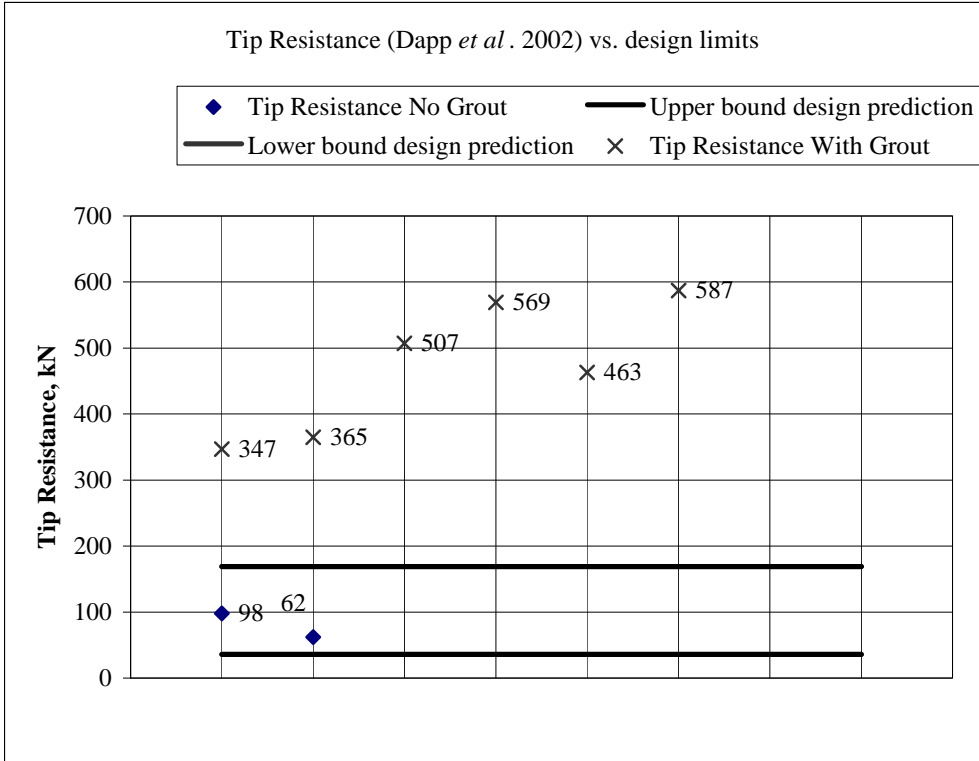


Figure 28 Tested tip resistance versus design limits (Dapp *et al.* 2002)

The remaining figures are from the case histories that provided information on side resistance.

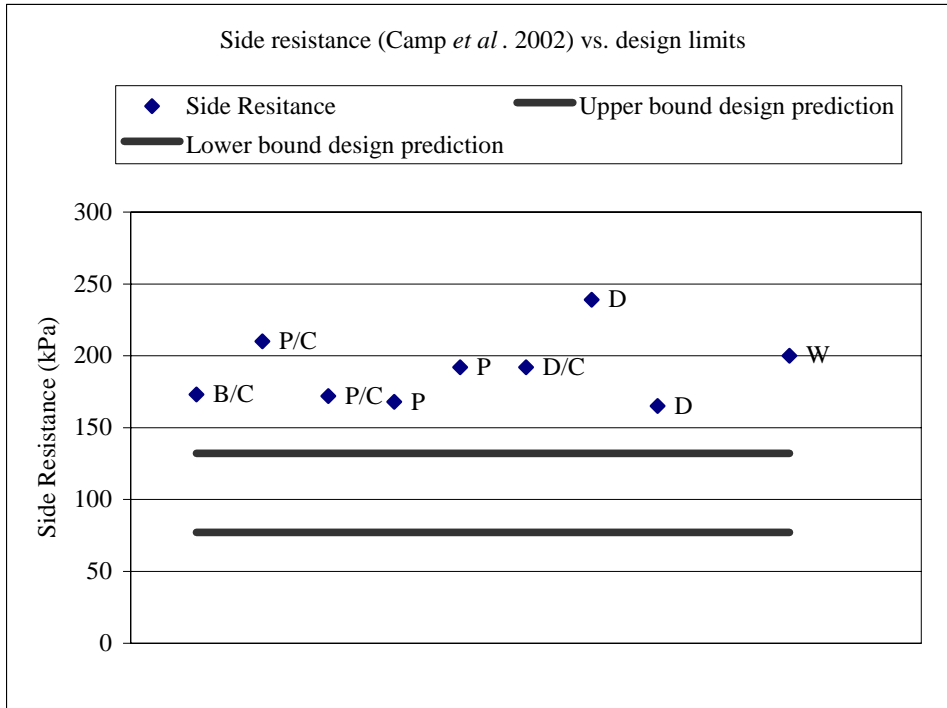


Figure 29 Tested side resistance versus design limits (Camp *et al.* 2002)

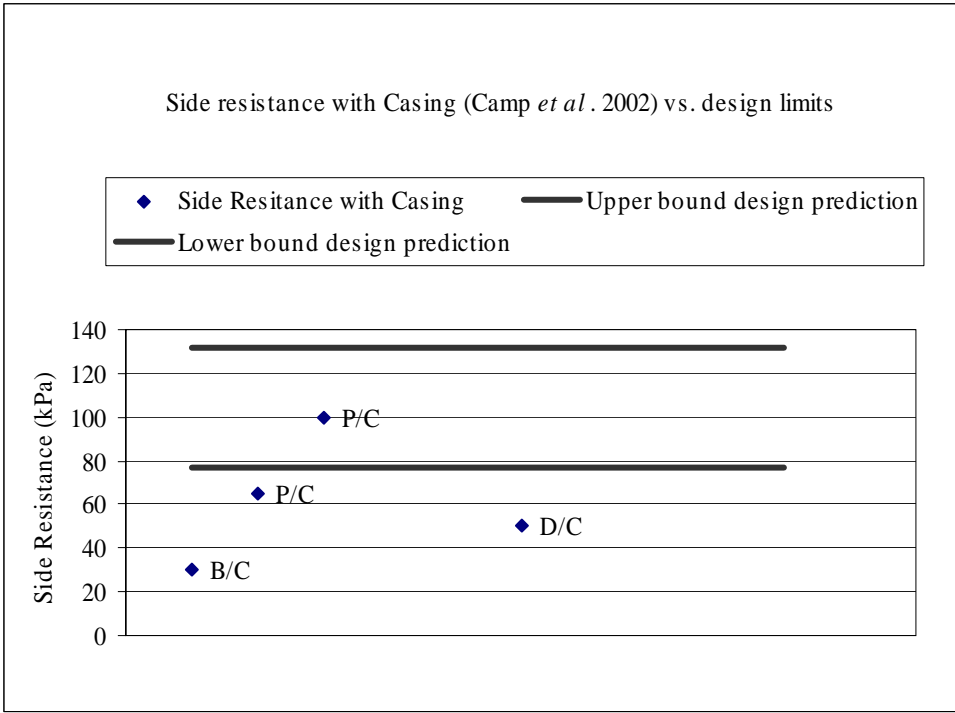


Figure 30 Tested side resistance with casing versus design limits (Camp *et al.* 2002)

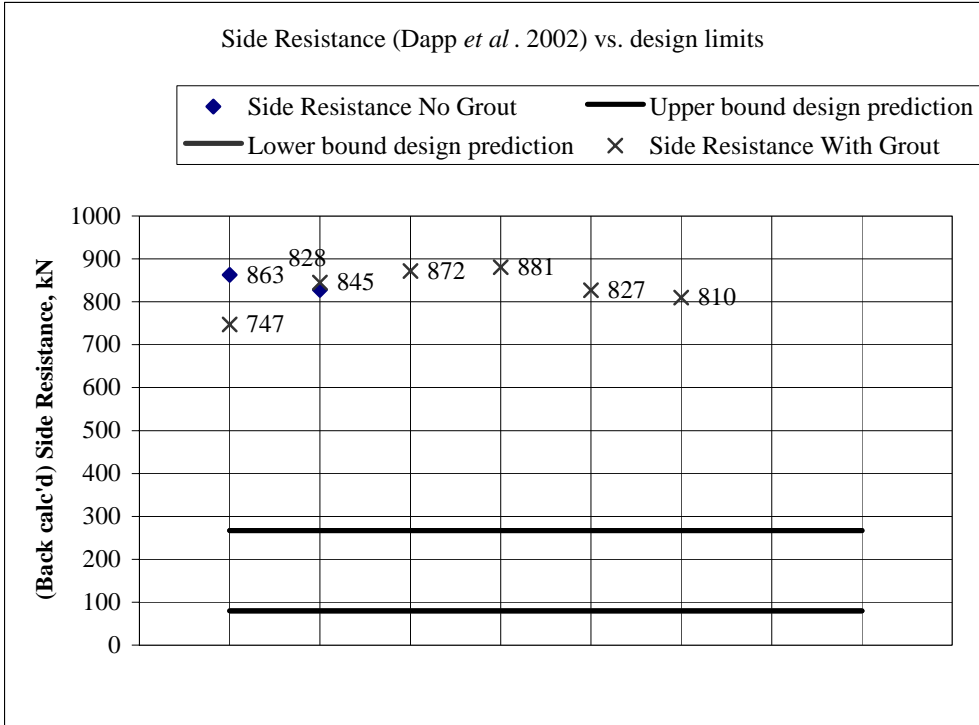


Figure 31 Tested side resistance versus design limits (Dapp *et al.* 2002)

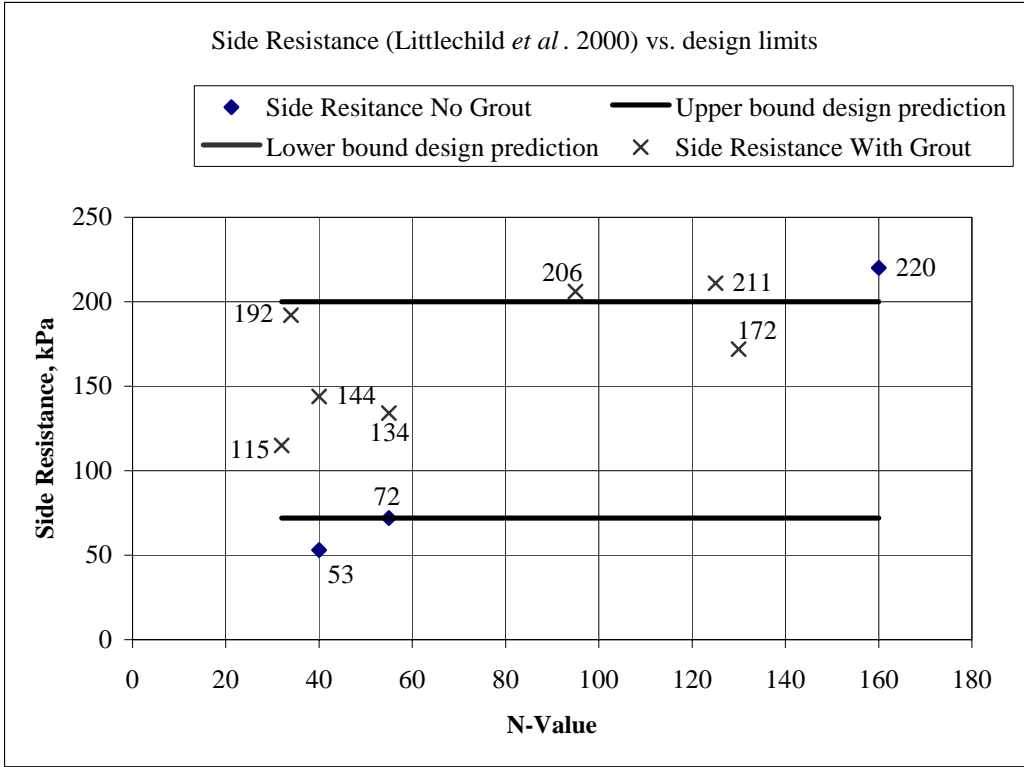


Figure 32 Tested side resistance versus design limits (Littlechild *et al.* 2000)

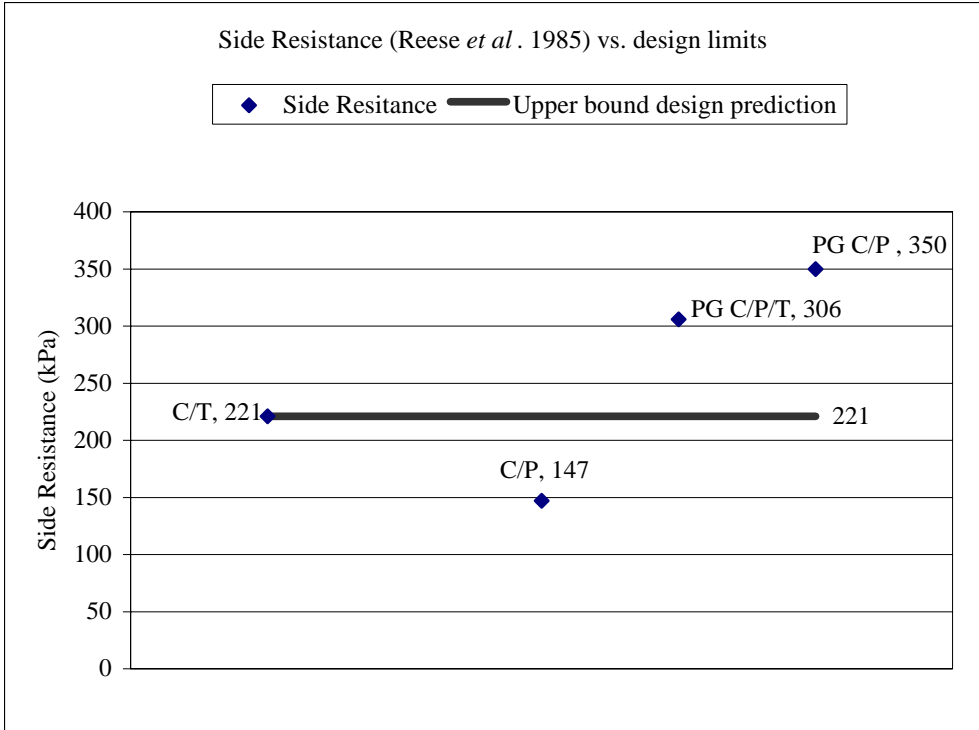


Figure 33 Tested side resistance versus design limits (Reese *et al.* 1985)

REFERENCES

ADSC: International Association of Foundation Drilling. <http://www.adsc-iafd.com/history.html>. 9/12/2002.

American Pile Driving Equipment (2002). <http://www.apevibro.com/asp/glossary.asp.4/15/03>.

Branagan, P., Vanderpool, W., Murvosh, H., Klein, M. (2000) "CSL Defines CIDH Defects; Coring Confirms Result." *New Technological and Design Developments in Deep Foundations*, Dennis, N.D., et al. (ed.), ASCE, Geo Institute, Vol. 100, pp 110-124.

Bruce, D.A., Traylor, R.P. (2000) "The Repair and Enhancement of Large Diameter Caissons by Grouting." *New Technological and Design Developments in Deep Foundations*, Dennis, N.D., et al. (ed.), ASCE, Geo Institute, Vol. 100, pp 59-71.

Brusey, W.G. (2000) "Post-Grouted Test Shafts at JFK International Airport". *New Technological and Design Developments in Deep Foundations*, Dennis, N.D., et al. (ed.), ASCE, Geo Institute, Vol. 100, pp 18-32.

The California Department of Transportation (Caltrans), personal correspondence. August, 2003.

CALTRANS: Memo To Designers 3-1. December 2000.

CALTRANS: Foundation Manual. Chapters 6, 9. July 1997.

Camp, W.M., Brown, D.A., and Mayne, P.W. (2002). "Construction Method Effects on Axial CIDH pile Performance." *DEEP FOUNDATIONS 2002: An International Perspective on Theory, Design, Construction, and Performance*, O'Neill, M.W. and Townsend, F.C. (ed.), ASCE, Geo-Institute, Publication No. 116, Vol. 1, pp 193-208.

Camp, W.M., Brown, D.A., and Mayne, P.W. (2002). "CIDH pile Axial Design Values: Predicted Versus Measure Response in a Calcareous Clay." *DEEP FOUNDATIONS 2002: An International Perspective on Theory, Design, Construction, and Performance*, O'Neill, M.W. and Townsend, F.C. (ed.), ASCE, Geo-Institute, Publication No. 116, Vol. 1, p. 1518.

Coduto, D.P. (1999). *GEOTECHNICAL ENGINEERING: Principles and Practices*. Prentice-Hall, Inc., Upper Saddle River, N.J.

Dapp, S.D., Mullins, G. (2002) "Pressure Grouting CIDH pile Tips: Full-Scale Research Investigation for Silty and Shelly Sands". *DEEP FOUNDATIONS 2002: An International Perspective on Theory, Design, Construction, and Performance*, O'Neill,

M.W. and Townsend, F.C. (ed.), ASCE, Geo-Institute, Publication No. 116, Vol. 1, pp 335-350.

Das, B.M. (1999). *Principles of Foundation Engineering*. PWS Publishing.

Ferraris, C.F., Brower, L., Ozyildirim, C., Daczko, J. (2000). "Workability of Self-Compacting Concrete." Contribution of the *National Institute of Standards and Technology*, reprinted from *The Economical Solution for Durable Bridges and Transportation Structures*, International Symposium on High Performance Concrete. Orlando, FL, 2000.

Finno, R.J., Chao, Hsiao-Chou, Gassman, S.L., Zhou, P. (2002). "Non-destructive Evaluation of CIDH piles at the Amherst NGES Test Section." *Geotechnical Special Publication*, ASCE. New York, N.Y.

Fisher, D.J., O'Neill, M.W., Contreras, J.C. (1995). "DS²: CIDH pile Decision Support System." *Journal of Construction Engineering Management*, ASCE. New York, N.Y.

(photo) Goodman, D.V., Guerrant, C.H. (2002) Virginia Department of Transportation, Lake Country Parkway. Greenhorne & O'Mara Inc. <http://www.clarksvillebypass.com/>

Greer, D.M. and Gardner, W.S. (1986) "Construction of drilled pier foundations". John Wiley & Sons, Inc., New York, N.Y.

Iskander, M., Roy, D., Ealy, C., Kelley, S. (2001). "Class-A Prediction of Construction Defects in CIDH piles." Proceedings of the 80th Annual Transportation Research Board Meeting. Washington, D.C. Record Number 1772.

Kulhawy, F.H. and Jackson, C.S. (1989) "Some Observations on Undrained Side Resistance of CIDH piles." *Proceedings*, Foundation Engineering: Current Principles and Practices, American Society of Civil Engineers, Vol. 2, pp. 1011-1025.

Liebich, B. (2002) "Acceptance Testing of CIDH piles by Gamma-Gamma Logging." Caltrans Foundation Testing Branch.

(photo) Liebich, B. (2002) Caltrans Foundation Testing Branch website. <http://www.dot.ca.gov/hq/esc/geotech/ft/>

Lin, M.S., Lin, T., Chang, L.T. (2000) "A Case Study for CIDH piles Base Mud Treatment". *New Technological and Design Developments in Deep Foundations*, Dennis, N.D., et al. (ed.), ASCE, Geo Institute, Vol. 100, pp 46-45.

Littlechild, B.D., Plumbridge, G.D., Hill, S.J., Lee, S.C. (2000) "Shaft Grouting of Deep Foundations in Hong Kong". *New Technological and Design Developments in Deep Foundations*, Dennis, N.D., et al. (ed.), ASCE, Geo Institute, Vol. 100, pp 33-45.

Lukas, R.G., and Baker, C.N., Jr. (1978) "Ground movement associated with drilled pier installations." *Preprint no. 3266*, ASCE. New York, N.Y.

Mullins, G., Dapp, S.D., and Lai, P., (2000) "Pressure Grouting CIDH pile Tips in Sand". *New Technological and Design Developments in Deep Foundations*, Dennis, N.D., et al. (ed.), ASCE, Geo Institute, Vol. 100, pp 1-17.

Olson Engineering, Inc. Website summary on CSL.

Osterberg, J. (2000) "Side Shear and End Bearing in CIDH piles". *New Technological and Design Developments in Deep Foundations*, Dennis, N.D., et al. (ed.), ASCE, Geo Institute, Vol. 100, pp 72-79.

Ouchi, Masahiro (1998) "History and Development and Applications of Self-Compacting Concrete in Japan". *Proceedings of the International Workshop on Self-Compacting Concrete*, Ozawa, K., Ouchi, M. (ed.), Self-Compacting Concrete Sub-Committee Concrete Committee, Japan Society of Civil Engineers. Tokyo, Japan. March 1999.

Petek, K., Felice, C.W., Holtz, R.D. (2002) "Capacity Analysis of CIDH piles with Defects." *DEEP FOUNDATIONS 2002: An International Perspective on Theory, Design, Construction, and Performance*, O'Neill, M.W. and Townsend, F.C. (ed.), ASCE, Geo-Institute, Publication No. 116, Vol. 2, pp 1120-1135.

Reese, L.C., Owens, M., Hoy, H. (1985) "Effects of Construction Methods on CIDH piles": Proceedings of a session / sponsored by the Geotechnical Engineering Division of the American Society of Civil Engineers in conjunction with the ASCE Convention, Denver, Colorado, May 1, 1985.

Robinson, B., Rausche, F., Garland, L., Ealy, C. (2002) "Dynamic Load Testing of CIDH piles at National Geotechnical Experimentation Sites." *DEEP FOUNDATIONS 2002: An International Perspective on Theory, Design, Construction, and Performance*, O'Neill, M.W. and Townsend, F.C. (ed.), ASCE, Geo-Institute, Publication No. 116, Vol. 2, pp 855-856.

Sarhan, H., Tabsh, S.W., O'Neill, M. (2002) "Flexural Behavior of CIDH piles with Minor Flaws." *DEEP FOUNDATIONS 2002: An International Perspective on Theory, Design, Construction, and Performance*, O'Neill, M.W. and Townsend, F.C. (ed.), ASCE, Geo-Institute, Publication No. 116, Vol. 2, pp 1136-1150.

Sarhan, H., O'Neill, M. (2002) "Aspects of Structural Design of CIDH piles for Flexure." *DEEP FOUNDATIONS 2002: An International Perspective on Theory, Design, Construction, and Performance*, O'Neill, M.W. and Townsend, F.C. (ed.), ASCE, Geo-Institute, Publication No. 116, Vol. 2, pp 1151-1165.

(photo) Stewart, J.P., Wallace, J.W., Taciroglu, E., Janoyan, K., Lermite, S., Ahlberg, E., Rha, C. (2001) "Field Testing of CIDH piles." Caltrans Sponsored Study

Turner, J.P. (1992) "Constructability of CIDH piles." *Journal of Construction Engineering Management*, ASCE. New York, N.Y.

Walter, B.G. (2000) "Post-Grouted Test Shafts at JFK International Airport". *New Technological and Design Developments in Deep Foundations*, Dennis, N.D., et al. (ed.), ASCE, Geo Institute, Vol. 100, pp 18-32.